Published in final edited form as:
Anat Rec (Hoboken). 2008 October 1; 291(10): 1301–1333. doi:10.1002/ar.20758.

Architectonic subdivisions of neocortex in the grey squirrel (*Sciurus carolinensis*)

Peiyan Wong[1] and **Jon H. Kaas**[1,*]

[1] Department of Psychology, Vanderbilt University, Nashville TN 37212

Abstract

Squirrels are highly visual mammals with an expanded cortical visual system and a number of well-differentiated architectonic fields. In order to describe and delimit cortical fields, subdivisions of cortex were reconstructed from serial brain sections cut in the coronal, sagittal, or horizontal planes. Architectonic characteristics of cortical areas were visualized after brain sections were processed with immunohistochemical and histochemical procedures for revealing parvalbumin, calbindin, neurofilament protein, vesicle glutamate transporter 2, limbic-associated membrane protein, synaptic zinc, cytochrome oxidase, myelin or Nissl substance. In general, these different procedures revealed similar boundaries between areas, suggesting that functionally relevant borders were being detected. The results allowed a more precise demarcation of previously identified areas as well as the identification of areas that had not been previously described. Primary sensory cortical areas characterized by sparse zinc staining of layer 4, as thalamocortical terminations lack zinc, as well as by layer 4 terminations rich in parvalbumin and vesicle glutamate transporter 2. Primary areas also expressed higher levels of cytochrome oxidase and myelin. Primary motor cortex was associated with large SMI-32 labeled pyramidal cells in layers 3 and 5. Our proposed organization of cortex in grey squirrels includes both similarities and differences to the proposed of cortex in other rodents such as mice and rats. The presence of a number of well-differentiated cortical areas in squirrels may serve as a guide to the identification of homologous fields in other rodents, as well as a useful guide in further studies of cortical organization and function.

Keywords

Rodents; cortical areas; visual cortex; motor cortex; somatosensory cortex; auditory cortex; cingulate cortex; retrosplenial cortex

INTRODUCTION

Over the last 55 million years of evolution, the rodent clade has had considerable success and diversification, radiating into some 28 families, 400 genera and over 2000 extant species (Huchon et al., 2002). Squirrels diverged from other rodents about 40 million years ago, diversified into 50 genera and 273 species (Mercer and Roth, 2003), and developed distinguishing characteristics that make them attractive for neurobiological studies. Most notably, grey squirrels and other squirrels have been used in a number of studies of the visual system because this system is especially well developed (Van Hooser and Nelson, 2006). As a result of such studies, the visual system in squirrels can be productively compared to other well-developed visual systems, such as those of primates, cats and tree

[*]Correspondence to: Jon H. Kaas, Vanderbilt University, 301 Wilson Hall, 111 21st Avenue South, Nashville, TN 37203, Phone: 615-322-6029, Fax: 615-343-8449, jon.kaas@vanderbilt.edu.

shrews, for common features and alternative specializations. As examples of specializations of the visual system, diurnal squirrels have large eyes with a majority of cones over rods in their retina (West and Dowling, 1975; Long and Fisher, 1983; Szél and Röhlich, 1988), a distinctly laminated dorsal lateral geniculate nucleus (Kaas et al., 1972; Cusick and Kaas, 1982; Major et al., 2003), and a patently laminated superior colliculus (Abplanalp, 1970; Lane et al., 1971; Cusick and Kaas, 1982) that is approximately ten times larger than in rats matched for body size (Kaas and Collins, 2001). In the neocortex, primary visual cortex is large, with a fine-grain retinotopic map (Hall et al., 1971), the second visual area, V2, is well-defined, and additional visual areas have been proposed (Kaas et al., 1989; Sereno et al., 1991). Given that tree squirrels are also skilled in climbing and exploring the fine branches of their arboreal niche, and use their forepaws to manipulate food items, as do most primates, it is not surprising that their sensorimotor system and cortex are well-developed and proportionately large with as many as five somatosensory areas (Krubitzer et al., 1986; Slutsky et al., 2000). The auditory cortex has also been explored in squirrels and several auditory areas have been described (Luetheke et al., 1988). These studies on aspects of cortical organization and function in squirrels have produced results that can be compared with architectonic studies of how the cortex is subdivided into areas, as the borders of cortical areas are most reliably defined when architectonic evidence is congruent with evidence from neurophysiological and anatomical studies (Kaas, 1972; 1989).

Most studies of cortical architecture in rodents have focused on laboratory rats (e.g., Krieg, 1946; Schober, 1986; Wise and Donoghue, 1986; Zilles and Wree, 1995; Swanson, 1992; 2003; Uylings et al., 2003) and, to a lesser extent, on laboratory mice (e.g., Rose, 1912; Caviness 1975; Wallace, 1983; Lorente de Nó, 1992; Paxinos and Franklin, 2003). Compared to rats and mice, cortical organization and function in squirrels has been limited to a few investigations. This is surprising considering the characteristic functional adaptations of squirrels that cannot be gleaned from examining rat brains. In the present study, we reexamine the cortical architecture of the grey squirrel using a number of recently developed immunohistochemical stains with the goal of defining and describing the areas that form the functional subdivisions of the neocortex.

For the present study, an important additional procedure was to use a histochemical procedure to reveal unbound ionic zinc (Zn^{2+}) in cortical tissues (Danscher, 1981; 1982; Danscher and Stoltenberg, 2005). Detectable levels of synaptic zinc are contained in cortical neurons, especially in the synaptic vesicles of cortical neuron terminations and synaptic clefts. As thalamocortical neurons and their cortical terminations are not synaptic zinc positive, cortical areas with dense or sparse thalamocortical inputs can be distinguished by reactions for zinc (e.g., Valente et al., 2002). As a notable example, primary sensory areas can be distinguished by an almost total lack of zinc in layer 4. Some brain sections were processed for cytochrome oxidase, which is expressed at high levels in layer 4 of sensory areas (Wong-Riley, 1979). Other brain sections were immunostained with a monoclonal selective neurofilament marker, SMI-32, parvalbumin (PV), calbindin (CB), vesicle glutamate transporter 2 (VGluT2) and limbic-associated membrane protein (LAMP). SMI-32 is a monoclonal antibody that reacts with non-phosphorylated epitopes in neurofilaments M and H (Lee et al., 1988), and reveals a subset of pyramidal cells (Campbell and Morrison, 1989). PV is a calcium-binding protein and PV immunoreactive neurons include subsets of GABAergic, non-pyramidal cells, thought to be basket and double bouquet interneurons (Celio, 1986; Condé et al., 1996; DeFelipe, 1997; Hof et al., 1999). Perhaps, more importantly for the present study, PV also labels afferent cortical terminals from sensory thalamic nuclei (Van Brederode et al., 1990; DeFelipe and Jones, 1991; DeVencia et al., 1998; Hackett et al., 1998; Latawiec et al., 2000; Cruikshank et al., 2001). The large to medium PV positive thalamic neurons projecting to sensory cortex belong to the “leminiscal” subsystem of relay cells that project most densely to layer 4 (e.g.,

Jones and Hendry, 1989; Rausell and Jones, 1991; Diamond et al., 1993). Another calcium-binding protein, calbindin (CB) reveals a different subset of GABA immunoreactive interneurons compared to PV (Van Brederode et al., 1990). VGluT2 immunostaining also reveals thalamocortical terminations in layer 4, but not those of cortical neurons (Fujiyama et al., 2001; Kaneko and Fujiyama, 2002; Nahami and Erisir, 2005). The limbic-associated membrane protein (LAMP) is a cell-surface glycoprotein expressed in limbic areas (Levitt, 1984; Horton and Levitt 1988; Côté et al., 1995).

By using this battery of additional procedures, together with traditional Nissl and myelin stains, we were able to more fully characterize the areal subdivisions of neocortex in grey squirrels. A brief abstract of the present findings has appeared (Wong and Kaas, 2006).

MATERIALS AND METHODS

Architectonic subdivisions of the neocortex were studied in nine grey squirrels (*Sciurus carolinensis*). All procedures were approved by the Vanderbilt Institutional Animal Care and Use Committee and followed NIH guidelines.

Tissue preparation

All animals were given a lethal dose of sodium pentobarbital (100mg/kg). To reveal synaptic zinc, the animals were given 200mg/kg body weight of sodium sulfide with 1ml of heparin in 0.1M phosphate buffer, (PB), pH 7.2, intravenously. The animals were perfused transcardially, in sequence, with 0.9% saline, 4% paraformaldehyde in 0.1M PB and subsequently with 4% paraformaldehyde and 10% sucrose. The brains were removed from the skull, bisected and post-fixed for about 3 hrs in 4% paraformaldehyde and 10% sucrose in 0.1M PB. The hemispheres were immersed in 30% sucrose solution for cryoprotection until they sank to the bottom of the vial before being cut into 40μm–thick coronal, parasagittal or horizontal sections on a freezing microtome. Serial sections were divided into four or up to six series. For some cases, after an injection of sodium sulfide, the animals were perfused with 0.9% saline, 2% paraformaldehyde in 0.1M PB, followed by 2% paraformaldehyde with 10% sucrose. The brains were then removed, artificially flattened, and then cut tangentially, parallel to the pia.

Zinc Histochemistry

Our protocol followed that outlined by Ichinohe and Rockland (2004). Brain sections were washed thoroughly with 0.1M PB, pH 7.2, followed by 0.01M PB, pH 7.2. The IntenSE M Silver enhancement kit (Amersham International, Little Chalfont Bucks, UK) was used to visualize the Zn^{2+}-enriched terminals. A one-to-one cocktail of the IntenSE M kit solution and a 50% gum arabic solution was used as the developing reagent. When a dark brown/black signal was seen, which usually takes about 4 hours to appear, the development of reaction products was terminated, by rinsing the sections in 0.01M PB. Sections were then mounted and dehydrated in an ascending series of ethanols, (70% for 20 min, 95% for 10 min, 100% for 10 min), cleared in xylene and coverslipped using Permount (Fisher Scientific, Pittsburgh, PA).

Immunohistochemistry

In some cases, a series of one in four or five brain sections was immunostained for SMI-32 (mouse monoclonal anti-SMI-32 from Covance Inc. Princeton, NJ; 1:2000), parvalbumin (PV) (mouse monoclonal anti-PV from Sigma-Aldrich, St. Louis, Mo; 1:2000), calbindin (CB) (mouse monoclonal anti-CB from Swant, Bellinzona, Switzerland; 1:5000), vesicle glutamate transporter 2 (VGluT2) (mouse monoclonal anti-VGluT2 from Chemicon now part of Millipore, Billerica, MA; 1:2000), or Limbic Associated Membrane protein (mouse

monoclonal anti-LAMP) (kindly provided by Drs Aurea Pimenta and Pat Levitt; Horton and Levitt, 1998; Reinoso et al., 1996; 1:1000). Sections processed for PV, CB, VGluT2 and SMI-32 were reacted using the protocol described in Ichinohe et al. (2003). Briefly, sections were incubated in a blocker of 01.M PBS, pH 7.2, with 0.5% Triton X-100 and 5% normal horse serum for an hour at room temperature before incubation in their respective primary antibodies in the blocker for 40 to 48 hours at 4°C. After rinsing, the sections were incubated in the blocker containing biotynylated horse anti-mouse IgG (Vector, Burlinggame, CA; 1:200) for 90 minutes at room temperature. followed by ABC incubation (one drop each of reagent A and B per 7ml of 0.1M PB, pH 7.2; ABC kits, Vector, Burlingame, CA) for 90 minutes, also at room temperature. Immunoreactivity was visualized by developing sections in diaminobenzidine histochemistry with 0.03% nickel ammonium sulfate. Processing procedures for LAMP have been described in Chesselet et al., (1991) and a brief description follows. Sections were incubated in 0.1M PBS, pH 7.2, containing 4% non-fat dry milk and the anti-LAMP antibody for 24h at 4°C. Procedures for the secondary antibody and immunoreactivity visualization are as described above.

Antibody characterization

For further details on antibody characterization obtained from manufacturer's technical information, with the exception of the LAMP antibody, please refer to Table 2.

The mouse monoclonal anti-calbindin antibody is produced by the hybridization of mouse myeloma cells with spleen cells from mice immunized with the calbindin D-28k that was purified from the chicken gut. This monoclonal antibody is not known to cross-react with other known calcium binding-proteins and specifically stains the 45Ca-binding spot of calbindin D-28k (MW 28,000, IEP 4.8) from human, monkey, rabbit, rat, mouse and chicken in a two-dimensional gel (manufacturer's technical information).

The mouse monoclonal anti-parvalbumin antibody specifically recognizes PV in a calcium ion-dependent manner, and does not react with other members of the EF-hand family. This anti-parvalbumin antibody specifically reacts with the Ca-binding spot of parvalbumin (MW = 12,000) from human, bovine, goat, pig, rabbit, canine, feline, rat, frog and fish on an two-dimensional gel (manufacturer's technical information).

The mouse monoclonal anti-SMI-32 antibody specifically recognizes the 200-kD nonphosphorylated epitope in neurofilament H of most mammalian species. Anti-SMI-32 antibody visualizes neuronal cell bodies, dendrites and some thick axons in the nervous system, and is not found in other cells and tissues. Anti-SMI-32 antibody epitope shows up as two bands (200 and 180kDa) that merge into a single neurofilament H line on two-dimensional blots (manufacturer's technical information).

The mouse monoclonal anti-VGluT2 antibody has shown species reactivity to the mouse and rat. The antibody epitope for VGluT2 from Millipore is not known. However, preadsorption of this monoclonal antibody (MAB5504) by Wässle et al., (2006) with the C-terminal peptide (562–582) did not block staining.

The mouse monoclonal anti-LAMP antibody shows up as a single band on Western blot analysis between 64–68 kDa on a 10% SDS-polyacrylamide gel. On a two-dimensional gel, LAMP is a single protein that visualizes as a single spot at approximately 68kDa, with a p*I* of 5.2–5.5 (Zacco et al., 1990).

Histochemistry

Apart from the sections processed with the antibodies stated above, one section from each parasagittal or coronal series was processed for Nissl substance (with thionin). In cases cut

in the horizontal plane, one series of sections was processed for Nissl substance (with thionin) and another series of sections was processed for myelin using the Gallyas (1979) silver procedure. In flattened brain sections, one in every three sections was processed for cytochrome oxidase (CO) (Wong-Riley, 1979).

Light microscopy

A number of histological procedures were used to delineate architectonic borders in brain sections, including those for Nissl substance, myelin, CO, zinc, PV, CB, VGluT2, SMI-32 and LAMP. Cortical borders were revealed by laminar and cell density changes in the processed sections. The locations of borders were established by viewing sections with a high-powered microscope. Nissl and zinc preparations were the most useful for defining primary sensory areas, while Nissl and SMI-32 preparations were useful for defining cortical areas in the sensorimotor cortex. Other histochemical procedures were used for corroborating otherwise ambiguous borders. Processed sections were viewed under a Nikon E800 microscope (Nikon Inc., Melville, NY) and digital photomicrographs of sections were acquired using a Nikon DXM1200 camera (Nikon Inc., Melville, NY) mounted on the microscope. Digitized images were adjusted for levels, brightness and contrast using Adobe Photoshop (Adobe Systems Inc., San Jose, CA), but they were not otherwise altered.

Anatomical reconstruction

The first brain section in every series was projected onto a white sheet of paper using a Bausch and Lomb Microprojector (Bausch & Lomb, Rochester, NY) and the outline of the section was drawn. Blood vessels and other landmarks were marked on the outline so that sections from adjacent series could be aligned. Areal borders of adjacent sections processed for different preparations in a series were independently assessed and marked on the outline. The locations of the independently identified borders in the different preparations were within 500μm, usually less, of each other. On rare occasions where the deviation in distances between the identified borders is greater than 500μm, it would usually be the result of histological artifacts, such as tears in the section. These sections were not included in the analysis. Borders are assigned only when changes in architectonic characteristics were observed in at least three preparations and the location of the changes were within 500μm of each other.

The outlines of the brain sections with the architectonic borders marked out were then digitized and imported into Adobe Illustrator (Adobe Systems Inc., San Jose, CA), where they are aligned into stacks using the contour of the outlined section and the landmarks stated above. For brains that were cut coronally, straight lines drawn parallel, perpendicular, and at a 45° angle to the midline on the image of each outline served as axes of reference to obtain the lateral, dorsal and dorsolateral view of the brain respectively. Brains cut in the sagittal and horizontal planes were used to reconstruct the dorsal and lateral view of the brain respectively by drawing an axis of reference parallel to the midline. The rostral and caudal poles of the section, and the position of the borders were marked along these axes, and subsequently charted on their respective views of the brain. The points on the brain chart were then joined, thus obtaining the areal boundaries. In general, the different histological procedures revealed nearly identical boundaries between areas, suggesting that functionally relevant borders were being detected.

Summary diagrams of the arrangement of proposed cortical areas were constructed as guides to viewing the histological material by transposing the most reliably identified areal borders from reconstructed cases cut in the coronal, sagittal or horizontal planes. The coronal plane was most useful for charting borders that coursed predominantly in the rostrocaudal direction, sagittal sections were most useful for mediolateral coursing borders of the dorsal

surface, and horizontal sections were most useful for mediolateral borders of the lateral and medial brain surfaces. Some areal borders have been included, even though architectonic distinctions have not been well documented here, either because these borders were well described in pervious publications, or because distinctions depend on previously published electrophysiological results. For example, the temporal anterior field, Ta, contains several auditory areas that have been defined electrophysiologically, but were not distinguished architectonically in the present study. In some of the diagrams of cortical areas in squirrels, these areas are depicted. Likewise, we did not find clear architectonic differences between part of the previously identified parietal lateral field, Pl, that contains the electrophysiologically identified second somatosensory area, S2 and remaining caudal region, but S2 is distinguished in some of the figures.

RESULTS

The present results provide further evidence for the validity of several previously proposed subdivisions of cortex in squirrels (Kaas et al., 1972), while providing evidence for the modification of the boundaries of some areas, and evidence for other areas not previously described. The proposed areas are outlined on a dorsolateral view of a squirrel brain in Fig. 1f and in figures that follow. Descriptions of cortical areas, region by region, follow.

Occipital cortex

The occipital region of the grey squirrel comprises of three areas, 17, 18 and 19, following Brodmann's (1909) terminology (Fig. 1–4).

Area 17—The striate area 17 is very distinct, and its borders are easily identified. The greater extent of area 17 in squirrels compared to other rodents can be appreciated in low magnification photomicrographs of coronal (Fig. 1) and sagittal brain sections (Fig. 2). Note that even at low magnification, the borders of area 17 are apparent in Nissl, zinc, PV, VGluT2 and SMI-32 preparations. Much of the border of area 17 is with the laterally adjoining area 18, or V2, where the distinctive laminar appearance of area 17 disappears (Fig. 1). Area 17 extends onto the medial wall and even well onto the ventral surface of the hemisphere where it is bordered by the agranular division of the retrosplenial cortex (Fig. 2). A rostral segment of area 17 is bordered medially by cortex presumed to be a subdivision of limbic cortex, termed area L after Kaas et al., 1972. A ventromedial portion of V1 is bordered by cortex widely described as prostriata (PS) (e.g., Rosa, 1999). All borders of area 17 are sharp and easily identified in all the preparations used in the present study.

The myeloarchitecture of area 17 and other visual areas can be compared to the cytoarchitecture in figure 3. Note that the inner half of layer 3 of area 17 is occupied by a band of densely myelinated fibers, known as the outer band of Baillarger. This band corresponds to a light zone of more sparsely distributed cells in inner layer 3 in Nissl-stained sections (layer 3C). Layer 4 of area 17, in contrast, is lightly myelinated, with very few myelinated horizontal fibers. Layers 5 and 6 in area 17 are again densely myelinated. These two densely myelinated bands are characteristic of area 17 and other primary sensory areas in other mammals (e.g., Annese et al., 2004). While the outer band of Baillarger, also known as the line of Gennari in area 17 is usually attributed to layer IVb of V1, comparative studies suggest that layer IVa and IVb of area 17 of anthropoid primates are actually sublayers of layer 3 (e.g., Hässler, 1966; see Casagrande and Kaas, 1994 for review). The outer band of Baillarger in area 17 of squirrels is external to layer 4 of densely packed granule cells and is thicker in the dorsal binocular portion than the ventral monocular portion of area 17.

The laminar pattern of staining in area 17 is more fully appreciated in brain sections shown at a higher magnification (Fig. 4). Nissl preparations (Fig. 4B) reveal a layer 4 that is

densely populated with small cells that give it a dark appearance. In some regions, a lighter, more sparsely populated zone in the middle of layer 4 suggests that sublayers exist (Kaas et al., 1972). Medially, layer 4 thins (Fig. 1A) at the point where area 17 changes from being binocular to monocular (Hall et al., 1971). Laterally, layer 4 tapers somewhat near the border with area 18 (see Figs. 3,4,6), corresponding to a narrow transition zone that has callosal connections with the other cerebral hemisphere (Gould, 1984). Other layers in area 17 are also quite distinct in Nissl preparations. Layer 2 is densely populated with small cells. Layer 3 is broad and has a mixture of cell types, with an inner sublayer of less densely packed cells that has been identified as layer 3C in squirrels (Fig. 3A,5A;Kaas et al., 1972). A similar sublayer has been identified in tree shrews (Jain et al., 1994) and monkeys (see Casagrande and Kaas, 1994 for review).

In Nissl preparations of areas 17 and 18 (Figs. 1, 4, and 6) and elsewhere, a narrow band of cells can be seen below layer 6. Reep (2000) has identified this deeper layer of cells in a range of mammalian species, including grey squirrels and other rodents, but not in cats and monkeys. This layer appears to consist of subplate cells that persist rather than undergoing apoptosis. In other preparations, area 17 is also distinct. In zinc preparations, layer 4 is nearly devoid of synaptic zinc, standing out as a white band (e.g., Figs. 2B,4C). The adjoining area 18 and agranular retrosplenial area (RSA) have much more synaptic zinc in layer 4 (Fig. 2B). Layer 3, especially inner layer 3, and layer 6 of area 17 also express less synaptic zinc than the corresponding layers in adjoining cortex, but more synaptic zinc than layer 4 (Fig. 4C). The reduction of synaptic zinc in layers 3 and 6 suggests that a greater proportion of axon terminals in these layers represent thalamic inputs than in adjoining areas of cortex. The vesicle glutamate transporter, VGluT2, is densely expressed in layer 4, and to a lesser extent in layer 6 of area 17, so the extent of area 17 is very obvious in this preparation (Fig. 1E,5C). Adjoining cortical areas express much less VGluT2 in these layers. The VGluT2 protein is expressed in the terminals of thalamocortical connections (Nahamani and Erisir, 2005). In a similar manner, PV is expressed at higher levels in layers 4 and 6 in area 17 compared to adjacent cortex (Figs. 1C,4D,5B), but the density contrast in these layers is less than that in VGluT2 preparations (Figs. 1E,5C). PV preparations differed somewhat, with the section in Fig. 1C reflecting the staining of the thalamocortical terminals in layer 4, and to a lesser extent in layer 6, whereas the preparation in Fig. 4D more clearly stains the subset of GABAergic interneurons that express the calcium-binding protein, parvalbumin (Celio, 1986). The distribution of PV positive interneurons was similar in area 17 and 18 (Fig. 4D). SMI-32 labels dark bands of pyramidal neurons in layers 3 and 5, without labeling neurons in layer 4 (Figs. 1D, 4E). The stained pyramidal cells in layer 3 are largely within layer 3C, where they are much smaller than those in layer 5. Layers 4 and 6 express more cytochrome oxidase (CO) protein than other layers, and the layers were more CO-dense in area 17 than in adjoining cortex (not shown). The distinctiveness of layer 4 in PV and VGluT2 preparations is shown at higher magnification photomicrograph in Fig. 5. Also note the greater expression of these proteins in layer 5b. In contrast, layer 5a expresses more calbindin (Fig. 5D).

In summary, area 17 is easily distinguished in most preparations in squirrels. Layer 4 is densely packed with granule cells, is lightly myelinated, expresses little synaptic zinc, is densely populated with PV- and VGluT2- immunoreactive thalamocortical terminations and lacks SMI-32 stained pyramidal cells. Layer 4 is thinner in the monocular than the binocular portion of area 17.

Area 18—The lateral border of area 17 in squirrels is bound by area 18, which corresponds to the second visual area, V2 (Hall et al., 1971). The representation of the contralateral visual hemifield in V2 approximates a mirror reversal of that in V1, and the common border of V1 and V2 represents the zero vertical meridian through the center of gaze. Thus, area 18

(V2) borders area 17 along the complete representation of the vertical meridian (Hall et al., 1971), which extends from the rostral border of area 17 with area L, and continues caudally over the occipital pole and even somewhat onto the ventral surface of the hemisphere. As area 18 is only about 2mm wide, it forms a long band, with area 19 on its lateral border.

In Nissl preparations, the layers of area 18 are less distinct than those of either of the bordering areas, 17 and 19 (Figs. 1A, 2A, 3A, 4B). Layers 4 and 6 are less densely packed with cells, and these cells are less darkly stained then in area 17 and 19 (Fig. 2A, 4B) such that the density contrast between layers is lower. While layer 4 and, to a lesser extent, layer 6 in area 17 are relatively free of synaptic zinc, and therefore unstained in zinc preparations, there is only a moderate reduction of synaptic zinc in layers 4 and 6 of area 18. Hence, these layers are darker in area 18 than in area 17 (Figs. 2B, 4C). This indicates that there are fewer inputs to area 18 from the thalamus, especially the pulvinar (Robson and Hall, 1977), and more are from other areas of cortex, including dense layer 4 inputs from area 17 (Kaas et al., 1989). Area 19 resembles area 18 in zinc preparations, although slightly more synaptic zinc is expressed in layers 4 and 6. Layers 4 and 6 also express less PV and VGluT2 in area 18 than in area 17, and slightly less than in area 19 (Figs. 1C, 1E,4D,6C, 6E). Areas 17, 18 and 19 all have high levels of neuropil and pyramidal cell labeling in layers 3 and 5 in SMI-32 preparations, but the labeled zone in layer 3 is broader in binocular area 17 than in area 18 (Fig. 6D), whereas layer 5 of area 18 has somewhat larger pyramidal cells than area 17 (Fig. 4E). Area 18 is not densely myelinated as area 17 and has distinct bands of Baillarger than both areas 17 and 19 (Fig. 3B), and does not express high levels of CO in layers 4 and 6 (not shown). Overall, area 18 is one of the more clearly defined areas of the neocortex in squirrels. In the present preparations, area 18 was relatively uniform in appearance, without obvious architectonic subdivisions. However, in sections cut parallel to the cortical surface and stained for myelin, area 18 has a series of myelin-light patches along its length (Kaas et al., 1989). The patches receive most of the inputs from area 17, while the myelin-dense surround receive dense callosal inputs (Gould, 1984).

In summary, area 18 has a less densely packed layer 4 than area 17, and is less densely myelinated as well. Area 18 expresses less PV and VGluT2 in layers 4 and 6 compared to area 17.

Area 19—As noted above, area 19 has slightly more distinct lamination than area 18 in Nissl preparations as indicated by somewhat more darkly stained neurons in layers 4 and 6 (Figs. 2A, 3A; see Kaas et al., 1972 for more documentation). As several areas border area 19 laterally, the distinction between area 19 and these adjoining areas in Nissl preparations varies, but typically, layers 4 and 6 are more darkly stained in area 19 (Fig. 6A). In zinc preparations (Figs. 2B, 6B), middle layers express less synaptic zincin area 19 than adjoining temporal mediodorsal area, Tm, and other layers have less synaptic zincas well (Fig. 6B). Area 19 has higher PV and VGluT2 levels than more lateral cortex (e.g., Figs. 6C, 6E), and increased SMI-32staining in layers 3 and 5 (Fig. 6D). Overall, area 19 is not as well defined as area 18. The architectonic evidence, although not completely compelling, suggests that area 19 is a single subdivision of occipital cortex.

In summary, area 19 is more myelinated than area 18, and the neurons in layers 4 and 6 are more darkly stained in area 19 than area 18, giving area 19 a more distinct lamination pattern. In addition, area 19 stained more darkly for PV, VGluT2 and SMI-32 compared to the adjacent temporal areas.

Temporal Cortex

Temporal cortex in squirrels is a large region that contains areas devoted to visual and auditory functions. Kaas et al. (1972) divided the region into three large fields, an anterior

temporal field, Ta, with auditory functions, an intermediate temporal field, Ti, possibly with auditory functions, and a posterior temporal field, Tp, with visual functions (Fig. 7). Ta includes the primary auditory field, A1, first identified by Merzenich et al., (1976), a rostral auditory field, R (Leutheke et al., 1988), as well as an intermediate (Ta_i) and a ventral (Ta_v) subdivisions. A redefined temporal mediodorsal region, Tm, was formerly considered to be a peripheral extension of area 19, 19p (Kaas et al., 1972), but pulvinar connections (see Fig. 1D of Robson and Hall, 1977) and architecture align this region more with Tp.

The temporal posterior region, Tp—Previously, Tp was characterized as a field with densely myelinated inner and outer bands of Baillarger (Kaas et al., 1972). In Nissl-stained sections, layer 4 is well developed. Although layer 4 is not developed to the extent seen in primary sensory areas, it is more prominent than in adjoining cortices (Figs. 6A, 7B). Tp stands out as a densely myelinated field (Fig. 7D), bordered rostrally and caudally by less myelinated fields, areas Ti and perirhinal cortex, respectively. In zinc preparations, Tp resembles primary sensory cortex in that layer 4 expresses little synaptic zinc and only moderate levels of synaptic zinc are present in outer layer 3, layer 2 and layer 5 (Figs. 6B, 7C). Tp also has features of sensory cortex in PV preparations, as layer 4 is much more darkly stained with PV-positive thalamocortical terminals than layer 4 in adjoining regions of cortex. There are also two thin PV-dense bands are present in layer 6 (Fig. 6C). In addition, Tp expresses high levels of VGluT2 in the thalamocortical terminations in layer 4 (Figs. 6E, 7E). Finally, SMI-32 processing reveals three distinct bands of labeled pyramidal cells in Tp, one in deep layer 3, one in layer 5, and another in deep layer 6 (Figs. 6D, 7F). Thus, Tp has architectonic features that are much like those of sensory cortex. Although Tp is not a primary sensory area, Tp does receive dense inputs from a caudal division of the visual pulvinar, which relays visual information from the superior colliculus (Robson and Hall, 1977).

The temporal mediodorsal region, Tm—Area Tm was previously defined as a distinct part of area 19, area 19p. We now include Tm as a separate field that has less distinct bands in layer 4 and 6 in VGluT2 preparations than adjoining area 19 and Tp, but more than in Ti (Fig. 6E). The darker appearance of Tm in zinc preparations suggests that Tm receives less dense thalamic inputs than area 19 or Tp (Fig. 6B). The SMI-32 band of smaller pyramidal cells is less densely stained in Tm than area 19 (Fig. 6D).

The temporal intermediate area, Ti—The large Ti region was originally characterized as a field of sparse myelination (Kaas et al., 1972). This feature is especially apparent in figure 7D, where a brain section in the horizontal plane was stained for myelin, allowing the adjoining myelin-dense Ta and Tp fields to be distinctly contrasted with myelin-poor Ti. In Nissl preparations, layer 4 of Ti is less dense in appearance than in Ta and Tp, as neurons are less darkly stained and packed (Fig. 7B). Thus, Ti is easily distinguished from Ta and Tp in traditional Nissl and myelin preparations.

In our sections processed for zinc, Ti expresses more synaptic zinc, especially in layers 2, 3 and 5, than Ta and Tp (Fig. 7C). As there is a moderate level of synaptic zinc present even in layer 4, much of the input to Ti must come from other cortical areas, rather than the thalamus. Ti expresses only low levels of PV (not shown) and VGluT2 (Fig. 7E). The SMI-32 preparations reveal few darkly stained pyramidal cells (Fig. 7F). Overall, Ti can be reliably distinguished from Ta and Tp. The lack of architectonic characteristics of sensory fields suggests that Ti receives relatively few inputs from the thalamus and likely functions as a higher-order processing area.

Region Ta and its subdivisions—In Nissl and myelin preparations, Ta was described as a region where a broad layer 4 was densely packed with small, darkly stained neurons,

whereas prominent outer and inner myelinated bands of Baillarger occupied inner layer 3, and layers 5 and 6 respectively (Kaas et al., 1972). However, these features were not uniform in Ta, as they were more pronounced in dorsal than in ventral Ta. Subsequently, Luethke et al., (1988) demonstrated that dorsal Ta corresponds to two primary auditory areas, the rostral area, R, and the caudal area, A1. In addition, intermediate (Ta_i) and ventral (Ta_v) divisions of Ta were identified by connections as secondary auditory areas. Our observations from Nissl and myelin preparations (Figs. 7B, 7D) agree that layer 4 is more developed in the A1 and R regions of Ta (R is actually more ventral than rostral to A1), and that A1 and R are more myelinated than other parts of Ta. Areas A1 and R are very similar in Nissl and myelin preparations. Thus, the outlines of these areas (Fig. 7A) are estimates based on the microelectrode mapping results of Luetheke et al. (1988).

In zinc preparations, A1 and R express little synaptic zinc, and layers 4, 6 and inner layer 3 are almost devoid of staining (Fig. 7C). This is expected for primary sensory cortex with dense thalamic projections from the medial geniculate complex. More ventral portions of Ta also have little synaptic zinc, although more than in A1 and R. A1 and R also show higher expression of PV than adjoining areas Ti and Pv (not shown). As layer 4 is densely stained, and layers 6 and inner 5 are moderately stained, this part of Ta stands out as a field with these PV-dense bands. Layer 3 is also moderately stained. Layer 4 of dorsal Ta also expresses more VGluT2 than adjoining areas (Fig. 7E). In SMI-32 preparations, stained pyramidal cells and their apical dendrites are densely stained in inner layer 3, outer layer 5 and inner layer 6, such that three dense bands of labeled cells are apparent (Fig. 7F).

Overall, region Ta is very distinct from surrounding cortex in a number of preparations, including those for myelin, zinc, PV and SMI-32. The dorsal part of Ta is more sharply and distinctly defined than the ventral part, but no obvious difference is detected between the territories of A1 and R in dorsal Ta.

Parietal cortex

Parietal cortex includes areas that can be considered to be primarily somatosensory in function (Figs. 8, 10). These include the parietal anterior area, Pa(S1), which corresponds to the primary somatosensory area, S1 (Sur et al., 1978). A strip of dysgranular cortex, 3a/dy, borders Pa(S1) rostrally, separating Pa(S1) from motor cortex. The parietal medial area, Pm, forms the medial half of the caudal border of Pa(S1). The parietal lateral area, Pl, of Kaas et al. (1972) is retained here, but subdivided into a rostral half that is coextensive with second somatosensory area, S2 (Nelson et al., 1979), and a caudal half that has uncertain functions. The parietal ventral area, Pv, just ventral to S2, is a secondary somatosensory area first identified in squirrels (Krubitzer et al., 1986).

Anterior parietal cortex, Pa or S1—Pa(S1) is the largest division of the parietal cortex. The area has all the characteristic features of a primary sensory cortex, but the area is also not homogenous in structure. Instead, Pa(S1) is disrupted by zones of dysgranular cortex that relate to the way the contralateral body surface is represented in S1 (Sur et al., 1978; Krubitzer et al., 1986; Gould et al., 1989). In brief, a large, circular dysgranular zone with narrow rostral extensions separates the representation of the forepaw from that of the face (Figs. 8A, B, C). A second narrow ventral extension separates the representation of the upper lip from that of the lower lip. The large circular part of the dysgranular zone was termed the unresponsive zone (UZ) in microelectrode recording experiments (Sur et al., 1978), as neurons in this zone failed to respond to light tactile stimulation in anesthetized squirrels. The location of the UZ is indicated on the illustrations of the cortical areas on the squirrel brain in Fig. 6F and other subsequent figures. In all preparations, the UZ and its narrow extensions have the histological features of dysgranular cortex rather than primary

sensory cortex. As such, it is possible to consider this dysgranular cortex as outside of S1, and part of area 3a/dy. However, both S1 proper and the embedded dysgranular zone are included here as parts of Pa(S1).

In addition to the UZ, and its rostral and ventral extensions, brain sections cut parallel to the surface of flattened cortex reveal a modular organization that is similar to that described in rats (Dawson and Killackey, 1987; Remple et al., 2003), but not as clearly expressed (also see Woolsey et al., 1975). These modules constitute small zones where CO (Fig. 8D), or PV (Figs. 8C, E) is densely expressed. These zones are separated by narrow septa, where little CO or PV is expressed, as in the UZ and its extensions. In rats, such modules correspond to semi-isolated groups of body surface mechanoreceptors related to individual whiskers and other body hairs, as well as segregated parts of the body, such as pads on the palm and segments of digits. In squirrels, a correspondence of specific CO or PV modules in Pa(S1) with receptor groups in the skin has not yet been established, but they exist in the regions representing mystacial vibrissae and the hairs of the buccal pad (upper lip) and lower lip. In rats, and other rodents, the modules representing individual mystacial vibrissae are called barrels (Woolsey and Van der Loos, 1970).

Previously, Pa(S1) has been described from Nissl-stained sections as having a distinctive layer 4 that is densely packed with darkly stained cells, and darkly stained outer and inner bands of Baillarger in sections stained for myelin (Kaas et al., 1972). In agreement with these earlier findings, Pa(S1) proper has a thick layer 4 that is densely packed with small cells (Fig. 9A). This feature is more pronounced in Pa(S1) than in adjoining cortical areas. Thus, a border between Pa(S1) and Pm is obvious in Nissl-stained sections (Fig. 10B, 13A). A similar distinction is apparent between Pa(S1) and the dysgranular cortex along the rostral border of Pa(S1) (Fig 11B). The transition from Pa(S1) to Pv is somewhat different, in that layer 4 is somewhat thinner, but also denser in Pv (Fig. 12B). In sections stained for myelin, the inner and outer bands of Baillarger are darker in Pa(S1) than in adjoining cortex (Fig. 12C). Pa(S1) can also be seen as more densely myelinated than surrounding cortex in favorable sections cut parallel to the surface of flattened cortex, whereas the UZ and its ventrolateral extensions are less myelinated and resemble 3a/dy (Figs. 8A, B).

In brain sections processed for synaptic zinc, Pa(S1) clearly stands out as a primary sensory area. A broad middle zone, corresponding to layer 4 and the deepest part of layer 3, expressed little synaptic zinc, indicating that many of the synaptic terminals in these layers belong to zinc free inputs from the thalamus (Figs. 10C, 11C, 12D, 13B). Pa(S1) is known to receive dense inputs from the ventroposterior nucleus (Krubitzer and Kaas, 1987). A narrower layer 4 stains darker in adjoining cortex, indicating more synaptic zinc and fewer thalamic inputs. A comparative reduction of synaptic zinc was also apparent in layer 6 of Pa(S1), indicating the presence of more thalamic inputs to this layer in Pa(S1) than in adjoining areas.

Pa(S1) is apparent as an area with a denser expression of PV in layer 4 than neighboring areas. This feature of Pa(S1) is best seen in the low magnification photomicrograph in Fig. 9E (also see Figs. 11D, 13C), where labeled thalamic afferents form a band in layer 4 and to a lesser extent in inner layer 3, as well as bands in layers 5 and 6. Distribution of PV-positive GABAergic neurons and their neuropil does not differ much between Pa(S1) and other areas. Pa(S1) expresses more VGluT2 in layer 4 than in adjoining cortex (Figs. 9D, 12F, 13E), but a clear difference between Pa(S1) and adjoining sensory areas (S2 and Pv) is not always apparent. In Pa(S1), the SMI-32 antibody labels pyramidal neurons and their apical dendrites in inner layers 3 and layer 5, so that two distinct bands are apparent (Fig. 11E, 12E, 13D). A deeper staining of neurons in layer 6 may be apparent in some

preparations (Fig. 12E). Overall, Pa(S1) does not stand out from adjoining parietal areas in SMI-32 preparations.

When viewed at higher magnification, the various preparations used in the present study reveal several obvious sublayers in Pa(S1) (Fig. 9). The Nissl-stained section shows that layer 4 is densely packed with small granule cells, whereas the adjoining sublayer 3c is less densely packed with cells than either layer 4 or the outer layer 3. This situation is similar to that observed in area 17 (Fig. 5A). Likewise, the dense myelination of the outer band of Baillarger is clearly co-extensive with sublayer 3c as defined in Nissl preparations, which is again similar to that of area 17 (Fig. 3B). As with other sensory areas, CO expression is most dense in layer 4 of Pa(S1), but layer 6a is also dense. PV-positive neuropil is nicely concentrated in layer 4, reflecting the terminations of PV-positive relay cells in the ventroposterior nucleus, whereas less dense neuropil staining is observed in layers 5b and 6b. VGluT2 neuropil densely populates layer 4, while extending somewhat into inner sublayers of layer 3, suggesting the presence of thalamic inputs, in addition to those from the ventroposterior nucleus. Pa(S1) also receives inputs from the posteriomedial nucleus (Krubitzer and Kaas, 1987), which possibly contributes to the VGluT2-positive staining in layer 3. The synaptic zinc-poor regions of Pa(S1) also suggest a distribution of thalamocortical terminations that is broader than layer 4, as the deeper sublayers of layers 3 and 6 are zinc-poor, whereas layers 2, outer 3 and 5B are synaptic zinc-rich. Layer 4 is CB-poor (Fig. 9F).

In summary, Pa(S1) is characterized by histological features that are typical of primary sensory cortex, including a thick layer 4 that is densely packed with small cells, and prominent inner and outer bands of Baillarger in myelin stains. The zinc stain reveals a layer 4 with little synaptic zinc and zinc poor bands in layer 6. The PV-positive thalamocortical afferents terminate in a similar laminar pattern. Pa(S1) also demonstrates specializations not found in other primary sensory areas, including a large dysgranular zone (UZ), with radiating dysgranular septa that separate the representations of body parts that are adjacent in S1, but separated on the receptor sheet (skin). Similar separating septa have been described in S1 of various mammals (see Qi and Kaas, 2004, for review). In addition, a modular organization in parts of S1, best seen in brain sections cut parallel to the surface, corresponds to those seen in the barrel field and other parts of S1 in rats and other rodents.

Area Pm—The parietal medial area, Pm is a subdivision of cortex between Pl rostrally, area 19 caudally, limbic L medially, and S2/Pl, laterally. In general, Pm lacks distinctive characteristics, as with other secondary or higher-order sensory fields. Due to the lack of marked identifying features, Pm possibly contains more than one functional division. In Nissl preparations, layer 4 is thinner and less pronounced than in Pa(S1) (Figs. 10B, 13A). The Pm and limbic (L) border is marked by the lack of a distinctive laminar pattern in L in the Nissl stain, whereas the lateral border with the parietal lateral area (Pl/S2) shows an increase in the thickness of layer 4 in Pl/S2. Pm expresses more synaptic zinc than Pa(S1) (Figs. 10C, 13B), especially in layer 4, but also in layers 3 and 6. However, Pm has similar levels of synaptic zinc with area 19, except in layer 6 where Pm has a slightly increased synaptic zinc expression. In VGluT2 preparations, Pm is distinct from area L, as layers 4 and 6 of area L express much less of the vesicle glutamate transporter protein (Fig. 13F). Layer 3 stains less darkly for PV in Pm than in either Pa(S1) or L, and outer layer 6 is more darkly stained in L than Pm (Fig. 13C). Pl/S2 has a darker, more prominent inner layer 3 in PV stain than Pm. In most preparations, Pm has obvious borders with L and Pa(S1), a reasonably clear border with Pl/S2, and a somewhat uncertain border with area 19.

Pl(S2) and Pv—The second somatosensory area, S2, occupies much of Pl, whereas the more ventrally located Pv constitutes an additional somatotopic representation of the

contralateral cutaneous mechanoreceptors (Krubitzer et al., 1986). In Nissl preparations, Pl/S2 has a thinner layer 4 than Pa(S1) and with a lower packing density of cells in both layer 4 and layer 6 (Fig. 13A). In myelin preparations, Pl/S2 has a more distinctive outer band of Baillarger than area 19, but is less myelinated overall than Pa(S1) (not shown). The lateral border between Pl/S2 and Ti stands out clearly with a decrease in myelination in Ti and an increase in myelination in A1 (not shown). In the zinc stain, Pl/S2 has more synaptic zincexpression in all layers than Pa(S1) (Fig. 13B), suggesting a greater proportion of cortical inputs. However the zinc staining is not homogenous, as the caudal part of Pl/S2 shows an increase in zinc staining across the layers. The border between Pl/S2 and area 19 is marked by the increase in zinc staining especially in the supragranular layers in Pl/S2. In the VGluT2 preparations, Pl/S2 show staining in layers 4 and 6 that is as pronounced as that in Pa(S1) (Fig. 13E). The pyramidal cells in inner layer 3 of Pl/S2 are less darkly stained in SMI-32 preparations than in Pa(S1) (Fig. 13D). In PV preparations, layer 4 of Pl/S2 is thinner and more lightly stained, whereas the outer layer 6 is more lightly stained than in Pa(S1) (Fig. 13C). A reduction in myelin stain marks the border of Pl/S2 with Ti (see Fig. 7F for the sparse myelination of Ti). With the staining preparations used here, the border between Pl/S2 and area 19 is not dependably determined. In general, most stains define Pl/S2 as an area that lacks the characteristics of a primary sensory area, allowing it to be reliably distinguished from Pa(S1) and A1.

Area Pv has a thinner layer 4 in the Nissl-stained sections (Fig. 12B) and less myelinated inner and outer bands of Baillarger in myelin-stained sections (Fig. 12C) than adjoining areas, Pa(S1) and Ta. The moderate zinc staining across the layers in Pv (Fig. 12D) suggests that Pv receives more cortical inputs, although thalamic inputs to layer 4 do exist (Krubitzer et al., 1986). Layer 4, and inner and outer layer 6 stain less darkly for PV in area Pv compared to areas Pa(S1) and Ta (Fig. 13C). Area Pv has less VGluT2 expression as well (Fig. 12F, 13E). In SMI-32 preparations, Pv is not distinct from adjoining cortical areas (Figs. 12E, 13D). The architectonic characteristics of Pv, as shown by the stains used here, are consistent with the view that the parietal ventral area (Pv) is a secondary rather than a primary sensory area.

The dysgranular strip (3a/dy)—A dysgranular strip of transition cortex, lies between the areas M and Pa(S1). As this dysgranular strip resembles area 3a of cats (Dykes et al., 1980; Felleman et al., 1983; Dykes et al., 1986; Avendaño and Verdu, 1992) and primates (Jones and Porter, 1980; Huffman and Krubitzer, 2001; Krubitzer et al., 2004) in location, shape and architectonic characteristics, we label the region 3a/dy. In Nissl preparations, 3a/dy combines, in a muted form, some of the laminar characteristics of Mand Pa(S1). A layer 4 of granular cells is present in 3a/dy, but it is less pronounced than in Pa(S1). Layer 5 pyramidal cells are larger in 3a/dy than in Pa(S1), but not as large as in M. Layer 5 of 3a/dy is also much thinner than that of M(Fig. 11B). Layer 3 of 3a/dy is less myelinated than Pa(S1) (Fig. 14D). In the zinc stain, 3a/dy has more staining than Pa(S1) in layers 4 and 5, although the intensity of staining in those layers is lower than that of M(Figs. 11C; 14C; 15C). Area 3a/dy also has less dense staining of layers 4 and 6 in sections prepared for PV (Figs. 11D; 15D) and VGluT2 (Fig. 14E) than Pa(S1). However, in the more lateral sections, dy showed concentrations of PV stain in layer 4 and inner 3, and inner and outer layer 6, similar to, but to a lesser extent, the tri-banded appearance of Pa(S1) in PV preparations. This results in a more distinct border between dy and M, as dy shows higher PV expression in those layers than M (Fig. 15D). In layer 5 of dy, pyramidal cells immunoreactive for the SMI-32 antibody had larger cell bodies and shorter apical dendrites than those in Pa(S1) (Figs. 11E, 14F).

Frontal cortex

The frontal cortex in squirrels (F) was not subdivided by Kaas et al. (1972). Here we divide frontal cortex into an “agranular” primary motor field (M) and the remaining frontal cortex (F). In rats, a complete motor map (Hall and Lindholm, 1974; Neafsey et al., 1986; Brecht et al., 2004) has been cytoarchitectonically matched to lateral agranular cortex (AGl), which is characterized by the absence of a granular layer 4 (Donoghue and Wise, 1982; Wise and Donoghue, 1986; Li et al., 1990; Neafsey, 1990). In squirrels, electrical stimulation of neurons in the caudal part of the frontal cortex with microelectrodes produced movements of different body parts, but these results were not illustrated (Sur et al., 1978). However, accesses to these and more recent microstimulation results from motor cortex of squirrels in our laboratory indicate that M as defined here corresponds closely to the extent of primary motor cortex, M1. Rats also have a second motor area on the rostromedial border of M1 (Neafsey et al., 1986), as well as ventrolateral (orbital) and medial prefrontal regions (Öngür and Price, 2000). These regions are only briefly described in squirrels here.

Area M—In Nissl preparations, area M is characterized by the lack of a distinct layer 4 (although a thin layer 4 seems to be present), a much thicker layer 5 than the surrounding cortex, and large cell bodies in layer 5 (Fig. 11B). In myelin preparations, area Mis less densely myelinated than caudally located 3a/dy and Pa(S1), and the bands of Baillarger are less distinct (Fig. 14D). Area Mexpresses high concentrations of synaptic zinc in layers 3, 5 and 6. Layers 3 and 4 of area M have more zinc staining than the adjoining 3a/dy and Pa(S1) cortex (Figs. 11C, 14C). The presence of zinc staining in the middle layers of area M in squirrels, is not surprising. In addition to receiving synaptic zinc-free inputs from the ventrolateral (VL) complex of the thalamus, the motor cortex in squirrels receives zinc-positive cortical inputs from areas such as S1, 3a/dy, and Pv (Krubitzer et al., 1986). Area Mhas reduced PV-immunopositive terminations in middle layers compared to the cingulate cortex located medially, but less PV staining than in Pa(S1) (Fig. 15D). Middle layers of area M stain lighter in sections prepared for VGluT2 than in area 3a/dy and area Pa(S1), as expected of the poorly developed granular layer 4 of area M. Layer 5 and inner layer 6 of area Mshow SMI-32 stained pyramidal cells with large cell bodies, a characteristic of motor areas (Fig. 11E).

In summary, area Mcan be distinguished from 3a/dy and Pa(S1) by the lower levels of myelin present in area M, a thin and indistinct layer 4, and a thick layer 5 with large pyramidal cell bodies. As expected from a poorly developed layer 4, there is less expression of PV and VGluT2 in the neuropil of middle cortical layers than in sensory areas. Unlike sensory cortices, area Mhad some zinc staining in layer 4, likely due to the presence of cortical inputs from other areas, such as S1.

The remaining frontal areas—We have simply defined a large frontal (F) region rostral and medial to area Mthat is not sharply distinguished from area M. The frontal region extends to the border of anterior cingulate cortex (Fig. 17A). Frontal cortex likely includes a granular rostral motor area (Neafsey et al., 1986), as well as medial and orbital prefrontal areas of rats (Öngür and Price, 2000). The borders between these proposed divisions were difficult to identify in our preparations and thus were left unmarked. There are, however, some cytoarchitectonic differences between the frontal and motor cortices. In Nissl preparations, the rostromedial border of area Mwith the frontal cortex is marked by the emergence of a well-developed layer 4, packed with granular cells, and a thinner layer 5 then in area M (Figs. 14B, 15B, 16A). Area F also has better defined cortical layers in Nissl preparations than the adjoining cingulate areas (Figs. 14B, 15B). In the myelin stain, there is no distinct difference between area F and M, whereas there is slightly increased myelination in area F than in the adjacent cingulate areas (Figs. 14D, 17D). The zinc stain in area F is

less intense across the cortical layers than in area M and the cingulate areas, with the decrement being especially marked in layer 4 (Figs. 15C, 16B, 17E). Area F shows increased VGluT2 staining, in layer 4 compared to area M(Figs. 14E, 16D, 17C), whereas in PV preparations, area F showed denser staining in layer 4 and inner layer 3, and outer layer 6 (Figs. 15D, 16C). Area F can be distinguished from the cingulate areas by the sharp decrease in PV staining of layer 4 in the cingulate regions (Fig. 15D). The large pyramidal cells in layer 5 that were revealed by SMI-32 immunostaining in area M are not observed in area F and the expression of SMI-32 immunopositive cells in layer 3 of area F is reduced compared to area M and the rostral cingulate area (Figs. 16E, 17F).

In summary, most of the staining methods applied show differences between the frontal cortex, F, and the adjacent motor and cingulate cortex. However, the myelin stain was less useful in delimiting the borders of area F.

Cingulate and retrosplenial cortex

Cingulate and retrosplenial cortex are parts of the classical limbic system that are found in all mammals. Cingulate cortex is located along much of the medial wall of the cerebral hemisphere, and is generally divided into anterior motor-related, and posterior sensory-related divisions (Vogt et al., 1992). Retrosplenial cortex forms the most caudal part of the medial limbic cortex. The cingulate and retrosplenial cortical areas receive inputs from the anterior and lateral dorsal nuclei of the thalamus (Jones, 2007). A comparison of the different nomenclature used for areas of cingulate and retrosplenial cortex can be found in Jones et al. (2005).

Cingulate cortex—Early investigators divided cingulate cortex into areas somewhat differently and used different nomenclatures in mice (Rose, 1929) and rabbits or ground squirrels (Brodmann, 1909). Those of Rose were retained by Domensick (1969) in studies using rats, whereas Vogt and Peters (1981) favored Brodmann's terminology. The three divisions identified in rats by Zilles and Wree (1995), cingulate areas 1, 2, and 3, are respectively identified here as dorsal (DCg), ventral (VCg) and rostral (RCg) subdivisions of the cingulate cortex in squirrels. DCg roughly corresponds to area 24b of Vogt and Peters (1981), VCg to much of area 24a, and RCg to the rostral part of 24a and adjoining area 32. The cingulate cortex of squirrels encompasses the rostral half of the cortex along the medial wall of cerebral hemisphere (Fig. 17A).

Dorsal cingulate area (DCg)—In Nissl preparations, DCg has a layer 2 that is densely packed, an indistinct layer 4, and a population of relatively large cell bodies in layer 5 (Fig. 16A). In myelin-stained sections, DCg is lightly myelinated with a faint outer band of Baillarger (not shown). Layer 2 of DCg is darkly stained for synaptic zinc ions compared to the adjoining frontal cortex (Fig. 16B) in zinc preparations. Layer 4 and inner layer 3 of DCg have increased staining in VGluT2 prepared sections compared to the frontal cortex and the ventrally adjacent cingulate region (Fig. 16D). In SMI-32 immunostained sections, DCg shows darkly stained pyramidal cell bodies in layer 5 that are larger than those in the frontal cortex (Fig. 16E) and a band of SMI-32 stained pyramidal cell neuropil in layer 3 that terminates at the DCg/RCg border (Fig. 16E).

Ventral cingulate area (VCg)—VCg is bordered dorsally by DCg, rostrally by RCg, and caudally by the retrosplenial cortex. In Nissl-stained sections, layer 2 of VCg has a higher packing density of cells and a thinner layer 5 than in DCg and inner layer 4 is very cell sparse (Figs. 14B, 15B, 17B). VCg shows higher myelination than RCg and can be delimited as such (Figs. 14D, 17D). VCg shows very dark zinc staining of layer 2 and slightly lighter zinc staining in outer layer 5 (Figs. 14C, 15C, 17E). Layers 4 and inner 3 of

VCg have moderate levels of synaptic zinc (Figs. 14C, 15C, 17E), suggesting the presence of cortical afferents. The level of zinc staining in VCg is higher than in DCg, but lower than in RCg (Figs. 14C, 15C, 17E). VCg shows a double banded staining pattern in sections prepared for PV, the outer band in layers 3 and 4, and the inner band in outer layer 6 (Fig. 15D). In VGluT2 immunostained sections, VCg shows light staining in layer 4 and 6 (Figs. 14E, 17C), whereas in SMI-32 immunostained sections, there are almost no stained pyramidal cells bodies in layer 3 and a very sparse population of SMI-32 immunopositive pyramidal cell bodies in layer 5 (Figs. 14F, 17F).

Rostral cingulate area (RCg)—In Nissl-stained sections, RCg does not have a well-developed laminar pattern and the large pyramidal cell bodies present in layer 5 of DCg and to a lesser extent, in VCg, are almost absent in RCg (Figs. 14B, 15B, 16A, 17B). RCg is the least myelinated out of the three cingulate areas (Figs. 14D, 17D). In zinc preparations, RCg shows some staining in layer 4 (Figs. 14C, 15C, 16B, 17E) and darker staining of layer 5 than VCg (Figs. 14C, 17E). The PV immunopositive band in layer 4 of VCg is almost absent in RCg, providing a distinct border between VCg and RCg (Fig. 15D) and layer 6 of RCg stains lighter in PV preparations than that in DCg (Fig. 16C). In VGluT2 immunostained sections, RCg has a moderately dark staining of layer 4, although no clear borders of RCg can be detected in these preparations (Figs. 14E, 16D, 17C). There are almost no SMI-32 immunopositive pyramidal cells in layer 3 of RCg and very few immunostained small pyramidal cells in layer 5 (Figs. 14F, 16E, 17F).

Retrosplenial cortex—Brodmann (1909) distinguished three subdivisions of retrosplenial cortex in ground squirrels, areas 29a, 29b and 29c. More recently, Vogt and Peters (1981) described four divisions (29a, b, c and d), and Domensick (1969) described only agranular and granular divisions in rats. Here, we follow Zilles and Wree (1985) and Domensick (1969) by distinguishing two main divisions of retrosplenial cortex, a granular area, RSG and an agranular area, RSA.

Retrosplenial granular area (RSG)—In Nissl sections, RSG is characterized by a conspicuous band in layer 2 that is densely packed with deeply stained cells (Fig. 2A). The underlying granular layer appears to be part of layer 3, just over a sparse granular layer 4 (Vogt and Peters, 1981). RSG is poorly myelinated, without marked inner and outer bands of Baillarger (Fig. 18B). RSG is poorly stained in sections processed for zinc, especially in layers 3 and outer 4, which are almost free of synaptic zinc (Fig. 2B). This suggests that most of the afferents to RSG in squirrels originate from the thalamus or other subcortical structures. With the PV stain, layer 4 of RSG is light, whereas layers 2 and 3 are very dark. Layer 6 has moderate staining, giving rise to a banded appearance (Fig. 6C). RSG shows a dark staining of layer 3, outer layer 4 and inner layer 6 in the VGluT2 stain (Fig. 6E). In SMI-32 prepared sections, RSG shows light staining of pyramidal cells in outer layer 3, some staining of pyramidal cells in inner layer 5, somewhat more stained pyramidal cells in outer layer 6, forming a tri-banded staining pattern as well (Fig. 6D). Layer 4 of RSG is immunopositive for the LAMP antibody, as well as layer 6, though to a lesser extent. The expression of LAMP in RSG is less compared to the ventrally adjacent subicular areas, but the LAMP-positive band in layer 4 of RSG is thicker than that in RSA (Fig. 18C).

Retrosplenial agranular area (RSA)—The retrosplenial agranular area neither shows well-defined laminar differentiation nor a developed granular layer 4 in the Nissl stain (Figs. 2A, 6A). RSA is poorly myelinated and has no obvious bands of Baillarger detected (Fig. 18B). In sections prepared for zinc, RSA shows higher intensity of staining, especially of layer 3, than RSG (Figs. 2B, 6B), suggesting that RSA receives more cortical afferents than RSG. There is very little PV staining in RSA, except in outer layer 6 (Fig. 6C). In the

VGluT2 stain, two thin, well-stained bands are seen in layer 4 and 6 (Fig. 6E). RSA shows almost no staining of pyramidal cells in SMI-32 prepared sections (Fig. 6D). RSA expressed more staining for LAMP than the adjoining prostriata area, but less than the granular region of the retrosplenial cortex (Fig. 18C).

Area prostriata (PS)

Cortex along the medial border of area 17, the portion representing peripheral vision of the contralateral visual hemifield, has been distinguished in primates as area prostriata by Sanides (1972). In cats and in several other non-primates, the prostriata region has been called the splenial visual area (see Rosa, 1999 for review). In rats and mice, the comparable region has been called the posteromedial visual area (Wang and Burkhalter, 2007), medial area 18b (Krieg, 1946; Caviness, 1975), Oc2MM (Zilles and Wrree, 1995), or part of the agranular retrosplenial cortex (Krettek and Price, 1977). We have used the term prostriata here for this area, with visual connections and visually responsive neurons, in an effort to standardize the nomenclature, and promote comparisons with primates. Area prostriata is considered part of the limbic, rather than occipital cortex. It is described here as an area bordering area 17 that is visual in function. As with primates (see Allman and Kaas, 1971), prostriata in squirrels has an indistinct layer 4 and is poorly myelinated (Figs. 3, 6). Thus, there is little evidence of layer 4 in PV or VGluT2 preparations. Layer 2 shows dense zinc staining and SMI-32 staining disappears in layer 3.

Perirhinal areas

Cortex along the dorsal bank of the rhinal fissure has been called transitional cortex, as the six distinct layers of most of neocortex are not always apparent (Zilles and Wree, 1995). Here, we define an insular region (Ins) of cortex, just ventral and rostral to primary somatosensory cortex Pa(S1), a more caudal perirhinal (PRh) region, and a caudal entorhinal (Ent) cortex. Ins likely has functional subdivisions related to gustatory, general visceral, somatosensory, and multisensory functions (Guldin and Markowitsch, 1983; Kosar et al., 1986; Cechetto and Saper, 1987). Perirhinal and entorhinal areas relate to hippocampal memory functions (Burwell and Amaral, 1998).

The insular cortex defined here in squirrels corresponds to the agranular insular cortex of previous descriptions in rats (e.g., Kosar et al., 1986; Cechetto and Saper, 1987). The granular and dysgranular insular regions are included in the parietal region of secondary somatosensory cortex. In Nissl preparations, Ins has a darkly stained layer 2 that is densely packed with cell bodies that does not form a continuous layer. Instead, the cells form groups, or islands giving the layer a ‘scallop-like’ pattern. There is a lack of a well-developed granular layer 4 (Fig. 19B). In myelin-stained sections, the Ins area stands out as an area with almost no myelination (Fig. 19D). Ins is darkly stained in zinc preparations, especially in layers 2 and 3 (Fig. 19C), indicating that most of the input is from other cortical areas. The laminar staining pattern in the Ins region is uniform in PV (not shown), VGluT2 (Fig. 19E) and SMI-32 (Fig. 19F) immunostained sections.

In Nissl preparations, the perirhinal (PRh) cortex does not have a distinct laminar pattern. However, layer 2 stands out due to the densely packed, Nissl-stained cell bodies that form a continuous layer (Figs. 18B, 19B, 20B). This feature allows the differentiation of PRh from the Ins cortex (Fig. 19B). Like the Ins area, PRh is very poorly myelinated (Figs. 18B, 19D) and does not have distinct laminar patterns in the PV (Fig. 20D), VGluT2 (Fig. 19E) and SMI-32 (Fig. 19F) immunostained sections. Area PRh, being part of the limbic cortex, expresses a higher amount of the LAMP antibody compared to surrounding cortical areas (Fig. 18C).

Entorhinal cortex in rats is generally divided into lateral and medial areas (Blackstad, 1956; Hevner and Wong-Riley, 1992). In the entorhinal cortex of squirrels, we distinguish the lateral (LEnt), intermediate (IEnt) and medial (MEnt) entorhinal areas. In Nissl-stained sections, all three areas have almost no cell bodies in layer 4 (Figs. 19B, 20B). Layer 2 of LEnt shows higher packing density of cell bodies than IEnt, whereas in MEnt, the cells in layer 2 are grouped into 'islands' in Nissl preparations (see Figs. 19B, 20B). The entorhinal cortex has very low levels of myelination, with MEnt having the lowest level of myelination (not shown). Layer 2 of the MEnt region stains darkly for synaptic zinc, IEnt has much lighter staining and LEnt has the lowest levels of staining (Fig. 19C). In PV immunostained sections, layer 2 of LEnt has the darkest staining, followed by MEnt and IEnt as the most lightly stained region (Fig. 20D). MEnt has lighter staining through the layers than IEnt and LEnt in VGlut2 immunostained sections (Fig. 19E). SMI-32 immunopositive pyramidal cells are present in the upper cortical layer of LEnt and IEnt, and in the lower cortical layer of MEnt (Fig. 19F).

DISCUSSION

The focus of the present research effort was to provide an improved overview of how the neocortex in squirrels is subdivided into areas, the 'organs' of cortex (Brodmann, 1909). Just as how the early taxonomic system of Linnaeus was fundamental to the subsequent advances in the field of biology, the efforts of Brodmann (1909) and other early neuroanatomists in dividing cortex into a patchwork of areas with supposed functional significance usefully guided following generations of neuroscientists. The classification scheme of Linnaeus (c.f. Benton, 2005) was corrected and extended by subsequent research. Likewise, the early architectonic cortical maps of many studied mammals have been revisited and altered as a result of further study. Here we present a revised interpretation of how the neocortex is organized in the common grey squirrel, based on our study of an extensive battery of histological preparations. The results are expected to provide a more detailed and accurate portrayal of how the neocortex of squirrels is subdivided into areas, as squirrels, with their well-developed visual system, have become useful in neuroscience research (Van Hooser and Nelson, 2006; Kaas, 2002). In addition, these results on the well-differentiated areas of the squirrel cortex reflect on theories of how the cortex of other rodents, in particular the extensively studied rats and mice, is subdivided, as the brains of various rodents likely resemble each other in how they are organized. Thus, our broader goal is to understand what features of cortical organization are shared by the various species of rodents, and how the differences that do exist evolved. The present results are discussed in relation to previous architecture studies, especially on rodents, and other portrayals of the areal organization of cortex.

Most architectonic studies in rodents, such as rats and mice, employed the use of Nissl, myelin, and occasionally the acetylcholinesterase stains to subdivide the neocortex (e.g., Krieg, 1946; Caviness, 1975; Swanson, 1992; 2003; Zilles and Wree 1985, 1995; Paxinos and Franklin, 2003; see Kaas et al., 1972 for squirrels). However, the potential use of other histochemical procedures now provides a richness that can greatly enhance architectonic studies. Thus, the immunoreactivity and staining patterns produced by antibodies, such as VGluT2 (Nahami and Erisir, 2005), PV (Condé et al., 1996; Budinger et al., 2000; Cruikshank et al., 2001), and SMI-32 (Voelker et al., 2004; Boire et al., 2005) have been analyzed in the cortex of rodents, and there is a chemoarchitectonic atlas for rats (Paxinos et al., 1999). Yet, variations in staining patterns produced with these antibodies have not often been used as criteria for parcellating the neocortex. Similarly, the distribution of zinc-enriched terminals has been described in the neocortex of rodents, such as mice (Garrett et al., 1991; Brown and Dyck, 2004; Czupryn and Skangiel-Kramska, 1997), rats (Ichinohe et al., 2003; Miro-Bernie et al., 2006), and in the visual cortex of parma wallabies (Garrett et

al., 1994). These zinc-enriched terminals originate from a subset of glutamatergic neurons in the neocortex, as well as neurons in the claustrum and amygdala, and they are not found in terminals of neurons that originate in the thalamus (Danscher, 1982; Frederickson and Moncrieff, 1994; Frederickson et al., 2000, Ichinohe et al., 2003; Ichinohe and Rockland, 2004). Of course, all cortical areas get thalamic inputs, and layer 4 of all areas has intrinsic connections that presumably use zinc ions. Nevertheless, cortical areas, and especially layer 4, vary greatly in zinc expression, and a high density of zinc-stained terminals in layer 4 of any cortical area likely reflects a dominance of corticocortical inputs, whereas a low density suggests a dominance of thalamocortical inputs. As such, the zinc stain that reveals these zinc-enriched terminals can act as a marker that allows a parcellation of cortical areas based on differences in the proportions of cortical and thalamic inputs to layer 4. Thus, we have used VGluT2, PV, and synaptic zinc, as well as Nissl, myelin, SMI-32, LAMP, CB and CO preparations in our study of cortical architecture in squirrels.

Visual areas of occipital cortex

Area 17—The occipital cortex of squirrels contains three large areas, areas 17, 18 and 19 after Brodman (1909). These designations and the boundaries of these areas have been retained from Kaas et al., (1972). Area 17 is an area common to most, if not all mammals, and it is especially well developed in squirrels. The area is large, extending from the dorsomedial surface of the hemisphere, along the cortex of the medial wall and onto the cortex of the ventral surface. As with other mammals, area 17 of squirrels contains a systematic representation of the contralateral visual hemifield (Hall et al., 1971) and projects to the other occipital fields, areas 18 and 19 (Kaas et al., 1989). Area 17 is thicker and more developed in its lateral, binocular portion (Hall et al., 1971). Area 17 is bordered on the ventral surface by a subdivision of the cortex that may correspond to the visual limbic area, or prostriata, of primates and other mammals (Sanides, 1970; Rosa et al., 1997; Morecraft et al., 2000). The longer border of area 17, on the dorsolateral surface and extending onto the medial wall and the posterior pole of the hemisphere, is with area 18 (V2). Area 17 has a sharply defined layer 4 of densely packed granule and stellate cells, with suggestions of sublayers, as described previously (Kaas et al., 1972). The area is also very distinct in most preparations. Here we described the characteristics of area 17 of squirrels for the first time in sections processed for parvalbumin, SMI-32, VGluT2 and synaptic zinc. Layer 4 stands out in these preparations as a layer conspicuously poor in zinc, and densely expressing PV and VGluT2.

The low level of synaptic zinc in layer 4 of area 17 is consistent with the evidence that thalamocortical terminations do not have synaptic zinc, and that layer 4 of area 17, as a primary sensory area, receives dense thalamic inputs from the lateral geniculate nucleus of the dorsal thalamus, and few other inputs (e.g., Casagrande and Kaas, 1994; see Robson and Hall, 1975; Weber et al., 1977 for lateral geniculate projections to area 17 in squirrels). In addition to the low level of synaptic zinc expression in layer 4, layer 3 and outer layer 5 have considerably less synaptic zinc than the corresponding layers in extrastriate cortex (Fig. 4C). This implies that these layers also receive a high proportion of inputs from the thalamus. In squirrels, the lateral geniculate nucleus projects densely to layer 4, and much less densely to the outer half of layer 6 (Robson and Hall, 1975). These less dense terminations in layer 6 may account for most or all of the thalamic input to this layer that results in the reduction of the presence of synaptic zinc. In these earlier studies in squirrels, there was no evidence for notable lateral geniculate projections to layer 3, although such projections may exist as they do in primates (Casagrande and Kaas, 1994). Another source of thalamic projections to superficial layers of area 17 in mammals is from nuclei of the pulvinar complex (Kaas and Lyon, 2007). Although the cortical projections of pulvinar nuclei in squirrels have been studied in the past (Robson and Hall, 1977), and projections to

area 17 have not been directly demonstrated, they likely exist. Lesions of visual cortex that are confined to area 17 (Kaas et al., 1972) do not cause retrograde degeneration of nuclei in the pulvinar complex of squirrels, indicating that any projections to area 17 would have sustaining collaterals to other visual areas. If areas 18 and 19 are included in the cortical lesions, the anterior half of the pulvinar becomes massively degenerated. Possibly the anterior pulvinar in squirrels also projects to area 17, thereby accounting for the reduction of synaptic zinc in layer 3.

Area 17 of squirrels resembles area 17 of other rodents in its general location, architectonic features, and retinotopic organization, but area 17 of other less visual rodents is smaller and less distinctly differentiated. Area 17 and other areas have been repeatedly described in rats (Krieg, 1946; Swanson, 1992; 2003; Zilles et al., 1980; 1984; Reid and Juraska, 1991), and mice (Rose, 1930; Caviness, 1975; Paxinos and Franklin, 2003; Van der Gucht et al., 2007), and less frequently in other rodents, such as guinea pigs (Rose, 1912), hamsters (Lent, 1982; Dursteler et al., 1979) and agoutis (Picanço-Diniz et al., 1989). In a surface view, brain sections cut parallel to the cortical surface, and processed for cytochrome oxidase activity, or most other markers, area 17 is one of the most easily recognized and delimited areas of the mammalian brain. Here, we defined area 17, distinguished binocular and monocular sections of area 17, and described layers and significant sublayers of area 17.

Area 18—The concept of a medial area 18 (18b) and a lateral area 18 (18a) in rodents comes from Krieg (1946) in answer to a dilemma. In squirrels and rabbits, Brodmann (1909) described an area 18 along the medial border of area 17, but other areas, rather than area 18, were placed along the lateral border of area 17. At least in the squirrel, it seems likely by location that Brodmann was identifying the thinner, less-developed, monocular portion of area 17 as area 18. Rose (1912) soon followed with descriptions of an area 17 bordered medially, but not laterally, by an area 18 in guinea pigs and mice. The position of this medial area 18 was subsequently recognized as incompatible with the location of Brodmann's area 18 in carnivores and primates, and thus Krieg (1946) added a lateral area 18 to the cortex of rats. In modern studies of rodents, the medial "area 18" usually corresponds to the limbic visual area, prostriata (Sanides, 1970), also identified as the splenial visual area (Kalia and Whitteridge, 1973), rather than a part of area 18 (See Rosa, 1999 for review). Somewhat differently, cortex along the medial margin of area 17 has been divided into several proposed visual areas in mice and rats (e.g., Van der Gucht et al., 2007; Wang and Burkhalter, 2007). In either case, the medial region is not area 18 of other mammals, and the misidentification of this cortex as area 18 should be discouraged. As Krieg (1946) recognized, the proposed medial area 18 (18b) and the lateral area 18 (18a) do not resemble each other histologically.

In the present study, we used our battery of histological stains to characterize a highly distinct band of cortex along the lateral border of area 17. The location of this band, along the complete representation of the zero vertical meridian of area 17, corresponds to the second visual area, V2 (Hall et al., 1971), as it does in a wide range of mammals, including carnivores, primates, and fruit bats (see Rosa and Krubitzer, 1999, for review). Area 18 in squirrels was defined earlier in Nissl and myelin preparations (Kaas et al., 1972). In Nissl preparations, layer 4 and 6 are less densely stained than in adjacent areas, giving the appearance of less distinct lamination. The increase in zinc staining in layer 4 and other layers of area 18 is marked (Fig. 4C), consistent with the evidence that layer 4 of area 18 gets a massive input from area 17 (Kaas et al., 1989). However, the lateral geniculate nucleus does provide some thalamic input to layer 4 of area 18 in squirrels (Weber et al., 1977), and inputs to the supragranular layers are likely to originate from the pulvinar complex. The adjoining area 19 has somewhat more synaptic zinc, suggesting less thalamic input. There is no evidence for significant geniculate projections to area 19. Area 18 also has

a more pronounced laminar pattern of neurofilament protein staining than area 19, as does the cortex laterally adjoining area 17 in mice (Van der Gucht et al., 2007). Sections processed for VGluT2 or PV also reveal laminar differences in density of staining between areas 18 and 19. Finally, in surface-view of brain sections cut parallel to the brain surface and stained for myelin, area 18 is quite distinct as a slightly less densely myelinated strip along the outer border of area 17. However, the myelin pattern is not homogenous within area 18 (Kaas et al., 1989). Rather, the strip contains a series of six to eight 500μm wide patches along its length, indicating that area 18, as with primates (Casagrande and Kaas, 1994), has a modular organization in squirrels. This supposition is supported by the results of a study of the corpus callosum connections in squirrels (Gould, 1984), as interhemispheric projections terminate broadly in area 18, while avoiding a series of patch-like regions that resemble the myelin-poor patches in size and number. It seems likely that the callosal-poor zones are those where area 17 projections are concentrated, just as with rats (Olavarria and Montero, 1984; Malach, 1989) and other rodents (Olavarria and Montero, 1989; Bravo et al., 1990).

As further support for the concept of an area 18 or V2 in rodents, an area 18 along the lateral border of area 17 has been defined architectonically in the large South American hystricomorph (related to guinea pigs) rodent, the agouti (*Dasyprocta aguti*). The area 18 is distinct in cytochrome oxidase preparations as a band of less dense staining, and characteristics in Nissl and myelin preparations are similar to those in squirrels (Picanço-Diniz, 1987; Picanço-Diniz et al., 1989). Microelectrode recordings from this area 18 revealed a simple representation of the contralateral visual hemifield, which was termed V2.

We conclude from this review of the histological evidence that area 18 is a valid subdivision of visual cortex, with a regular pattern of modular subdivisions relating to callosal and area 17 inputs. Other types of evidence support this conclusion. Most importantly, microelectrode recordings across the width of area 18 in a series of penetrations from rostral to caudal reveal a systematic representation of the contralateral visual hemifield in area 18 (Hall et al., 1971), one that conforms to the retinotopic organization of V2 of other mammals, such as cats and monkeys. Thus, there is a reversal of retinotopic order at the area 17/18 border of squirrels so that forward vision is represented along the border and successively more temporal vision is represented away from the border in both V1 and V2. Lower vision is represented ventrally and upper vision is represented caudally in both areas. Highly similar results appear to have been obtained in microelectrode mapping studies in ground squirrels (Sereno et al., 1991). A summary of the Sereno et al. (1991) study has been published in a review by Van Hooser and Nelson (2006). It shows a V2 along the lateral border of V1 with the vertical meridian represented at the V1–V2 border, peripheral vision along the outer border of V2, and the lower quadrant is rostral to the upper quadrant. This proposed organization of area 18 in cortex lateral to V1 in grey squirrels and ground squirrels is highly consistent with the connection patterns between area 17 and area 18. Injections of tracers in area 17 labeled several patches of cells in area 18, but rostral injections labeled more rostral patches than caudal injections (Kaas et al., 1989). Thus, the connection pattern was less precise than the physiologically determined V1 and V2 representations would suggest, but the anatomical and physiological patterns of organization in V2 were globally consistent.

The reason for this lengthy discussion of what seems to be an uncontroversial point is that squirrels are rodents, and a different type of organization has been proposed for cortex lateral to area 17 of rodents with a less developed visual system, such as rats and mice (e.g., Olavarria and Van Sluyters, 1982; Olavarria and Montero, 1984; 1990; Montero, 1993; Wang and Burkhalter, 2007). Thus, a series of six visual areas have been proposed along the lateral border of area 17, where V2 (area 18) is in squirrels and other studied mammals. This

proposal, based on a combination of anatomical and physiological results, is partly compatible with the classic cytoarchitecture map of mouse cortex by Rose (1930), which showed several architectonic fields along the lateral border of area 17. However, it is informative to note that Brodmann (1909) had previously failed to identify an area 18 along the lateral border of area 17 of squirrels, and instead portrayed a string of areas along this border (areas 7, 22, 21, 20 and 36). As the existence of a lateral area 18, or V2, in squirrels now seems clear, we conclude that at least the squirrel branch of the rodent radiation retained a visual area, V2 or area 18, an area that is basic to nearly all other mammals (See Rosa and Krubitzer, 1999 for review). We question whether other less visual branches of the rodent radiation abandoned this broadly conserved feature.

Not all investigators have placed a series of visual areas exist on the lateral border of area 17 in rodents. In the first extensive cytoarchitectonic and myeloarchitectonic study of cortical areas in rats, Krieg (1946) illustrated an area 18a along the complete lateral border of area 17. Subsequently, Caviness (1975) retained an area 18a lateral to area 17 in mice, as did Zilles and collaborators in several studies of rodent neocortex, with the modifications that the region of area 18a was termed occipital area 2 lateral (Oc2L) and it was extended rostrally, to include parts of Krieg's area 17 (e.g., Zilles et al., 1980; Zilles and Wree, 1995). A more recent architectonic study (Van der Gucht et al., 2007) of visual cortex in mice, based on patterns of immunoreactivity for the neurofilament protein, SMI-32, distinguished a narrow area V2L (with anterior and posterior halves) along the lateral border of V1 (area 17) that corresponds closely to the territory of V2 (area 18) expected from microelectrode mapping data (see Wagor et al., 1980; also see Tiao and Blakemore, 1976). Interestingly, Olavarria and Mendez (1979) in their microelectrode mapping study of the diurnal rodent, *Octodon degus*, illustrated a much longer lateromedial area (LM) than usual for this proposed area. This LM, though incompletely mapped, had the shape and retinotopy expected in V2. While connection patterns, and some of the microelectrode mapping results, can be viewed as supporting the proposal of six or so areas along the lateral border of area 17 (e.g., Olavarria and Montero, 1984; Montero, 1993; Olavarria et al., 1982; Olavarria and Montero, 1990; Wang and Burkhalter, 2007), sometimes in a rather convincing manner (e.g., Wang and Burkhalter, 2007), Malach (1989) concluded, in a study of area 17 connections in rats, that the cortex adjoining lateral striate cortex contains a single, global map, V2. In a similar manner, Kaas et al., (1989) suggested that the acallosal modules of area 18 in squirrels and other rodents overlap slightly in visuotopic organization, so that injections in any region of area 17 could label several, but not all modules. Thus, rostral modules in area 18 would be labeled by rostral injections and caudal modules by caudal injections. After a review of the distribution of V2 across mammalian taxa, Rosa and Krubitzer (1999) concluded that rodents have a V2, and that an elongated LM in rats and other rodents corresponds to V2.

Area 19—The third division of occipital cortex that we have defined in squirrels is area 19. This area was also retained from the earlier study of Kaas et al. (1972). Overall, area 19 is less well-defined, and therefore more questionable as a valid visual area than areas 17 and 18. However, area 19 constitutes a band of cortex that is distinctly different in architectonic appearance from area 18 and the adjoining temporal areas. Yet, presently defined area 19 may contain rostral and caudal subdivisions, as suggested by connection patterns (Kaas et al., 1989). On the other hand, area 19 is a subdivision of the cortex that has long been associated with the concept of a third representation of the contralateral visual hemifield. This seems to be the case in cats, and perhaps other carnivores, where cortex defined architectonically as area 19 corresponds to a third visual representation, one along the outer border of area 18 (V2), and forming a mirror reversal of representation in V2 (Hubel and Wiesel, 1965; Tusa et al., 1979; Albus and Beckmann, 1980). Presently, there is good evidence for such a V3 along the outer border of area 18 (V2) in primates (Kaas and Lyon,

2001), although it should be recognized that area 18 has been redefined in some primates and it does not correspond to the area 18 of Brodmann (1909). Except for the description of visual cortex in agoutis (Picanço-Diniz et al., 1989), other architectonic descriptions of the organization of occipital cortex in rodents do not include an area 19. Yet, the existence of a narrow V3, about half the width of V2, has been described in the visual cortex of ground squirrels (Sereno et al., 1991). Given the long history of uncertainties about the existence of V3 in monkeys and the difficulties in obtaining conclusive evidence (see Kaas and Lyon, 2001), it seems possible that squirrels have a V3. However, the V3 proposed by Sereno et al. (1991) would occupy only the medial half of the area 19 depicted here. For now, we know that area 19 of squirrels receives visual inputs from areas 17 and 18 (Kaas et al., 1989), and that the pattern of connections appears to be more complicated that would be expected from the retinotopy proposed for V3.

Areas of the temporal cortex

Three major divisions of temporal cortex, areas Ta, Ti and Tp, are easily distinguished in squirrels. Ta and Tp have histological characteristics of sensory cortex, whereas Ti has the features of a secondary field. Thus, Ta and Tp have a conspicuous layer 4 of granule cells, dense myelination, express little synaptic zinc, have three obvious bands of stained pyramidal cells in SMI-32 preparations, and a darkly stained layer 4 in VGluT2 and CO preparations. In marked contrast, Ti lacks these distinguishing features. Ta, Ti and Tp were previously recognized by Kaas et al. (1972) in squirrels, and these three subdivisions of temporal cortex are retained here. We have also added a fourth subdivision, Tm.

Area Ta—The sensory nature of Ta is known, as it contains two primary auditory fields, A1 and R, as wells as several secondary auditory fields (Luetheke et al., 1988; Merzenich et al., 1976). In our unpublished studies of temporal cortex connections in squirrels, injections in Ta labeled neurons in the medial geniculate complex of the dorsal thalamus. Although Ta is not uniform in appearance, we were unable to reliably distinguish differences in architecture between the auditory fields contained within Ta. However, in brain sections cut parallel to the flattened cortex, the core areas, A1 and R, do appear to be slightly more myelinated than the rest of Ta (Krubitzer et al., 1986). In such myelin-stained, flat-mounted sections from the brains of ground squirrels, Ta has been identified as such (Slutsky et al., 2000), or simply referred to as auditory cortex (Paolini and Sereno, 1998).

There is no complete agreement on how auditory cortex is divided into areas across rodent taxa, but all rodents appear to have at least two core or primary-like areas, as well as a number of associated secondary fields (e.g., Wallace et al., 2000; Thomas et al., 1993; Rutkowski et al., 2003; Polley et al., 2007). The core areas generally include an area identified as A1, and a more rostral area, the anterior auditory field. These areas receive inputs from the ventral nucleus of the medial geniculate complex, as well as other subdivisions (Ryugo and Killackey, 1974). These areas, and possibly adjoining auditory areas, have been included in an architectonic zone that has the sensory characteristics of Ta in squirrels. The region was termed *area auditoria* or area 41 in rats by Krieg (1946). Caviness (1975) described a similar area 41 in mice. Zilles and colleagues called the same region Te1 (temporal area 1) in rats (Zilles et al., 1980; Zilles and Wree, 1995). Given the distinctiveness of the auditory region, it is surprising that the region was not recognized in rodents by Brodmann (1909) or Rose (1930). Although Ta, area 41, or Te1 correspond to auditory cortex, the field includes at least two core areas and likely several secondary areas.

Area Tp—Area Tp is the other subdivision of temporal cortex in squirrels with architectonic characteristics suggestive of a core sensory field. This is a very distinct area in squirrels and has been delimited in a number of previous studies (Kaas et al., 1973;

Krubitzer et al., 1986; Paolini and Sereno, 1998; Kaas et al., 1989; Slutsky et al., 2000). A comparable area Tp has been described in the agouti, identified by its dense myelination and ventroposterior position (Picanço-Diniz, 1987; Picanço-Diniz et al., 1989). Microelectrode recordings from Tp of agoutis indicate that the area responds to visual stimuli and possibly has a retinotopic organization. The source of the activating visual input to Tp of squirrels is uncertain. It appears to get no input from area 17 and, at best, sparse inputs from area 18. However, Robson and Hall (1977) demonstrated a dense projection from the caudal part of the pulvinar complex to Tp in squirrels, and this subdivision of the pulvinar that receives inputs from the retinal-recipient layer of the superior colliculus. Thus, a relay from the retina to the superior colliculus, followed by the pulvinar, and finally to Tp, likely provides activating input to Tp. The superior colliculus of squirrels is about ten times larger than expected for a rat of similar size (Kaas and Collins, 2001), and it provides a massive input to the caudal pulvinar. As removal of all of area 17 in squirrels fails to completely abolish the components for visual discrimination (Levey et al., 1973; Kicliter et al., 1977; Wagor, 1978), a pathway from the superior colliculus to the cortex via the pulvinar may be the source for most of the preserved visual abilities. While considerable vision remains after a loss of primary visual cortex in such a diverse array of mammalian species such as cats, monkeys, tree shrews, and humans (see Payne et al., 1996 for review), the role of a pathway from the superior colliculus to cortex in preserving visual abilities remains uncertain (Fendrich et al., 2001).

No visual area comparable to Tp has been described in rats and mice. Krieg (1946) considered temporal cortex caudal to auditory cortex in rats to be poorly developed and of uncertain identity. The caudal division of temporal cortex of Zilles and Wree (1985), Te2, would seem to occupy the position of both Ti and Tp of squirrels, but the low level of myelination of Te2 and evidence of auditory functions suggest that this region more closely corresponds to Ti than Tp. Quite possibly, rats and mice, with less developed visual systems, have little cortex that corresponds to Tp.

Area Ti—Area Ti is the region between Ta and Tp. Ti has none of the pronounced architectonic features of a core sensory area of Ta and Tp, but rather has the appearance of a higher-order or association area. The functions of Ti are not known, but its position between visual and auditory fields suggest that is might be responsive to both modalities. As suggested above, much of Ti may correspond to area Te2 of Zilles and Wree (1985) in rats.

Area Tm—The fourth subdivision of temporal cortex in squirrels is the most dorsal or medial portion, Tm. As the architecture of Tm resembles that of Tp, some of Tm was included in Tp by Kaas et al., (1972). However, part of the Tm region was distinguished as area 19p, as it differed from area 19 proper by having a somewhat denser layer 4 of granule cells and a somewhat greater expression of myelin. Together with Tp, Tm or parts of it may receive inputs from the caudal division of the inferior pulvinar (Robson and Hall, 1977). The Tm region appears to have connections with area 18 of grey squirrels (Kaas et al., 1989), and it is within the territory of temporal cortex that is responsive to visual stimuli in ground squirrels. Tm possibly overlaps with the proposed middle lateral (ML) visual field, where neurons were found to be directionally selective (Paolini and Sereno, 1998). Anatomical studies are needed to determine if the connections of Tm are distinct from those of Tp.

Areas of the parietal cortex

Areas Pa(S1), Pm, Pl, PV and dy are subdivisions of somatosensory cortex in squirrels. Areas Pa(S1), Pm and Pl have been retained from Kaas et al. (1972). Here we add the 3a/dy area and the parietal ventral area.

Area Pa(S1)—The largest subdivision of somatosensory cortex is area Pa(S1). As somatosensory koniocortex (area 3b), Pa(S1) is characterized by a layer 4 that is densely packed with granule cells. Amongst other architectonic features of primary sensory cortex, layer 4 is expresses very little synaptic zinc, and has a neuropil that is VGluT2 rich. This lack of synaptic zinc suggests that layer 4 receives inputs almost exclusively from the thalamus, rather than from other areas of cortex. As with primary somatosensory cortex (area 3b) of other mammals, Pa(S1) in squirrels receives dense inputs from the ventroposterior nucleus (Krubitzer and Kaas, 1987), and these inputs are expected to terminate largely within layer 4. Area Pa(S1) represents the contralateral body surface (Sur et al., 1978; Krubitzer et al., 1986; Slutsky et al., 2000) in a topographic pattern that conforms to the expected organization of the first somatosensory area, S1 (see Kaas, 1983 for review). Thus, the hindlimb and tail are represented medially, and the face is represented laterally in Pa(S1). As has been most clearly demonstrated in rats (e.g., Chapin and Lin, 1984; Dawson and Killackey, 1987; Remple et al., 2003), but also in other mammals including monkeys (see Qi and Kaas, 2004 for review), aspects of the somatotopy are reflected in the configuration of Pa(S1). Thus, protrusions of the rostral dysgranular area, dy, extend into Pa(S1), separating upper lip, lower lip and forepaw representations (Figure 8B; also see Figure 1 of Krubitzer et al., 1986). The two separate septa of dysgranular cortex merge in central Pa(S1), forming an oval of dysgranular cortex nearly 1mm wide where neurons fail to respond to light, tactile stimuli. This dysgranular oval was called “the unresponsive zone” (Sur et al., 1978), and it is known to have thalamic connections that implicate this and other parts of this dysgranular cortex in the processing of information from muscle spindle receptors (Gould, 1989). Functionally, the large dysgranular zones within Pa(S1) appear to be an extension of the rostral dysgranular cortex rather than part of Pa(S1).

The large forepaw region of Pa(S1) (Figure 8a; Sur et al., 1978) reflects the high density of cutaneous mechanoreceptors in the glaborous forepaw skin of tree squirrels (Brenowitz, 1980). Additional important sensory information in squirrels, as with other rodents, is relayed from the sinus hairs of the face, the mystiacal hairs and the smaller hairs on the skin adjoining the upper and lower lips. These regions of S1 of many rodents, and some other mammals, are subdivided histologically into a number of modules or barrel-like structures, first recognized by Woolsey and colleagues (1975). These modular subdivisions (called barrels), one for each whisker, can be seen in a number of histological preparations, including Nissl-stained sections cut parallel to the cortical surface. Such “barrels” have been described before in S1 of squirrels (Woolsey et al., 1975), and they are demonstrated here in brain sections processed for CO or PV (Fig. 8).

The primary somatosensory representation, S1, has been identified by microelectrode recordings in a number of rodent species and other mammals (see Johnson, 1985 for review). This primary representation has been consistently shown to be coextensive with an architectonically distinct zone of cortex that varies in histological differentiation, but always expresses more sensory characteristics than other areas of cortex, excluding primary auditory and primary visual cortex. As argued elsewhere, only the area 3b somatosensory representation of primates is homologous with S1 of other mammals (Kaas, 1983). Thus, the sensory cortex that is co-extensive with S1 can be termed as area 3b in all mammals, regardless of its degree of differentiation, as is now commonly done for area 17 as primary visual cortex. However, there has been a history of misidentification in architectonic studies. Brodmann (1909) identified much of the S1 region of squirrels as area 1. In rats, Krieg (1946) laterally divided the S1 region into a puzzling patchwork of areas 1, 2 and 3. Caviness (1975) divided the S1 region of mice into areas 3 and 1, placing most of area 2 caudal to area 3. More recently, the full extent of S1 in rats has been recognized, and Zilles and Wree (1985) have accurately outlined S1 in Nissl-stained sections cut parallel to the

flattened cortex as parietal area 1 (Par1), which includes both granular and dysgranular cortex of rats.

Although an overlap zone of S1 with motor cortex is commonly proposed in some rodents, especially rats (e.g., Donoghue et al., 1979; Donoghue and Wise, 1982; Hall and Lindholm 1974), the co-extensiveness of S1 with granular parietal cortex of rodents argues against this interpretation. Nevertheless, as Sanderson et al, (1984) noted, low-threshold movements can be elicited with electrical stimulation with microelectrodes from agranular, dysgranular, and even rostral granular parietal cortex in rats. This finding is similar to that obtained with microstimulation in primates, where low levels of current evoke movements from primary motor cortex (M1), dysgranular cortex (area 3a) between M1 and S1, and parts of S1 (area 3b) (see Wu et al., 2000; Burish et al., 2007). Yet, M1 (Area 4), area 3a, and S1(3b) areas are well established as separate areas without overlap. While some portions of S1(3b) in rodents may be more specialized for motor functions than others, these portions need not represent a more primitive overlap of functional areas, as often stated.

A second subdivision of parietal cortex, the dysgranular area, 3a/dy, lies along the rostral border of Pa(S1), while including the dysgranular zones that extend into Pa(S1). This arrangement is very much like the arrangement of dysgranular cortex relative to the granular cortex in rats (Chapin and Lin, 1984). Although a 3a/dy zone was not included in the earlier study of cortical architecture in squirrels of Kaas et al (1972), where brain sections were cut in the coronal plane, the 3a/dy area is obvious in sections cut in the more favorable horizontal and sagittal planes. The 3a/dy area is identified by a marked reduction in the density of cells packed in layer 4 compared to Pa(S1), but a more obvious layer 4 than in motor cortex. By relative position and architectonic appearance, 3a/dy is homologous to area 3a of primates, an area that also appears to exist in other mammals as the cortical target of a thalamic projection of proprioceptive information, largely from muscle spindle receptors (see Krubitzer et al., 2004 for review). The area along the rostral border of S1 in cats has long been considered to be area 3a (e.g., Dykes et al., 1980). The 3a/dy area in squirrels has also been called the rostral area (Slutsky et al., 2000). As for area 3a of primates and cats, R or dys contains a representation of largely “deep” receptors (non-cutaneous) in a somatotopic pattern that parallels that of S1. These inputs come from a proprioceptive nucleus of the thalamus (Gould et al., 1989), and cortical inputs come from S1 (Krubitzer et al., 1986).

Area Pm—The medial half of the parietal cortex along the caudal border of Pa(S1) was termed Pm (Kaas et al., 1972). This band of cortex has less pronounced sensory features than Pa(S1), but Pm differs only slightly from adjoining areas 19 and Pl, which have somewhat more pronounced sensory features. Much of Pm has connections with Pa(S1), S2 and PV (Krubitzer et al., 1986), and in ground squirrels, neurons in Pm have been shown to respond to strong somatosensory stimulation (Slutsky et al., 2000). As such, Pm can be regarded as a somatosensory area, or possibly a multisensory area. An area Pm has also been defined along the caudal border of S1 in rats (Li et al., 1990; Fabri and Burton, 1991). Similar to Pm in squirrels, Pm in rats receives projections from S1 in a topographic pattern that indicates that a somatosensory representation in Pm parallels the organization of S1. Pm in squirrels likely projects to motor cortex, as Pm does in rats (Donoghue and Parham, 1983; Reep et al., 1990; Reep et al., 1994; Wang and Kurata, 1998), and as cortex along the caudal border of S1 does in many mammals (see Remple et al., 2007 for review). The position of Pm, of course, is in the relative position of area 1 in primates, which contain a representation of cutaneous receptors in parallel to the S1 representation (see Kaas, 2004 for review). In rats, Pm has visual and perhaps auditory inputs, and functions as a multisensory area (Reep et al., 1994; Di et al., 1994; Wallace et al., 2004). In tree shrews, Pm consists of a rostral

strip that is dominated by somatosensory inputs and a caudal strip that is multisensory (Remple et al., 2006). This possibility has not been investigated in squirrels.

As Pm in squirrels is not architectonically very distinct from adjoining occipital and lateral parietal areas, it is not surprising that a Pm region has not been distinguished in the major architectonic studies of neocortex in rats and mice. However, Rose (1912) distinguished a larger area 7 in mice that covered much of the region, whereas regions designated as areas 1 and 2, and perhaps 18a covered the Pm region in the depiction of Caviness (1975). In rats, Krieg (1946) included the Pm region in a larger area 7, whereas Zilles and coworkers included Pm in a large occipital region, Oc2L (Zilles 1990; Zilles and Wree, 1995).

Areas Pl and Pv—The lateral parietal region, Pl, has been retained from Kaas et al (1972), and the parietal ventral area, Pv, is newly distinguished as an architectonic field between Ta and Pa(S1). The second somatosensory area, S2 occupies a little more than the rostral half of Pl (Krubitzer et al., 1986). However, the only distinctive differences in the architecture of the two parts of Pl, is that caudal Pl has less zinc staining. Pl has less dominant sensory characteristics than adjoining areas Pa(S1) and Ta, but more than Pm, Ti, and even area 19. S2 is known to receive direct thalamic connections from the ventroposterior nucleus in most mammals, as it does in squirrels (Krubitzer and Kaas, 1987). Other thalamic inputs are from the posterior medial nucleus. These thalamic inputs would reduce the expression of zinc in layer 4 and in supragranular layers of S2. However, S1 provides dense cortical inputs to S2, and Pv provides additional inputs (Krubitzer et al., 1987), increasing the expression of zinc. The significance of the more caudal part of Pl is unknown, but multisensory functions seem likely, given the adjacent somatosensory, auditory and visual regions.

Pv is a subdivision of somatosensory cortex that was first defined in squirrels, but has subsequently been identified in a range of mammalian species (see Slutsky et al., 2000, for review). As with S2, Pv contains a representation of the contralateral body surface. Typically, responses to auditory stimuli can be recorded in Pv as well. In squirrels, the sensory characteristics of Pv are less pronounced than in the adjoining areas Pa(S1) and Ta, as the cortical architecture resembles that of S2. Pv receives cortical inputs form S1 and S2 (Krubitzer et al., 1986) and thalamic inputs from the ventroposterior nucleus and parts of the medial geniculate complex (Krubitzer and Kaas, 1987). This mixture of thalamic and cortical inputs accounts for the increased expression of zinc in layer 4 and supragranular layers, compared to Pa(S1), but the increase is not as extensive as in area Ti, which appears to get fewer thalamic inputs.

Until recently, S2 and Pv were not distinguished from each other in other rodents, such as rats. However, the existence of both areas has now been well documented in rats (Fabri and Burton, 1991; Li et al., 1990; Remple et al., 2003). In surface-view sections, Pv of rats expresses less cytochrome oxidase than either of the adjoining S1 of primary auditory areas, but the expression is uneven, suggesting a relationship to the body surface repesentation (Remple et al., 2003). In rats, both S2 and Pv would be contained in the cortex identified by Zilles and Wree (1985) as parietal area 2.

Frontal cortex

In frontal cortex of squirrels, we have distinguished an agranular motor area that might be more properly called dysgranular because a trace of layer 4 is present. Here we described other architectonic characteristics of this field, including the presence of a thin synaptic zinc-poor layer 4. Unpublished microstimulation results from our laboratory indicate that this agranular field, M, corresponds to primary motor cortex, M1. This M1 is in the relative position of M1 in other mammals, and it corresponds to the map of contralateral body

movements that has been described in lateral agranular cortex of rats (Donoghue and Wise, 1982; Neafsey et al., 1986; Brecht et al., 2004). In rats, M1 appears to largely correspond to frontal area 1 (Fr1) of Zilles and Wree (1985), although not completely. Krieg (1946) defined an area 4 that overlaps with medial S1, and does not conform well to the extent of M1 in rats. In ground squirrels, Brodmann (1909) described a frontal region, with cytoarchitectonic features of both areas 4 and 6, that overlaps the present area M, whilst extending further rostrally.

The cortex rostromedial to area M is in the relative position of the second motor area of rats (Neafsey et al., 1986). In squirrels and rats, this rostromedial cortex has a more obvious layer 4, but this region is not fully characterized in the present report. The second motor area of rats, whether a premotor area or the supplementary motor area, corresponds to the Fr2 region of Zilles and Wree (1995).

Other frontal areas in squirrels include the lateral orbital frontal cortex and the medial frontal cortex of the frontal pole. These regions were not well distinguished in the present preparations. In rats and rabbits, lateral and medial frontal regions have different connections and behavioral functions (Uylings et al., 2003; Gabbott et al., 2005; Leal-Campanario et al., 2007). Although the prefrontal cortex of rats is considered to be agranular (Öngür and Price, 2000), and thereby lacking the highly granular prefrontal cortex of primates (Preuss, 1995), frontal polar regions of squirrel cortex, have a clear layer 4. The frontal pole has been variously divided in rats, with Ray and Price (1992) defining medial and lateral frontal polar areas.

Cingulate and retrosplenial cortex

Cingulate cortex—In squirrels, we distinguish these subdivisions of cingulate cortex as areas DCg, VCg, and RCg. DCg corresponds to the dorsal cingulate area, VCg to the ventral cingulate area, and RCg to the prelimbic area of Ray and Price (1992). DCg approximately corresponds to area 24b and b′, VCg to 24a′ and RCg to 24a of Vogt et al. (2004). The cingulate cortex in squirrels, like in other mammals such as monkeys (Vogt et al., 1992) and rats (Zilles, 1990), surrounds much of the anterior portion of the corpus callosum (Fig. 16A). The cingulate cortex, part of the limbic system and the Papez circuit (Vogt et al., 1992), has cytoarchitectonic features of both isocortex and allocortex (Zilles, 1990). The lack of well-defined cortical layers and an indistinct layer 4, characteristics of the cingulate cortex in rats (Zilles, 1990; Vogt et al., 2004), are observed in grey squirrels as well. SMI-32 preparations in grey squirrels showed that the dorsal part of the cingulate cortex, DCg, contains slightly more pyramidal neurons than the ventral areas, VCg and RCg (Fig. 16F). This is similar to the observation made by Jones and colleagues (2005) in Nissl preparation of rat brain sections, where this dorsal anterior cingulate (ACd) area (DCg here), contains slightly more pyramidal neurons than their ventral anterior cingulate (ACv) area (VCg and RCg). The cingulate cortex in rats receives diffuse projections from the mediodorsal, ventromedial and anteromedial portion of the thalamus (Domesick, 1969) and has been implicated in higher-order brain functions, such as attention, pain processing and motivational aspects of learning (Gabriel et al., 1980; Vogt et al., 1990; Jones et al., 2005).

Retrosplenial cortex—The retrosplenial cortex has a role in the processes of learning and memory (van Groen and Wyss, 1990). In grey squirrels, we have retained the retrosplenial granular (RSG), and retrosplenial agranular (RSA) nomenclature of Rose (1929) and these retrosplenial areas seem to correspond to areas 29a to c and 29d respectively, of Vogt (1993). The granular retrosplenial cortical area (RSG) in grey squirrels, as in rats (Vogt and Peters, 1981), is more dysgranular than agranular as there is some layer 4 stellate cells. Just as in rats, RSG in squirrels has a compressed layer 2 plus 3 that is densely packed with cells.

This band of cells is less distinct in the poorly laminated RSA (Fig. 2A)(Palomero-Gallagher and Zilles, 2004). Both RSG and RSA show characteristics of periallocortex, with poor laminar differentiation, making them easily distinguishable from adjacent cortical areas. The middle layers of RSG are poorly stained in sections processed for zinc, suggesting the presence of thalamic inputs. RSA has more zinc staining, especially in layer 3. In rats, RSG receives afferents from the anterodorsal (AD) and anteroventral (AV), and lateral dorsal (LD) thalamic nuclei (Domesick, 1969; 1972; van Groen and Wyss, 1990), as well as afferents from parts of the cingulate cortex, some visual areas (Vogt and Miller, 1983) and callosal fibers from the contralateral retrosplenial areas (Vogt et al., 1981). RSA has connections with the anteroventral (AV), anteromedial (AM) and the lateral dorsal (LD) nuclei of the thalamus (Sripanidkulchai and Wyss, 1986).

Perirhinal cortex

Perirhinal cortex forms a narrow belt along the dorsal bank of the rhinal fissure and the caudally adjoining cortex at the end of the rhinal sulcus. Traditionally, perirhinal cortex has been divided somewhat arbitrarily into a portion ventral and rostral to somatosensory cortex, the insular cortex, and a more caudal portion, the perirhinal cortex, of similar appearance. Even more caudoventrally, the entorhinal cortex has a distinct appearance that allows it to be identified as such in a wide range of mammalian species.

Insular cortex—The insular cortex (Ins) defined here is poorly laminated with an indistinct layer 4 (Fig. 19). In rats, this region corresponds to the “agranular” insular cortex (AI) of Zilles (1990) that lacks a distinct granular layer 4 and is poorly myelinated. Our insular cortex in squirrels does not include the granular insular cortex of other descriptions in rats and other rodents, as this cortex is included in our Pv region (Fig. 8A). As with rats (Zilles, 1990), the insular cortex in grey squirrels occupies the anterior half of the rhinal sulcus, with the claustrum marking the caudal border of the insular with the adjoining perirhinal cortex. The insular cortex has connections with several regions, including the cingulate, piriform, perirhinal and entorhinal cortices, and the mediodorsal and lateroposterior nuclei of the thalamus (Groenewegen, 1988;Zilles, 1990;Ray and Price, 1992). Proposed to be part of the gustatory cortex, the agranular region of the insular in rats may be involved in taste (Kosar et al., 1986;Sewards and Sewards, 2001), as well as to having introceptive functions (Cechetto and Saper, 1987;Contreras et al., 2007).

Perirhinal cortex—The perirhinal cortex, PRh, in squirrels is bordered by temporal, insular and entorhinal cortices. PRh is retained from Zilles and Wree (1985), and corresponds to the posterior region of area 35 of Krieg (1946) and the ectorhinal and perirhinal areas of Swanson (1992). PRh is poorly myelinated in both grey squirrels (Fig. 19B) and rats (Burwell, 2001; Palomero-Gallagher and Zilles, 2004). In grey squirrels, PRh receives large amounts of cortiocortical inputs, especially in the superficial layers, as shown by the zinc stain (Fig. 19C). In rats, PRh has connections with the piriform, frontal, temporal and insular cortices (Furtak, 2007) and the anterior thalamic nuclei (Palomero-Gallagher and Zilles, 2004). Connections of PRh with the hippocampal formation suggest that PRh has a role in memory processes (Burwell and Amaral, 1998; Palomero-Gallagher and Zilles, 2004; Furtak, 2007).

Entorhinal cortex—The entorhinal cortex, area 28 of Brodmann’s (1909) is part of the retrohippocampal field and is an important association pathway within the hippocampal region (Köhler, 1986). We have retained the term Ent of rats from Paxinos et al. (1999) and Zilles (Palomero-Gallagher and Zilles, 2004), which corresponds to the entorhinal cortex (EC) of Blackstad (1956) and Köhler (1986). EC cortex has been divided into medial (MEA) and lateral areas (LEA) (Köhler, 1986), or areas 28a and 28b respectively (Blackstad, 1956).

On the basis of cytoarchitecture, we have further subdivided LEA into intermediate (IEnt) and lateral (LEnt) portions. MEA corresponds to our MEnt.

CONCLUDING REMARKS

Squirrels are rodents that have become useful and interesting in studies of neocortical areas and functions, in part because of their well-developed visual system, but also because of a brain that is larger than those in rats and mice. Here, we show that a number of cortical areas are more distinct architectonically than in more commonly studied laboratory rodents. In particular, primary and secondary visual areas as well as three main divisions of the temporal lobe are obvious. The distinctiveness of these fields invites further study, as well as comparisons with other rodents where homologous regions are expected, but not as easily defined. Such comparisons could lead to a better understanding of cortical organization and function in the widely used rats and mice. Other comparisons might be made with other members of the Euarchontoglire clade of mammals, including the closely related lagomorphs and the more distantly related tree shrews and primates. We would expect more overall similarities in cortical organization across members of this clade, than between members of this clade and those of the other five major clades of mammals. In this regard, it is interesting that evidence for a third visual area, V3, exists for some ground squirrels, but not for rats and mice, where even the existence of V2 has been questioned. V3 has been described in primates of the Euarchontoglire clade, but also in cats of the Laurasiatherian clade. While it is possible that a V3-like area evolved independently in squirrels, primates and cats, the other possibility is that present comparative understandings of cortical organizations within and across clades are so incomplete and inaccurate that questions about the evolution of V3, and perhaps many cortical areas, cannot be fruitfully addressed without a host of further comparative studies. As such studies can be costly and labor-intensive, studies of brain organization and function have necessarily concentrated on a few species for practical or conceptual reasons. Further studies of brain organization in squirrels might promote a better understanding of cortical organization and evolution in members of the Euarchontoglire clade.

Acknowledgments

We thank Drs. Troy Hackett and Omar Gharbawie for helpful comments regarding the manuscript, Mark Burish for his assistance with the experiments, and Laura Trice and Mary Varghese for help with the histological procedures. Drs. Aurea Pimenta and Pat Levitt kindly provided the LAMP antibody.

This research was supported by a grant from the National Eye Institute, EY 02686 to J.H.K.

References

Abplanalp P. Some subcortical connections of the visual system in tree shrews and squirrels. Brain Behav Evol. 1970; 3(1):155–168. [PubMed: 5522341]

Albus K, Beckmann R. Second and third visual area of the cat: interindividual variability in retinotopic arrangement and cortical location. J Physiol. 1980; 299:276–297.

Allman JM, Kaas JH. Representation of the visual field in striate and adjoining cortex of the owl monkey (Aotus trivirgatus). Brain Res. 1971; 35(1):89–106. [PubMed: 5002564]

Annese J, Pitiot A, Dinov ID, Toga AW. A myelo-architectonic method for the structural classification of cortical areas. Neuroimage. 2004; 21(1):15–26. [PubMed: 14741638]

Avendaño C, Verdu A. Area 3a in the cat. I. A reevaluation of its location and architecture on the basis of Nissl, myelin, acetylcholinesterase, and cytochrome oxidase staining. J Comp Neurol. 1992; 321(3):357–72. [PubMed: 1380516]

Benton, MJ. Vertebrate Palaeontology. Oxford: Blackwell; 2005.

Blackstad TW. Commissural connections of the hippocampal region in the rat, with special reference to their mode of termination. J Comp Neurol. 1956; 105(3):417–537. [PubMed: 13385382]

Boire D, Desgent S, Matteau I, Ptito M. Regional analysis of neurofilament protein immunoreactivity in the hamster's cortex. J Chem Neuroanat. 2005; 29(3):193–208. [PubMed: 15820621]

Bravo H, Olavarria J, Torrealba F. Comparative study of visual inter and intrahemispheric cortico-cortical cnnections in five native Chilean rodents. Anat Embryol. 1990; 191:67–73. [PubMed: 2407148]

Brecht M, Krauss A, Muhammad S, Sinai-Esfahani L, Bellanca S, Margrie TW. Organization of rat vibrissa motor cortex and adjacent areas according to cytoarchitectonics, microstimulation, and intracellular stimulation of identified cells. J Comp Neurol. 2004; 479(4):360–373. [PubMed: 15514982]

Brenowitz GL. Cutaneous mechanoreceptor distribution and its relationship to behavioral specializations in squirrels. Brain Behav Evol. 1980; 17(6):432–453. [PubMed: 7437898]

Brodmann, K. Brodmann's 'Localisation in the Cerebral Cortex'. Garey, LJ., translator. London: Eldred Smith-Gordon; 1909.

Brown CE, Dyck RH. Distribution of zincergic neurons in the mouse forebrain. J Comp Neurol. 2004; 479(2):156–167. [PubMed: 15452827]

Budinger E, Heil P, Scheich H. Functional organization of auditory cortex in the Mongolian gerbil (Meriones unguiculatus). III. Anatomical subdivisions and corticocortical connections. Eur J Neurosci. 2000; 12(7):2425–2451. [PubMed: 10947821]

Burish M, Stepniewska I, Kaas JH. Microstimulation and architectonics of frontoparietal cortex in common marmosets (Callithrix jacchus). J Comp Neurol. 2007 (in press).

Burwell RD. Borders and cytoarchitecture of the perirhinal and postrhinal cortices in the rat. J Comp Neurol. 2001; 437(1):17–41. [PubMed: 11477594]

Burwell RD, Amaral DG. Cortical afferents of the perirhinal, postrhinal, and entorhinal cortices of the rat. J Comp Neurol. 1998; 398(2):179–205. [PubMed: 9700566]

Campbell MJ, Morrison JH. Monoclonal antibody to neurofilament protein (SMI-32) labels a subpopulation of pyramidal neurons in the human and monkey neocortex. J Comp Neurol. 1989; 282(2):191–205. [PubMed: 2496154]

Casagrande, VA.; Kaas, JH. The afferent, intrinsic and efferent connections of primary visual cortex in primates. Peters, A.; Rockland, KS., editors. New York: Plenum Press; 1994.

Caviness VS Jr. Architectonic map of neocortex of the normal mouse. J Comp Neurol. 1975; 164(2): 247–263. [PubMed: 1184785]

Cechetto DF, Saper CB. Evidence for a viscerotopic sensory representation in the cortex and thalamus in the rat. J Comp Neurol. 1987; 262(1):27–45. [PubMed: 2442207]

Celio MR. Parvalbumin in most gamma-aminobutyric acid-containing neurons of the rat cerebral cortex. Science. 1986; 231(4741):995–997. [PubMed: 3945815]

Chapin JK, Lin CS. Mapping the body representation in the SI cortex of anesthetized and awake rats. J Comp Neurol. 1984; 229(2):199–213. [PubMed: 6438190]

Chesselet M-F, Gonzales C, Levitt P. Heterogeneous distribution of the limbic system-associated membrane protein in the caudate nucleus and substantia nigra of the cat. Neuroscience. 1991; 40:725–733. [PubMed: 1676494]

Condé F, Lund JS, Lewis DA. The hierarchical development of monkey visual cortical regions as revealed by the maturation of parvalbumin-immunoreactive neurons. Brain Res Dev Brain Res. 1996; 96(1–2):261–276.

Contreras M, Ceric F, Torrealba F. Inactivation of the interoceptive insula disrupts drug craving and malaise induced by lithium. Science. 2007; 318:655–657. [PubMed: 17962567]

Cruikshank SJ, Killackey HP, Metherate R. Parvalbumin and calbindin are differentially distributed within primary and secondary subregions of the mouse auditory forebrain. Neuroscience. 2001; 105(3):553–569. [PubMed: 11516823]

Coté PY, Levitt P, Parent A. Distribution of limbic system-associated membrane protein (LAMP) immunoreactivity in primate basal ganglia. Neuroscience. 1995; 69:71–81. [PubMed: 8637634]

Cusick CG, Kaas JH. Retinal projections in adult and newborn grey squirrels. Brain Res. 1982; 256(3): 275–284. [PubMed: 6179578]

Czupryn A, Skangiel-Kramska J. Distribution of synaptic zinc in the developing mouse somatosensory barrel cortex. J Comp Neurol. 1997; 386(4):652–660. [PubMed: 9378858]

Danscher G. Histochemical demonstration of heavy metals. A revised version of the sulphide silver method suitable for both light and electron microscopy. Histochemistry. 1981; 71(1):1–16. [PubMed: 6785259]

Danscher G. Exogenous selenium in the brain. A histochemical technique for light and electron microscopical localization of catalytic selenium bonds. Histochemistry. 1982; 76(3):281–293. [PubMed: 6186642]

Danscher G, Stoltenberg M. Zinc-specific autometallographic in vivo selenium methods: tracing of zinc-enriched (ZEN) terminals, ZEN pathways, and pools of zinc ions in a multitude of other ZEN cells. J Histochem Cytochem. 2005; 53(2):141–153. [PubMed: 15684327]

Dawson DR, Killackey HP. The organization and mutability of the forepaw and hindpaw representations in the somatosensory cortex of the neonatal rat. J Comp Neurol. 1987; 256(2):246–256. [PubMed: 3558880]

de Nó R, Lorente. The cerebral cortex of the mouse (a first contribution--the “acoustic” cortex). Somatosens Mot Res. 1992; 9(1):3–36. [PubMed: 1317625]

de Venecia RK, Smelser CB, McMullen NT. Parvalbumin is expressed in a reciprocal circuit linking the medial geniculate body and auditory neocortex in the rabbit. J Comp Neurol. 1998; 400(3): 349–62. [PubMed: 9779940]

DeFelipe J, Jones EG. Parvalbumin immunoreactivity reveals layer IV of monkey cerebral cortex as a mosaic of microzones of thalamic afferent terminations. Brain Res. 1991; 562(1):39–47. [PubMed: 1799871]

DeFelipe J. Types of neurons, synaptic connections and chemical characteristics of cells immunoreactive for calbindin-D28K, parvalbumin and calretinin in the neocortex. J Chem Neuroanat. 1997; 14:1–19. [PubMed: 9498163]

Di S, Brett B, Barth DS. Polysensory evoked potentials in rat parietotemporal cortex: combined auditory and somatosensory responses. Brain Res. 1994; 642(1–2):267–280. [PubMed: 8032888]

Diamond IT, Fitzpatrick D, Schmechel D. Calcium-binding proteins distinguish large and small cells of the ventral posterior and lateral geniculate nuclei of the prosimian galago and tree shrew (Tupaia belangeri). Proc Natl Acad Sci USA. 1993; 90:1425–1429. [PubMed: 8434002]

Domesick VB. Projections from the cingulate cortex in the rat. Brain Res. 1969; 12(2):296–320. [PubMed: 4185473]

Domesick VB. Thalamic relationships of the medial cortex in the rat. Brain Behav Evol. 1972; 6(1): 457–483. [PubMed: 4122728]

Donoghue JP, Kerman KL, Ebner FF. Evidence for two organizational plans within the somatic sensory-motor cortex of the rat. J Comp Neurol. 1979; 183(3):647–663. [PubMed: 103941]

Donoghue JP, Wise SP. The motor cortex of the rat: cytoarchitecture and microstimulation mapping. J Comp Neurol. 1982; 212(1):76–88. [PubMed: 6294151]

Donoghue JP, Parham C. Afferent connections of the lateral agranular field of the rat motor cortex. J Comp Neurol. 1983; 217(4):390–404. [PubMed: 6886060]

Dursteler MR, Blakemore C, Garey LJ. Projections to the visual cortex in the golden hamster. J Comp Neurol. 1979; 183(1):185–204. [PubMed: 102666]

Dyck R, Beaulieu C, Cynader M. Histochemical localization of synaptic zinc in the developing cat visual cortex. J Comp Neurol. 1993; 329(1):53–67. [PubMed: 8384221]

Dykes R, Rasmussen D, Hoeltzell P. Ventroposterior thalamic regions projecting to cytoarchitectonic areas 3a and 3b in the cat. J Neurophysiol. 1980; 56:1527–1546. [PubMed: 7411175]

Dykes RW, Herron P, Lin CS. Ventroposterior thalamic regions projecting to cytoarchitectonic areas 3a and 3b in the cat. J Neurophysiol. 1986; 6(6):1521–41. [PubMed: 3027273]

Fabri M, Burton H. Topography of connections between primary somatosensory cortex and posterior complex in rat: a multiple fluorescent tracer study. Brain Res. 1991; 538(2):351–357. [PubMed: 2012978]

Felleman DJ, Wall JT, Cusick CG, Kaas JH. The representation of the body surface in S-I of cats. J Neurosci. 1983; 3(8):1648–69. [PubMed: 6875661]

Fendrich R, Wessinger CM, Gazzaniga MS. Speculations on the neural basis of islands of blindsight. Prog Brain Res. 2001; 134:353–366. [PubMed: 11702554]

Frederickson CJ, Moncrieff DW. Zinc-containing neurons. Biol Signals. 1994; 3(3):127–139. [PubMed: 7531563]

Frederickson CJ, Suh SW, Silva D, Frederickson CJ, Thompson RB. Importance of zinc in the central nervous system: the zinc-containing neuron. J Nutr. 2000; 130(5S Suppl):1471S–1483S. [PubMed: 10801962]

Fujiyama F, Furuta T, Kaneko T. Immunocytochemical localization of candidates for vesicular glutamate transporters in the rat cerebral cortex. J Comp Neurol. 2001; 435(3):379–387. [PubMed: 11406819]

Furtak SC, Wei SM, Agster KL, Burwell RD. Functional neuroanatomy of the parahippocampal region in the rat: the perirhinal and postrhinal cortices. Hippocampus. 2007; 17(9):709–22. [PubMed: 17604355]

Gabbott PL, Warner TA, Jays PR, Salway P, Busby SJ. Prefrontal cortex in the rat: projections to subcortical autonomic, motor, and limbic centers. J Comp Neurol. 2005; 492(2):145–177. [PubMed: 16196030]

Gabriel M, Orona E, Foster K, Lambert RW. Cingulate cortical and anterior thalamic neuronal correlates of reversal learning in rabbits. J Comp Physiol Psychol. 1980; 94(6):1087–1100. [PubMed: 7204699]

Gallyas F. Silver staining of myelin by means of physical development. Neurol Res. 1979; 1(2):203–209. [PubMed: 95356]

Garrett B, Geneser FA, Slomianka L. Distribution of acetylcholinesterase and zinc in the visual cortex of the mouse. Anat Embryol (Berl). 1991; 184(5):461–468. [PubMed: 1741478]

Garrett B, Osterballe R, Slomianka L, Geneser FA. Cytoarchitecture and staining for acetylcholinesterase and zinc in the visual cortex of the Parma wallaby (Macropus parma). Brain Behav Evol. 1994; 43(3):162–172. [PubMed: 8193908]

Gould HJ 3rd. Interhemispheric connections of the visual cortex in the grey squirrel (Sciurus carolinensis). J Comp Neurol. 1984; 223(2):259–301. [PubMed: 6200520]

Gould HJ 3rd, Whitworth RH Jr, LeDoux MS. Thalamic and extrathalamic connections of the dysgranular unresponsive zone in the grey squirrel (Sciurus carolinensis). J Comp Neurol. 1989; 287(1):38–63. [PubMed: 2477399]

Groenewegen HJ. Organization of the afferent connections of the mediodorsal thalamic nucleus in the rat, related to the mediodorsal-prefrontal topography. Neuroscience. 1988; 24(2):379–431. [PubMed: 2452377]

Guldin WO, Markowitsch HJ. Cortical and thalamic afferent connections of the insular and adjacent cortex of the rat. J Comp Neurol. 1983; 215(2):135–153. [PubMed: 6853769]

Hackett TA, Stepniewska I, Kaas JH. Subdivisions of auditory cortex and ipsilateral cortical connections of the parabelt auditory cortex in macaque monkeys. J Comp Neurol. 1998; 394(4): 475–495. [PubMed: 9590556]

Hall R, Lindholm E. Organization of motor and somatosensory neocortex in the albino rat. Brain Res. 1974; 66:23–38.

Hall WC, Kaas JH, Killackey H, Diamond IT. Cortical visual areas in the grey squirrel (Sciurus carolinensis): a correlation between cortical evoked potential maps and architectonic subdivisions. J Neurophysiol. 1971; 34(3):437–452. [PubMed: 5560040]

Hässler, R. Comparative anatomy of the central visual systems in day- and night-active primates. In: Hassler, R.; Stephen, H., editors. Evolution of the Forebrain. Stuttgart: 1966. p. 419-434.

Hevner RF, Wong-Riley MT. Entorhinal cortex of the human, monkey, and rat: metabolic map as revealed by cytochrome oxidase. J Comp Neurol. 1992; 326(3):451–469. [PubMed: 1334980]

Hof PR, Glezer, Conde F, Flagg RA, Rubin MB, Nimchinsky EA, Vogt Weisenhorn DM. Cellular distribution of the calcium-binding proteins parvalbumin, calbindin, and calretinin in the neocortex of mammals: phylogenetic and developmental patterns. J Chem Neuroanat. 1999; 16(2):77–116. [PubMed: 10223310]

Horton HL, Levitt P. A unique membrane protein is expressed on early developing limbic system axons and cortical targets. J Neurosci. 1988; 8:4653–4661. [PubMed: 3199199]

Hubel DH, Wiesel TN. Receptive Fields and Functional Architecture in Two Nonstriate Visual Areas (18 and 19) of the Cat. J Neurophysiol. 1965; 28:229–289. [PubMed: 14283058]

Huchon D, Madsen O, Sibbald M, Ament K, Stanhope M, Catzeflis F, de Jong W, Douzery E. Rodent phylogeny and a timescale for the evolution of Glires: evidence from an extensive taxon sampling using three nuclear genes. Mol Biol Evol. 2002; 19(7):1053–1065. [PubMed: 12082125]

Huffman KJ, Krubitzer L. Area 3a: topographic organization and cortical connections in marmoset monkeys. Cereb Cortex. 2001; 11(9):849–867. [PubMed: 11532890]

Ichinohe N, Fujiyama F, Kaneko T, Rockland KS. Honeycomb-like mosaic at the border of layers 1 and 2 in the cerebral cortex. J Neurosci. 2003; 23(4):1372–82. [PubMed: 12598625]

Ichinohe N, Rockland KS. Region specific micromodularity in the uppermost layers in primate cerebral cortex. Cereb Cortex. 2004; 14(11):1173–1184. [PubMed: 15142953]

Jain N, Preuss TM, Kaas JH. Subdivisions of the visual system labeled with the Cat-301 antibody in tree shrews. Vis Neurosci. 1994; 11(4):731–741. [PubMed: 7918223]

Johnson, JI. Comparative development of somatic sensory cortex. Jones, EG.; Peters, A., editors. New York: Plenum Press; 1985.

Jones BF, Groenewegen HJ, Witter MP. Intrinsic connections of the cingulate cortex in the rat suggest the existence of multiple functionally segregated networks. Neuroscience. 2005; 133(1):193–207. [PubMed: 15893643]

Jones, EG. The Thalamus. 2. Cambridge Univ Press; Cambridge, UK: 2007.

Jones EG, Hendry SHC. Differential calbium-binding protein immunoreactivity distinguishes classes of relay neurons in monkey thalamic nuclei. Eur J Neurosci. 1989; 1:222–246. [PubMed: 12106154]

Jones EG, Porter R. What is area 3a? Brain Res. 1980; 203(1):1–43. [PubMed: 6994855]

Kaas JH. What, if anything, is SI? Organization of first somatosensory area of cortex. Physiol Rev. 1983; 63(1):206–231. [PubMed: 6401864]

Kaas JH. Convergences in the modular and areal organization of the forebrain of mammals: Implications for the reconstruction of forebrain evolution. Brain Behavior Evol. 2002; 59:262–272.

Kaas JH, Collins CE. Evolving ideas of brain evolution. Nature. 2001; 411(6834):141–142. [PubMed: 11346770]

Kaas JH, Guillery RW, Allman JM. Discontinuities in the dorsal lateral geniculate nucleus corresponding to the optic disc: a comparative study. J Comp Neurol. 1973; 147(2):163–179. [PubMed: 4630151]

Kaas JH, Hall WC, Diamond IT. Visual cortex of the grey squirrel (Sciurus carolinensis): architectonic subdivisions and connections from the visual thalamus. J Comp Neurol. 1972; 145(3):273–305. [PubMed: 5030907]

Kaas JH, Krubitzer LA, Johanson KL. Cortical connections of areas 17 (V-I) and 18 (V-II) of squirrels. J Comp Neurol. 1989; 281(3):426–446. [PubMed: 2703555]

Kaas JH, Lyon DC. Visual cortex organization in primates: theories of V3 and adjoining visual areas. Prog Brain Res. 2001; 134:285–295. [PubMed: 11702549]

Kaas JH, Lyon DC. Pulvinar contributions to the dorsal and ventral streams of visual processing in primates. Brain Res Rev. 2007

Kalia M, Whitteridge D. The visual areas in the splenial sulcus of the cat. J Physiol. 1973; 232(2):275–283. [PubMed: 4727082]

Kaneko T, Fujiyama F. Complementary distribution of vesicular glutamate transporters in the central nervous system. Neurosci Res. 2002; 42(4):243–250. [PubMed: 11985876]

Kicliter E, Loop MS, Jane JA. Effects of posterior neocortical lesions on wavelength, light/dark and stripe orientation discrimination in ground squirrels. Brain Res. 1977; 122(1):15–31. [PubMed: 837217]

Köhler C. Cytochemical architecture of the entorhinal area. Adv Exp Med Biol. 1986; 203:83–98. [PubMed: 2431606]

Krettek JE, Price JL. The cortical projections of the mediodorsal nucleus and adjacent thalamic nuclei in the rat. J Comp Neurol. 1977; 171(2):157–191. [PubMed: 64477]

Kosar E, Grill HJ, Norgren R. Gustatory cortex in the rat. I. Physiological properties and cytoarchitecture. Brain Res. 1986; 379(2):329–41. [PubMed: 3742225]

Krieg W. Connections of the cerebral cortex. I. The albino rat. A. Topography of the cortical areas. J Comp Neurol. 1946; 84:221–275. [PubMed: 20982805]

Krubitzer L, Huffman KJ, Disbrow E, Recanzone G. Organization of area 3a in macaque monkeys: contributions to the cortical phenotype. J Comp Neurol. 2004; 471(1):97–111. [PubMed: 14983479]

Krubitzer LA, Kaas JH. Thalamic connections of three representations of the body surface in somatosensory cortex of gray squirrels. J Comp Neurol. 1987; 265(4):549–580. [PubMed: 2448348]

Krubitzer LA, Sesma MA, Kaas JH. Microelectrode maps, myeloarchitecture, and cortical connections of three somatotopically organized representations of the body surface in the parietal cortex of squirrels. J Comp Neurol. 1986; 250(4):403–430. [PubMed: 3760247]

Lane RH, Allman JM, Kaas JH. Representation of the visual field in the superior colliculus of the grey squirrel (Sciurus carolinensis) and the tree shrew (Tupaia glis). Brain Res. 1971; 26(2):277–292. [PubMed: 5547178]

Latawiec D, Martin KA, Meskenaite V. Termination of the geniculocortical projection in the striate cortex of macaque monkey: a quantitative immunoelectron microscopic study. J Comp Neurol. 2000; 419(3):306–319. [PubMed: 10723007]

Leal-Campanario R, Fairen A, Delgado-Garcia JM, Gruart A. Electrical stimulation of the rostral medial prefrontal cortex in rabbits inhibits the expression of conditioned eyelid responses but not their acquisition. Proc Natl Acad Sci U S A. 2007; 104(27):11459–11464. [PubMed: 17592148]

Lee VM, Otvos L Jr, Carden MJ, Hollosi M, Dietschold B, Lazzarini RA. Identification of the major multiphosphorylation site in mammalian neurofilaments. Proc Natl Acad Sci USA. 1988; 85:1988–2002. [PubMed: 3162320]

Lent R. The organization of subcortical projections of the hamster's visual cortex. J Comp Neurol. 1982; 206(3):227–242. [PubMed: 7085930]

Levey NH, Harris J, Jane JA. Effects of visual cortical ablation on pattern discrimination in the ground squirrel (Citellus tridecemlineatus). Exp Neurol. 1973; 39(2):270–276. [PubMed: 4702821]

Levitt P. A monoclonal antibody to limbic system neurons. Science. 1984; 223:299–301. [PubMed: 6199842]

Li XG, Florence SL, Kaas JH. Areal distributions of cortical neurons projecting to different levels of the caudal brain stem and spinal cord in rats. Somatosens Mot Res. 1990; 7(3):315–335. [PubMed: 2248004]

Long KO, Fisher SK. The distributions of photoreceptors and ganglion cells in the California ground squirrel, Spermophilus beecheyi. J Comp Neurol. 1983; 221(3):329–340. [PubMed: 6655087]

Luethke LE, Krubitzer LA, Kaas JH. Cortical connections of electrophysiologically and architectonically defined subdivisions of auditory cortex in squirrels. J Comp Neurol. 1988; 268(2):181–203. [PubMed: 3360984]

Major DE, Rodman HR, Libedinsky C, Karten HJ. Pattern of retinal projections in the California ground squirrel (Spermophilus beecheyi): anterograde tracing study using cholera toxin. J Comp Neurol. 2003; 463(3):317–34. [PubMed: 12820165]

Malach R. Patterns of connections in rat visual cortex. J Neurosci. 1989; 9(11):3741–3752. [PubMed: 2479724]

Mercer JM, Roth VL. The effects of Cenozoic global change on squirrel phylogeny. Science. 2003; 299(5612):1568–1572. [PubMed: 12595609]

Merzenich MM, Kaas JH, Roth GL. Auditory cortex in the grey squirrel: tonotopic organization and architectonic fields. J Comp Neurol. 1976; 166(4):387–401. [PubMed: 1270613]

Miro-Bernie N, Ichinohe N, Perez-Clausell J, Rockland KS. Zinc-rich transient vertical modules in the rat retrosplenial cortex during postnatal development. Neuroscience. 2006; 138(2):523–535. [PubMed: 16426767]

Montero VM. Retinotopy of cortical connections between the striate cortex and extrastriate visual areas in the rat. Exp Brain Res. 1993; 94(1):1–15. [PubMed: 8335065]

Morecraft RJ, Rockland KS, Van Hoesen GW. Localization of area prostriata and its projection to the cingulate motor cortex in the rhesus monkey. Cereb Cortex. 2000; 10(2):192–203. [PubMed: 10667987]

Nahmani M, Erisir A. VGluT2 immunochemistry identifies thalamocortical terminals in layer 4 of adult and developing visual cortex. J Comp Neurol. 2005; 484(4):458–473. [PubMed: 15770654]

Neafsey, E. The complete ratunculus: output organization of layer V of the cerebral cortex. In: Kolb, B.; Tees, RC., editors. The cerebral cortex of the rat. Cambridge, MA: MIT Press; 1990. p. 197-212.

Neafsey EJ, Bold EL, Haas G, Hurley-Gius KM, Quirk G, Sievert CF, Terreberry RR. The organization of the rat motor cortex: a microstimulation mapping study. Brain Res. 1986; 396(1): 77–96. [PubMed: 3708387]

Nelson RJ, Sur M, Kaas JH. The organization of the second somatosensory area (SmII) of the grey squirrel. J Comp Neurol. 1979; 184(3):473–489. [PubMed: 422752]

Olavarria J, Mendez B. The representations of the visual field on the posterior cortex of Octodon degus. Brain Res. 1979; 161(3):539–543. [PubMed: 421136]

Olavarria J, Montero V. Elaborate organization of visual cortex in the hamster. Neurosci Res. 1990; 8(1):40–47. [PubMed: 2163048]

Olavarria J, Montero VM. Relation of callosal and striate-extrastriate cortical connections in the rat: morphological definition of extrastriate visual areas. Exp Brain Res. 1984; 54(2):240–252. [PubMed: 6723844]

Olavarria J, Montero VM. Organization of visual cortex in the mouse revealed by correlating callosal and striate-extrastriate connections. Vis Neurosci. 1989; 3(1):59–69. [PubMed: 2487092]

Olavarria J, Van Sluyters RC. The projection from striate and extrastriate cortical areas to the superior colliculus in the rat. Brain Res. 1982; 242(2):332–336. [PubMed: 6180800]

Öngür D, Price JL. The organization of networks within the orbital and medial prefrontal cortex of rats, monkeys and humans. Cereb Cortex. 2000; 10(3):206–219. [PubMed: 10731217]

Palomero-Gallagher, N.; Zilles, K. Isocortex. In: Paxinos, G., editor. The Rat Nervous System. London: Elsevier; 2004.

Paolini M, Sereno MI. Direction selectivity in the middle lateral and lateral (ML and L) visual areas in the California ground squirrel. Cereb Cortex. 1998; 8(4):362–371. [PubMed: 9651131]

Paxinos, G.; Franklin, KBJ. The Mouse Brain in Stereotaxic Coordinates. Academic Press; 2003.

Paxinos, G.; Kas, L.; Ashwell, KWS.; Watson, C. Chemoarchitectonic Atlas of the Rat Forebrain. Academic Press; 1999.

Payne BR, Lomber SG, Macneil MA, Cornwell P. Evidence for greater sight in blindsight following damage of primary visual cortex early in life. Neuropsychologia. 1996; 34(8):741–774. [PubMed: 8817506]

Picanço-Diniz CW, Oliveira HL, Silveira LC, Oswaldo-Cruz E. The visual cortex of the agouti (Dasyprocta aguti): architectonic subdivisions. Braz J Med Biol Res. 1989; 22(1):121–138. [PubMed: 2758167]

Picanço-Diniz, CW. Doctoral thesis. Universidade Federal do Rio de Janerio; 1987. Organizacao do sistema visual de roedores da Amazonia: topografia das areas visuais da Cutia, Dasyprocta aguti.

Polley DB, Read HL, Storace DA, Merzenich MM. Multiparametric auditory receptive field organization across five cortical fields in the albino rat. J Neurophysiol. 2007; 97(5):3621–3638. [PubMed: 17376842]

Preuss TM. Do rats have prefrontal cortex? The Rose-Woolsey-Akert program reconsidered. J Cogn Neurosci. 1995; 7:1–24.

Preuss TM, Stepniewska I, Jain N, Kaas JH. Multiple divisions of macaque precentral motor cortex identified with neurofilament antibody SMI-32. Brain Res. 1997; 767(1):148–153. [PubMed: 9365028]

Qi HX, Kaas JH. Myelin stains reveal an anatomical framework for the representation of the digits in somatosensory area 3b of macaque monkeys. J Comp Neurol. 2004; 477(2):172–187. [PubMed: 15300788]

Rausell E, Jones EG. Chemically distinct compartment of the thalamic VPM nucleus in monkeys relay principal and spinal trigeminal pathway to different layers of the somatosensory cortex. J Neurosci. 1991; 11:226–237. [PubMed: 1702464]

Ray JP, Price JL. The organization of the thalamocortical connections of the mediodorsal thalamic nucleus in the rat, related to the ventral forebrain-prefrontal cortex topography. J Comp Neurol. 1992; 323(2):167–197. [PubMed: 1401255]

Reep RL. Cortical layer VII and presistant subplate cells in mammalian brains. Brain Behav Evol. 2000; 56:212–234. [PubMed: 11155000]

Reep RL, Chandler HC, King V, Corwin JV. Rat posterior parietal cortex: topography of corticocortical and thalamic connections. Exp Brain Res. 1994; 100(1):67–84. [PubMed: 7813654]

Reep RL, Goodwin GS, Corwin JV. Topographic organization in the corticocortical connections of medial agranular cortex in rats. J Comp Neurol. 1990; 294(2):262–280. [PubMed: 2332532]

Reid SN, Juraska JM. The cytoarchitectonic boundaries of the monocular and binocular areas of the rat primary visual cortex. Brain Res. 1991; 563(1–2):293–296. [PubMed: 1786543]

Reinoso BS, Pimenta AF, Levitt P. Expression of the mRNAs encoding the limbic system-associated membrane protein (LAMP): I. Adult rat brain. J Comp Neurol. 1996; 375(2):274–288. [PubMed: 8915830]

Remple MS, Reed JL, Stepniewska I, Lyon DC, Kaas JH. The organization of frontoparietal cortex in the tree shrew (Tupaia belangeri): II. Connectional evidence for a frontal-posterior parietal network. J Comp Neurol. 2007; 501(1):121–49. [PubMed: 17206607]

Remple MS, Reed JL, Stepniewska I, Kaas JH. Organization of frontoparietal cortex in the tree shrew (Tupaia belangeri). I. Architecture, microelectrode maps, and corticospinal connections. J Comp Neurol. 2006; 497(1):133–54. [PubMed: 16680767]

Remple MS, Henry EC, Catania KC. Organization of somatosensory cortex in the laboratory rat (Rattus norvegicus): Evidence for two lateral areas joined at the representation of the teeth. J Comp Neurol. 2003; 467(1):105–118. [PubMed: 14574683]

Robson JA, Hall WC. Connections of layer VI in striate cortex of the grey squirrel (Sciurus carolinensis). Brain Res. 1975; 93(1):133–139. [PubMed: 49213]

Robson JA, Hall WC. The organization of the pulvinar in the grey squirrel (Sciurus carolinensis). II. Synaptic organization and comparisons with the dorsal lateral geniculate nucleus. J Comp Neurol. 1977; 173(2):389–416. [PubMed: 853144]

Rosa MG. Topographic organization of extrastriate areas in the flying fox: implications for the evolution of mammalian visual cortex. J Comp Neurol. 1999; 411(3):503–523. [PubMed: 10413783]

Rosa MG, Krubitzer LA. The evolution of visual cortex: where is V2? Trends Neurosci. 1999; 22(6): 242–248. [PubMed: 10354599]

Rosa MGP, Casagrande VA, Preuss TM, Kaas JH. Visual field representation in striate and prestriate cortices of a prosimian primate (Galago garnetti). The American Physiological Society. 1997:3193–3217.

Rose M. Histologische Localization der Grosshirnide der kleinen Saugetire (Rodentia, Insectivora, Chiroptera). JF Phychol U Neur. 1912; 19:389–479.

Rose M. Cytoarchitektonischer Atlas der Großhirnrinde der Maus. J Psychol Neurol. 1929; 35:65–173.

Rose M. Cytoarchitektonischer Atlas der Großhinrinde der Maus. J Psychol Neurol. 1930; 40:1–51.

Rutkowski RG, Miasnikov AA, Weinberger NM. Characterization of multiple physiological fields within the anatomical core of rat auditory cortex. Hear Res. 2003; 181(1–2):116–130. [PubMed: 12855370]

Ryugo DK, Killackey HP. Differential telencephalic projections of the medial and ventral divisions of the medial geniculate body of the rat. Brain Res. 1974; 82(1):173–177. [PubMed: 4611594]

Sanderson KJ, Welker W, Shambes GM. Reevaluation of motor cortex and of sensorimotor overlap in cerebral cortex of albino rats. Brain Res. 1984; 292(2):251–260. [PubMed: 6692158]

Sanides, F. Functional architecture of motor and sensory cortices in primates in the light of a new concept of neocortex evolution. In: Montagna, W., editor. The primate brain. New York: Appleton-Century-Crofts; 1970. p. 137-208.

Schober W. The rat cortex in stereotaxic coordinates. J Hirnforsch. 1986; 27(2):121–143. [PubMed: 3722803]

Sereno M, Rodman H, Karten H. Organization of visual cortex in the california ground squirrel. Society for Neuroscience Abstract. 1991

Sewards TV, Sewards MA. Cortical association areas in the gustatory system. Neurosci Biobehav Rev. 2001; 25(5):395–407. [PubMed: 11566478]

Slutsky DA, Manger PR, Krubitzer L. Multiple somatosensory areas in the anterior parietal cortex of the California ground squirrel (Spermophilus beecheyii). J Comp Neurol. 2000; 416(4):521–539. [PubMed: 10660882]

Sripanidkulchai K, Wyss JM. Thalamic projections to retrosplenial cortex in the rat. J Comp Neurol. 1986; 254(2):143–165. [PubMed: 3794004]

Sur M, Nelson RJ, Kaas JH. The representation of the body surface in somatosensory area I of the grey squirrel. J Comp Neurol. 1978; 179(2):425–449. [PubMed: 417097]

Swanson, LW. Brain Maps: Structure of the Rat Brain. 1. New York: Elsevier; 1992.

Swanson, LW. Brain Maps: Structure of the Rat Brain. Academic Press; 2003.

Szél A, Röhlich P. Four types of photoreceptors in the ground squirrel retina as evidenced by immunocytochemistry. Vision Research. 1988; 28:1297–1302. [PubMed: 3256146]

Thomas H, Tillein J, Heil P, Scheich H. Functional organization of auditory cortex in the mongolian gerbil (Meriones unguiculatus). I. Electrophysiological mapping of frequency representation and distinction of fields. Eur J Neurosci. 1993; 5(7):882–897. [PubMed: 8281300]

Tiao YC, Blakemore C. Functional organization in the visual cortex of the golden hamster. J Comp Neurol. 1976; 168(4):459–481. [PubMed: 939818]

Tusa RJ, Rosenquist AC, Palmer LA. Retinotopic organization of areas 18 and 19 in the cat. J Comp Neurol. 1979; 185(4):657–678. [PubMed: 447876]

Uylings HB, Groenewegen HJ, Kolb B. Do rats have a prefrontal cortex? Behav Brain Res. 2003; 146(1–2):3–17. [PubMed: 14643455]

Valente T, Auladell C, Pérez-Clausell J. Postnatal development of zinc-rich terminal fields in the brain of the rat. Exp Neurol. 2002; 174:215–229. [PubMed: 11922663]

Van Brederode JF, Mulligan KA, Hendrickson AE. Calcium-binding proteins as markers for subpopulations of GABAergic neurons in monkey striate cortex. J Comp Neurol. 1990; 298(1): 1–22. [PubMed: 2170466]

van Groen T, Wyss JM. Connections of the retrosplenial granular a cortex in the rat. J Comp Neurol. 1990; 300(4):593–606. [PubMed: 2273095]

Van der Gucht E, Hof PR, Van Brussel L, Burnat K, Arckens L. Neurofilament protein and neuronal activity markers define regional architectonic parcellation in the mouse visual cortex. Cereb Cortex. 2007

Van Hooser SD, Nelson SB. The squirrel as a rodent model of the human visual system. Vis Neurosci. 2006; 23(5):765–778. [PubMed: 17020632]

Voelker CC, Garin N, Taylor JS, Gahwiler BH, Hornung JP, Molnar Z. Selective neurofilament (SMI-32, FNP-7 and N200) expression in subpopulations of layer V pyramidal neurons in vivo and in vitro. Cereb Cortex. 2004; 14(11):1276–1286. [PubMed: 15166101]

Vogt, BA.; Vogt, L.; Farber, NB. Cingulate Cortex and Disease Models. In: Paxinos, G., editor. The Rat Nervous System. London: Elsevier; 2004.

Vogt, BA. Structural organization of cingulate cortex: areas, neurons, and somatodendritic transmitter receptors. In: Vogt, BA.; Gabriel, M., editors. Neurobiology of Cingulate Cortex and Limbic Thalamus. Birkhäuser; Boston: 1993. p. 19-70.

Vogt BA, Finch DM, Olson CR. Functional heterogeneity in cingulate cortex: the anterior executive and posterior evaluative regions. Cereb Cortex. 1992; 2(6):435–443. [PubMed: 1477524]

Vogt BA, Plager MD, Crino PB, Bird ED. Laminar distributions of muscarinic acetylcholine, serotonin, GABA and opioid receptors in human posterior cingulate cortex. Neuroscience. 1990; 36(1):165–174. [PubMed: 1977100]

Vogt BA, Miller MW. Cortical connections between rat cingulate cortex and visual, motor, and postsubicular cortices. J Comp Neurol. 1983; 216(2):192–210. [PubMed: 6863602]

Vogt BA, Peters A. Form and distribution of neurons in rat cingulate cortex: areas 32, 24, and 29. J Comp Neurol. 1981; 195(4):603–625. [PubMed: 7462444]

Vogt BA, Rosene DL, Peters A. Synaptic termination of thalamic and callosal afferents in cingulate cortex of the rat. J Comp Neurol. 1981; 201(2):265–283. [PubMed: 7287929]

Wagor E. Pattern vision in the grey squirrel after visual cortex ablation. Behav Biol. 1978; 22(1):1–22. [PubMed: 623604]

Wagor E, Mangini NJ, Pearlman AL. Retinotopic organization of striate and extrastriate visual cortex in the mouse. J Comp Neurol. 1980; 193(1):187–202. [PubMed: 6776164]

Wallace MN. Organization of the mouse cerebral cortex: a histochemical study using glycogen phosphorylase. Brain Res. 1983; 267(2):201–216. [PubMed: 6871673]

Wallace MN, Rutkowski RG, Palmer AR. Identification and localization of auditory areas in guinea pig cortex. Exp Brain Res. 2000; 132(4):445–456. [PubMed: 10912825]

Wallace MT, Ramachandran R, Stein BE. A revised view of sensory cortical parcellation. Proc Natl Acad Sci U S A. 2004; 101(7):2167–2172. [PubMed: 14766982]

Wang Q, Burkhalter A. Area map of mouse visual cortex. J Comp Neurol. 2007; 502(3):339–357. [PubMed: 17366604]

Wang Y, Kurata K. Quantitative analyses of thalamic and cortical origins of neurons projecting to the rostral and caudal forelimb motor areas in the cerebral cortex of rats. Brain Res. 1998; 781(1–2): 135–47. [PubMed: 9507093]

Wassle H, Regus-Leidig H, Haverkamp S. Expression of the vesicular glutamate transporter vGluT2 in a subset of cones of the mouse retina. J Comp Neurol. 2006; 496(4):544–555. [PubMed: 16572432]

Weber JT, Casagrande VA, Harting JK. Transneuronal transport of [3H]proline within the visual system of the grey squirrel. Brain Res. 1977; 129(2):346–352. [PubMed: 69471]

West RW, Dowling JE. Anatomical evidence for cone and rod-like receptors in the gray squirrel, ground squirrel, and prairie dog retinas. J Comp Neurol. 1975; 159(4):439–460. [PubMed: 1127139]

Wise, SP.; Donoghue, JP. Motor cortex of rodents. New York: Plenum; 1986. p. 243-269.

Wong P, Kaas JH. Architectonic subdivisions of neocortex in the grey squirrel (Sciurus carolinensis). Soc for Neurosci Abstract. 2006

Wong-Riley M. Changes in the visual system of monocularly sutured or enucleated cats demonstrable with cytochrome oxidase histochemistry. Brain Res. 1979; 171(1):11–28. [PubMed: 223730]

Woolsey TA, Van der Loos H. The structural organization of layer IV in the somatosensory region (SI) of mouse cerebral cortex. The description of a cortical field composed of discrete cytoarchitectonic units. Brain Res. 1970; 17(2):205–242. [PubMed: 4904874]

Woolsey TA, Welker C, Schwartz RH. Comparative anatomical studies of the SmL face cortex with special reference to the occurrence of “barrels” in layer IV. J Comp Neurol. 1975; 164(1):79–94. [PubMed: 809494]

Wu CW, Bichot NP, f Kaas JH. Converging evidence from microstimulation, architecture, and connections for multiple motor areas in the frontal and cingulate cortex of prosimian primates. J Comp Neurol. 2000; 423(1):140–177. [PubMed: 10861543]

Zacco A, Cooper V, Chantler PD, Fisher-Hyland S, Horton HL, Levitt P. Isolation, biochemical characterization and ultrastructural analysis of the limbic system-associated membrane protein (LAMP), a protein expressed by neurons comprising functional neural circuits. J Neurosci. 1990; 10(1):73–90. [PubMed: 1688937]

Zilles, K. Organization of the Neocortex. In: Tees, B.; Kolb, RC., editors. The Cerebral Cortex of the Rat. MIT Press; 1990.

Zilles, K.; Wree, A. Cortex: Areal and laminar structure. In: Paxinos, G., editor. The Rat Nervous System. 2. San Diego: Academic Press; 1995. p. 649-685.

Zilles, K.; Wree, A. Cortex: Areal and laminar structure. In: Paxinos, G., editor. The Rat Nervous System, Vol. 1: Forebrain and Midbrain. New York: Academic Press; 1985. p. 375-415.

Zilles K, Wree A, Schleicher A, Divac I. The monocular and binocular subfields of the rat's primary visual cortex: a quantitative morphological approach. J Comp Neurol. 1984; 226(3):391–402. [PubMed: 6611357]

Zilles K, Zilles B, Schleicher A. A quantitative approach to cytoarchitectonics. VI. The areal pattern of the cortex of the albino rat. Anat Embryol (Berl). 1980; 159(3):335–360. [PubMed: 6970009]

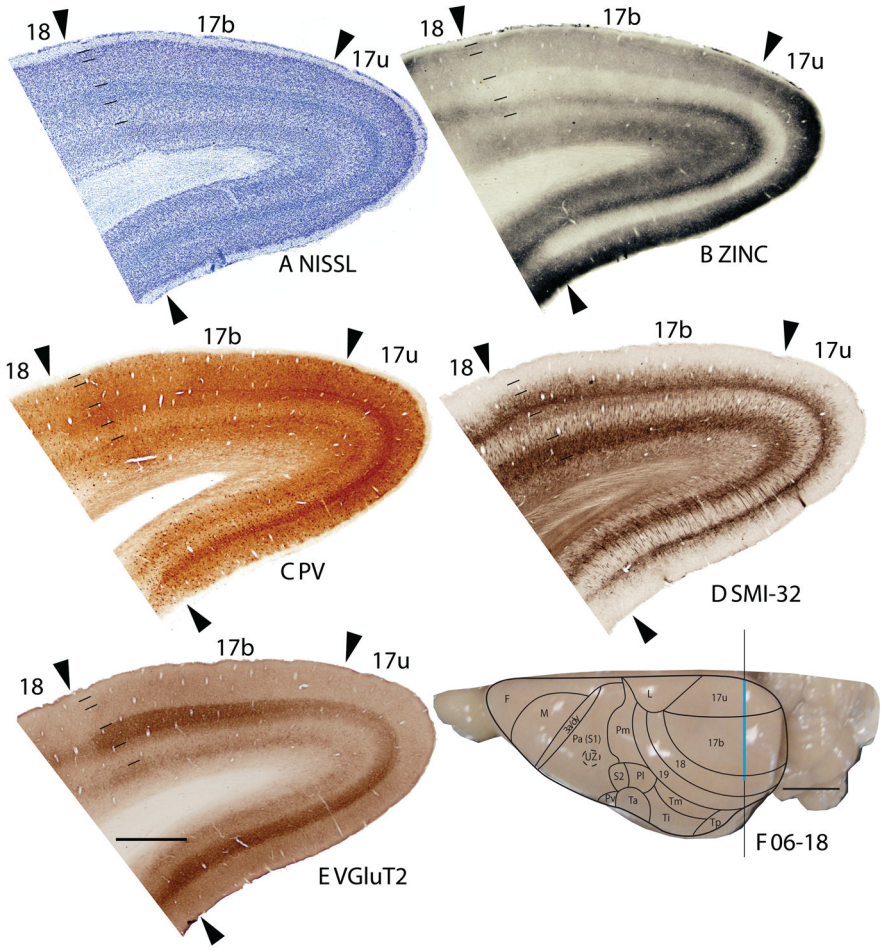

Figure 1.

Architectonic characteristics of visual areas 17 and 18. Coronal sections from occipital cortex were processed for (A) Nissl substance, (B) synaptic zinc, (C) parvalbumin (PV), (D) neurofilaments with the SMI-32 antibody, or (E) the vesicle glutamate transporter 2 (VGluT2). The boundaries of proposed cortical areas are shown on a dorsal view of a squirrel brain in panel F. The vertical line through areas 17 and 18 indicates the locations where sections were taken for panels A–E. The blue line marks the regions shown in these sections. Occipital areas 17, 18 and 19 are adopted from Brodmann (1909). 17u refers to the monocular region, while 17b refers to the binocular region of area 17. Arrowheads mark architectonic boundaries. Short lines under 17/18 arrow heads separate cortical layers 1–6. See table 1 for abbreviations for other areas. The scale bar for brain sections (panel E) = 2mm. The scale bar on the brain (panel F) = 5mm. Sections were from squirrel 06-18.

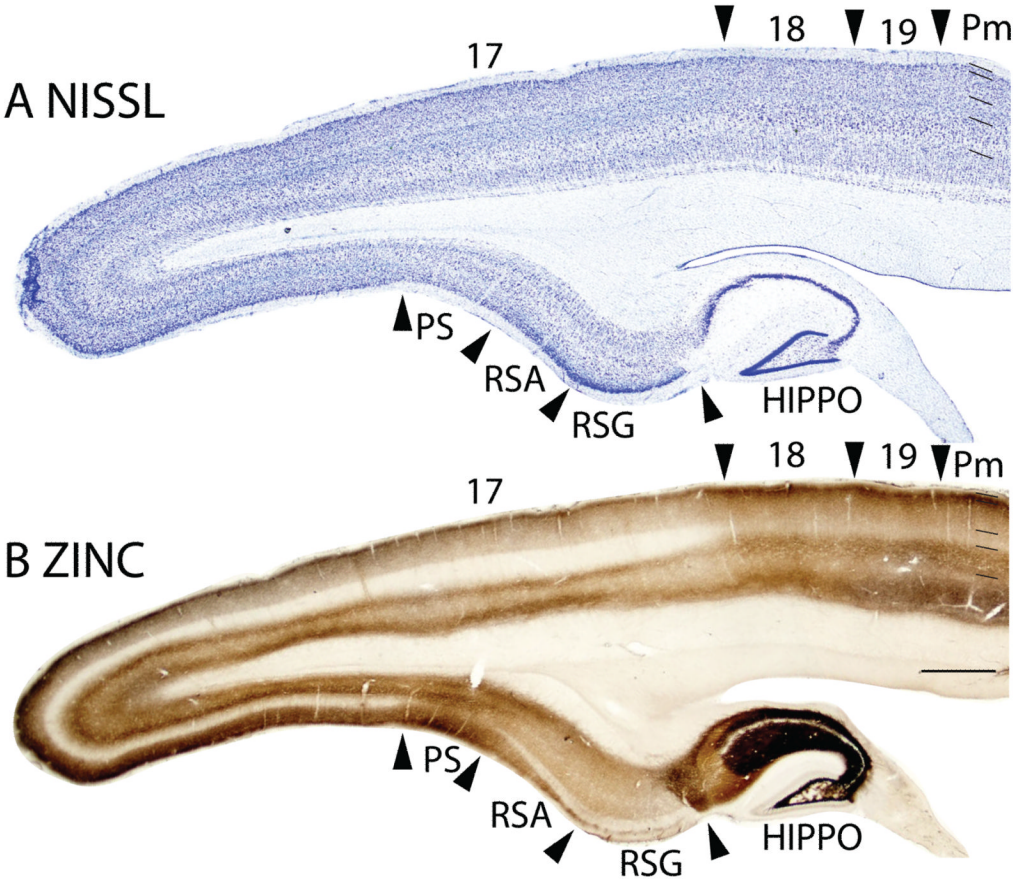

Figure 2.

Architectonic characteristics of visual and adjoining retrosplenial cortex. Brain sections were cut in the parasagittal plane. The sections processed for Nissl substance (A) and zinc (B) were from near the medial wall of the caudal hemisphere. See table 1 for abbreviations. Scale bar = 2mm. Sections were from 05-19. 2. Architectonic characteristics of visual and adjoining retrosplenial cortex. Brain sections were cut in the parasagittal plane. The sections processed for Nissl substance (A) and zinc (B) were from near the medial wall of the caudal hemisphere. See table 1 for abbreviations. Scale bar = 2mm. Sections were from 05-19.

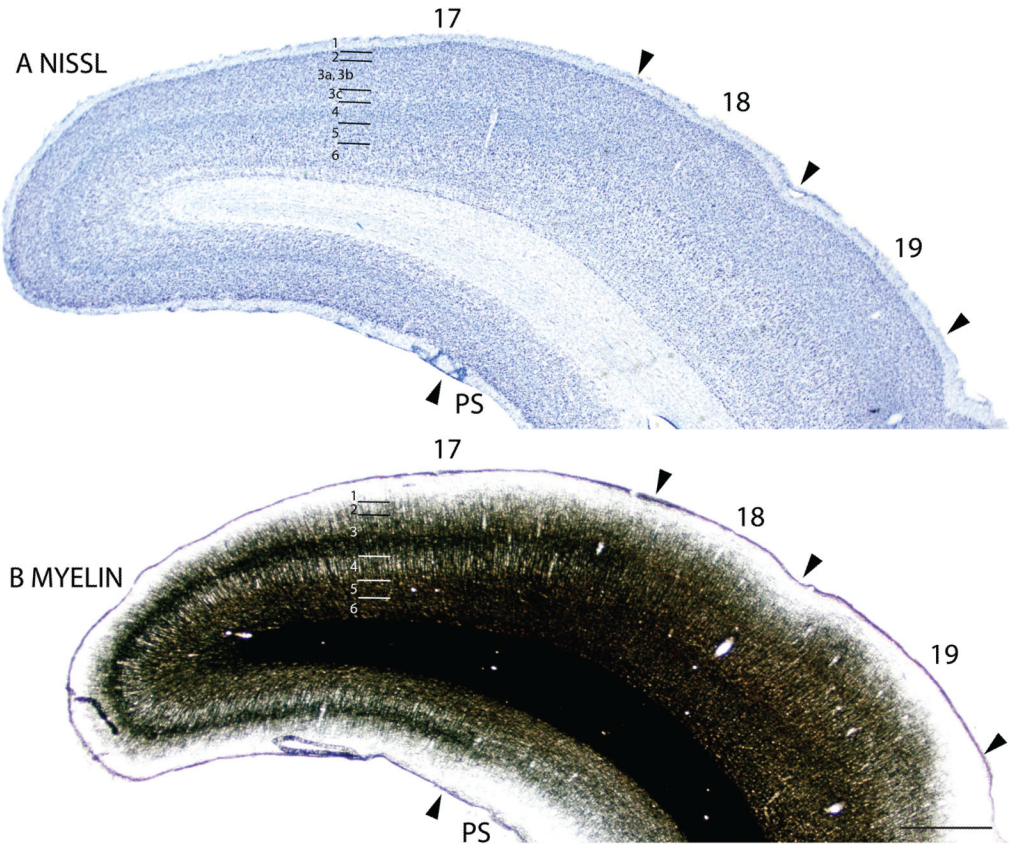

Figure 3.
Adjacent coronal brain sections through occipital cortex stained for Nissl substance (A) or myelin (B). Scale bar = 2mm. Sections were from 06-60.

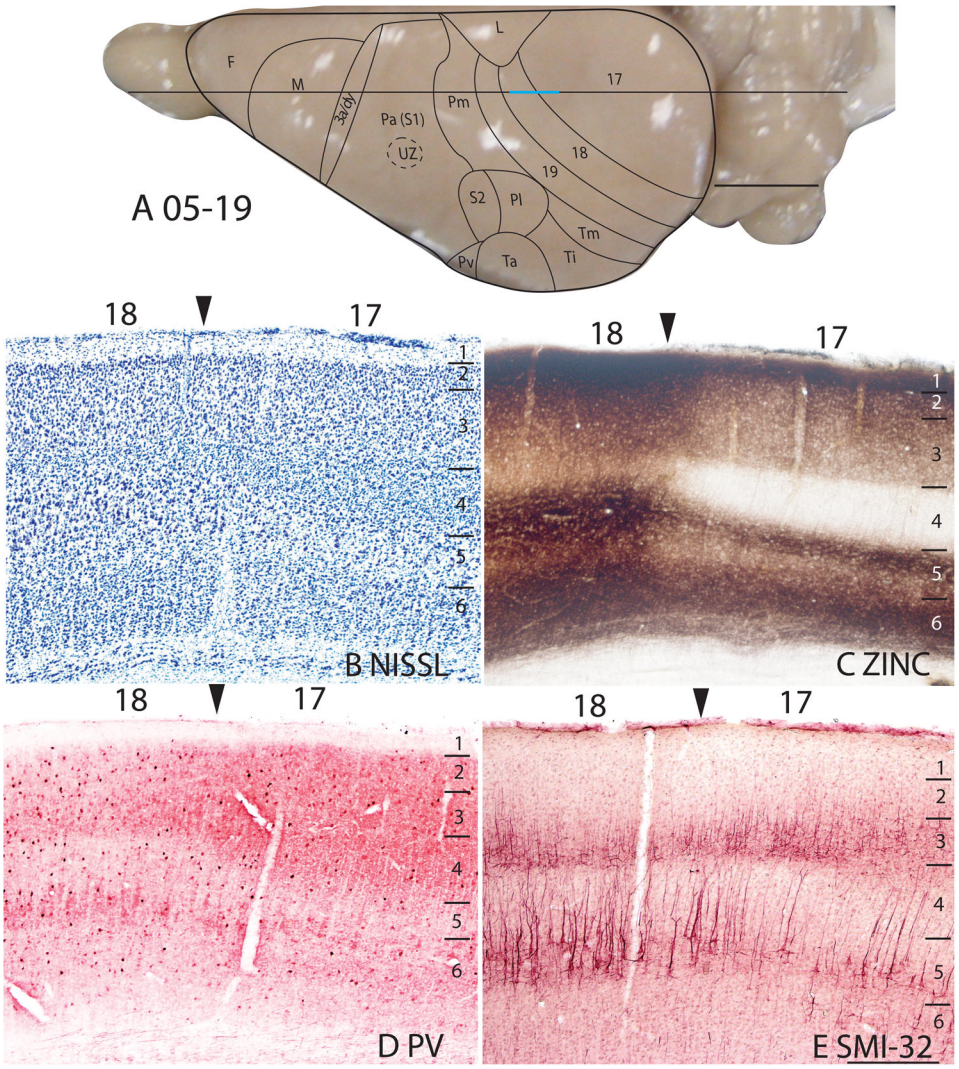

Figure 4.

Architectonic characteristics of the bordering region between area 17 and 18. The horizontal line across the dorsal view of the brain in panel A indicates the location of the sagittal sections used in this figure, and the blue line marks the extent of the sections shown in panels B–E. The higher magnification of these panels than in previous figures allows some of the laminar features of area 17 and 18 to be seen more distinctly. The scale bar in panel A = 5mm, panel E = 0.5mm. Squirrel 05-19. The cortical areas depicted on the dorsal view of a squirrel brain in Panel A and similar views in subsequent figures are based on present and previous architectonic and physiological results (see Methods).

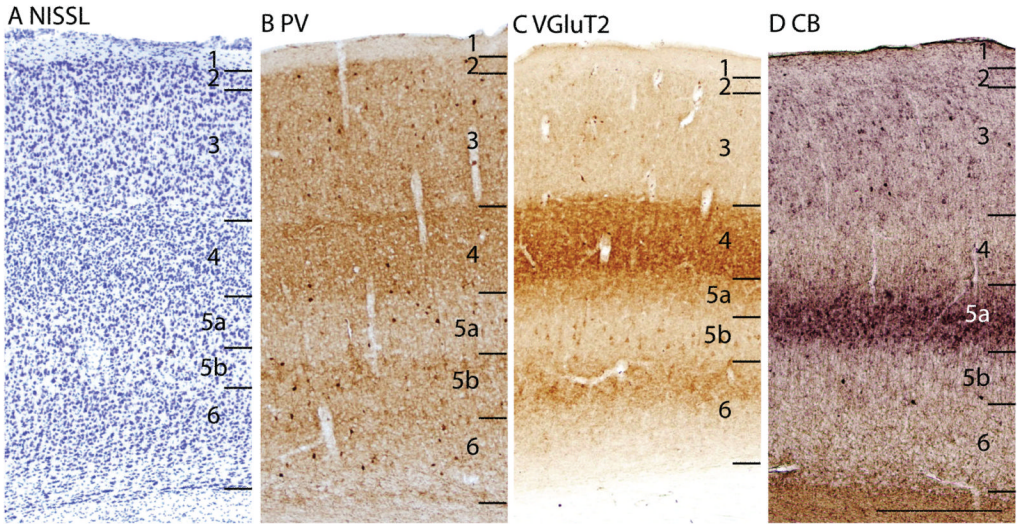

Figure 5.
The laminar architecture of area 17 at higher magnification. Note how the PV, VGluT2 and CB preparations reveal sublayers. Scare bar = 0.5mm. Sections are in the sagittal plane, from case 05-19.

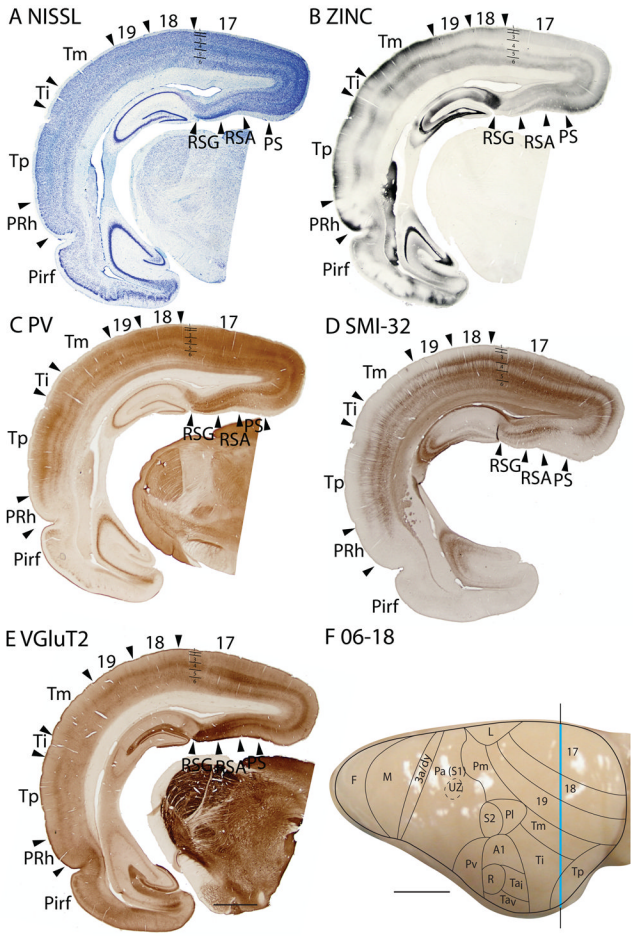

Figure 6.

Architectonic characteristics of subdivisions of occipital and temporal cortex in squirrel 06-18. Borders of cortical layers are marked at the 17/18 boundary. The blue portion of the vertical line across the cortex indicates the location where the coronal brain sections in panels A–E were obtained. Scale bar in panel E = 2mm, panel F = 5mm.

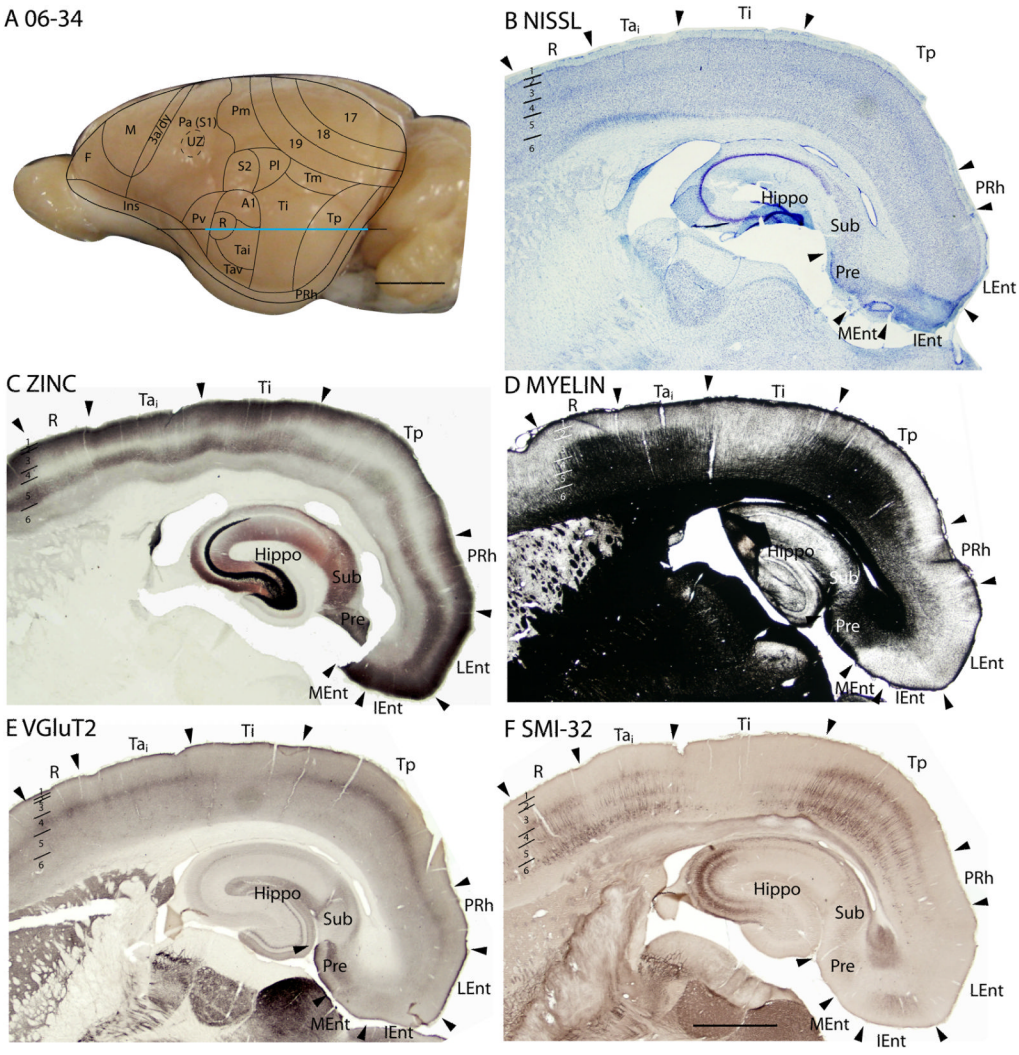

Figure 7.

Architectonic characteristics of subdivisions of temporal cortex in squirrel 06-34. Cortical areas are shown on a lateral view of the left caudal hemisphere in panel A. The blue part of the horizontal line across the brain indicates the location of the horizontal brain sections illustrated in panels B–F. Scale bar in panel A = 5mm, panel F = 2mm.

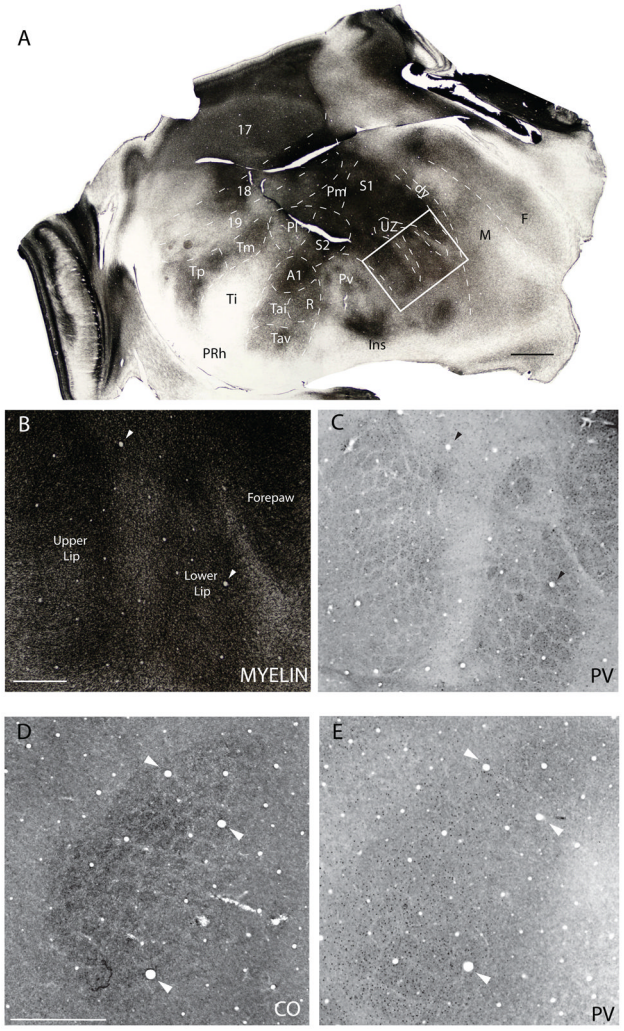

Figure 8.

Barrel field of the grey squirrel. A. A myelin stained section cut parallel to the surface of an artificially flattened cerebral hemisphere. Dashed lines show approximate cortical boundaries comparable to the reconstructed dorsal view of the brain in Fig. 1. The boxed region in A is shown in B and C at higher magnification in myelin and PV preparations respectively. D and E are from a separate case and show the barrel field in cytochrome oxidase (CO) and PV preparations respectively. See table 1 for abbreviations. Scale bar for flattened section = 2.0mm, for B and C = 1.0mm, for D and E = 2.0mm.

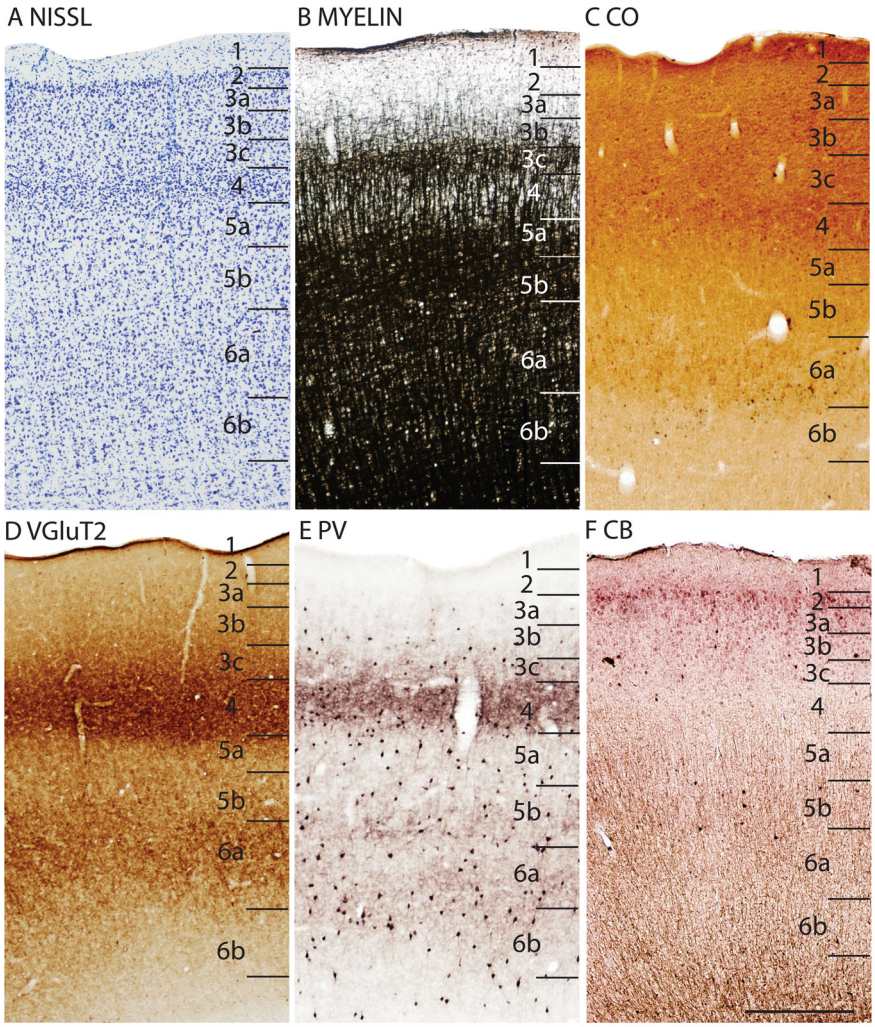

Figure 9.
The laminar architecture of area Pa(S1) at higher magnification. Scale bar = 0.5mm.

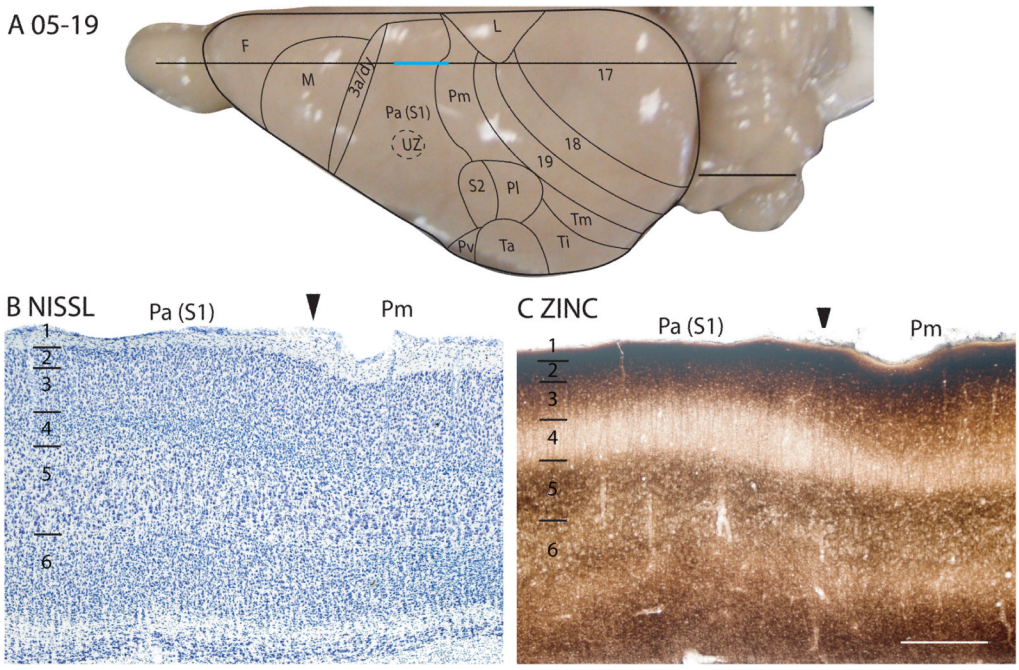

Figure 10.

Architectonic characteristics of subdivisions of the somatosensory cortex in squirrel 05-19. The horizontal line across the dorsal view of the brain in panel A indicates the location of the sagittal sections used in this figure, and the blue line marks the extent of the sections shown in panels B and C. The extent of each cortical layers 1 to 6 is indicated by the short horizontal lines on panels B–E. The scale bar on the brain (panel A) = 5mm. The scale bar for brain sections (panel E) = 0.5mm.

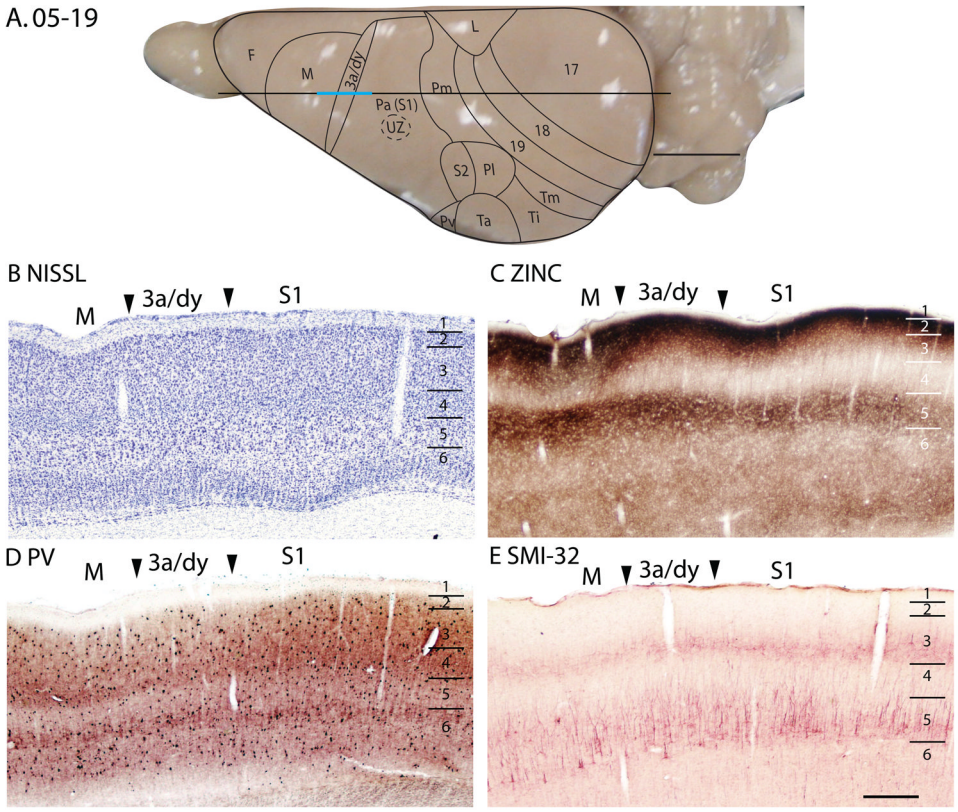

Figure 11.

Architectonic characteristics of subdivisions of the motor and somatosensory cortex in squirrel 05-19. The horizontal line across the dorsal view of the brain in panel A indicates the location of the sagittal sections used in this figure, and the blue line marks the extent of the sections shown in panels B–E. The extent of each cortical layers 1 to 6 is indicated by the short horizontal lines on panels B–E. Scale bar on the brain (panel A) = 5mm. Scale bar for brain sections (panel E) = 0.5mm.

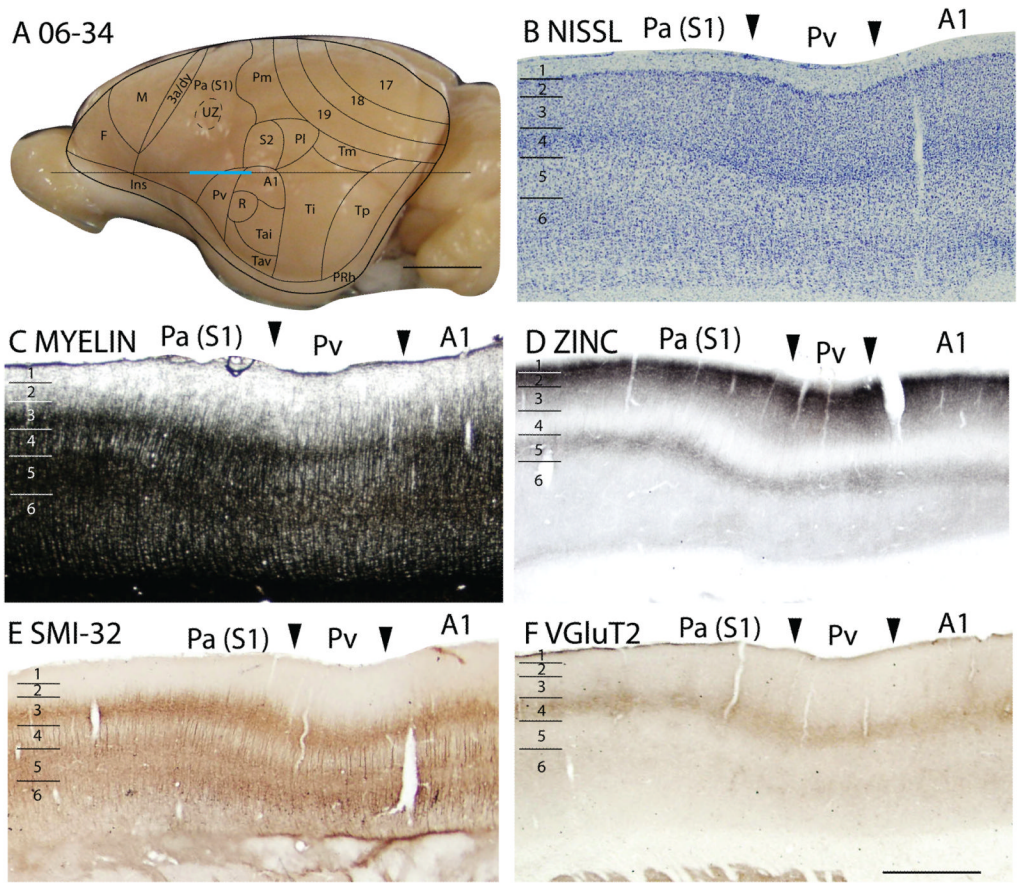

Figure 12.

Architectonic characteristics of subdivisions of parietal and primary auditory cortices in squirrel 06-34. Cortical areas are shown on a lateral view of the left hemisphere in panel A. The blue horizontal line across the brain indicates the location of the brain sections illustrated in panels B–F. Short horizontal lines on panels B–F indicate the extent of the 6 cortical layers. Scale bar on the brain (panel A) = 5mm. Scale bar for brain sections (panel F) = 1mm.

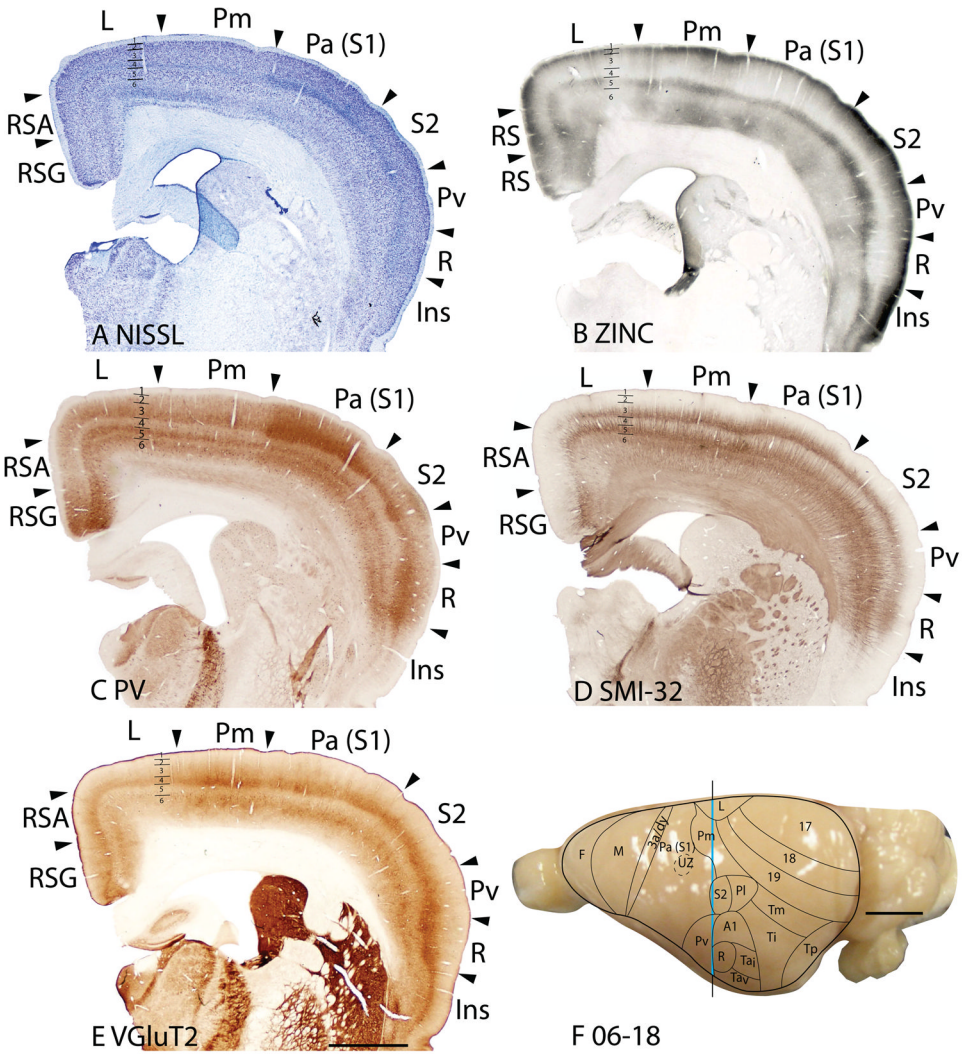

Figure 13.

Architectonic characteristics of subdivisions of the parietal and limbic cortices in squirrel 06-18. Borders of cortical layers are marked at the limbic (L) area. The blue vertical line across the cortex (panel F) indicates the location where the brain sections in panels A–E were obtained. Short horizontal lines on panels A–E indicate the extent of the 6 cortical layers. Scale bar in panel E = 2mm, panel F = 5mm.

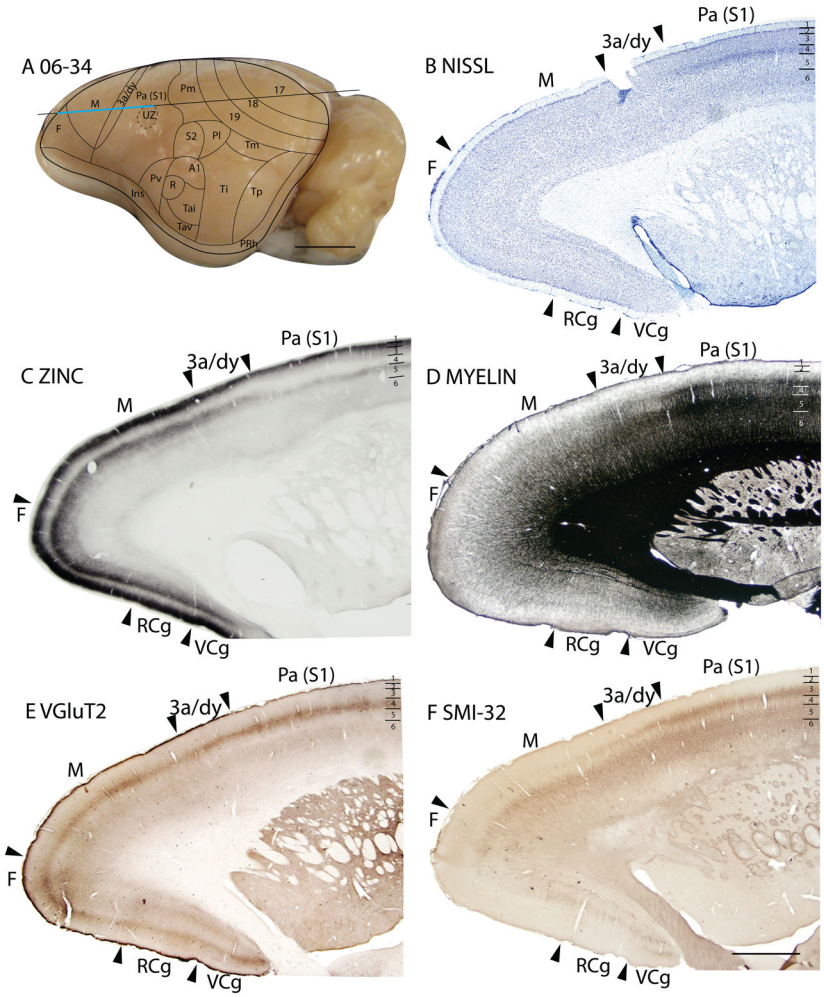

Figure 14.

Architectonic characteristics of subdivisions of frontal and cingulate cortices in squirrel 06-34. Cortical areas are shown on a lateral view of the left rostral hemisphere in panel A. The blue horizontal line across the brain indicates the location of the brain sections illustrated in panels B–F. Short horizontal lines on panels B–Fshow the extent of the cortical layers. Scale bar on the brain (panel A) = 5mm. Scale bar for brain sections (panel F) = 2mm.

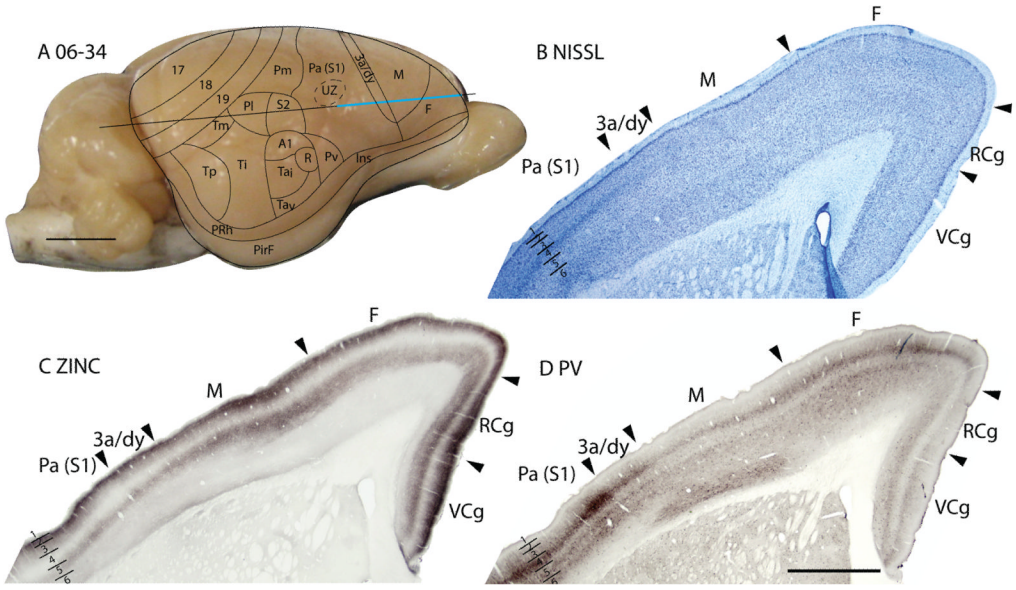

Figure 15.

Architectonic characteristics of subdivisions of frontal and cingulate cortices in squirrel 06-34. Cortical areas are shown on a lateral view of the right rostral hemisphere in panel A. The blue horizontal line across the brain indicates the location of the brain sections illustrated in panels B–D. Short horizontal lines on panels B–D show the extent of the cortical layers. Scale bar on the brain (panel A) = 5mm. Scale bar for brain sections (panel D) = 2mm.

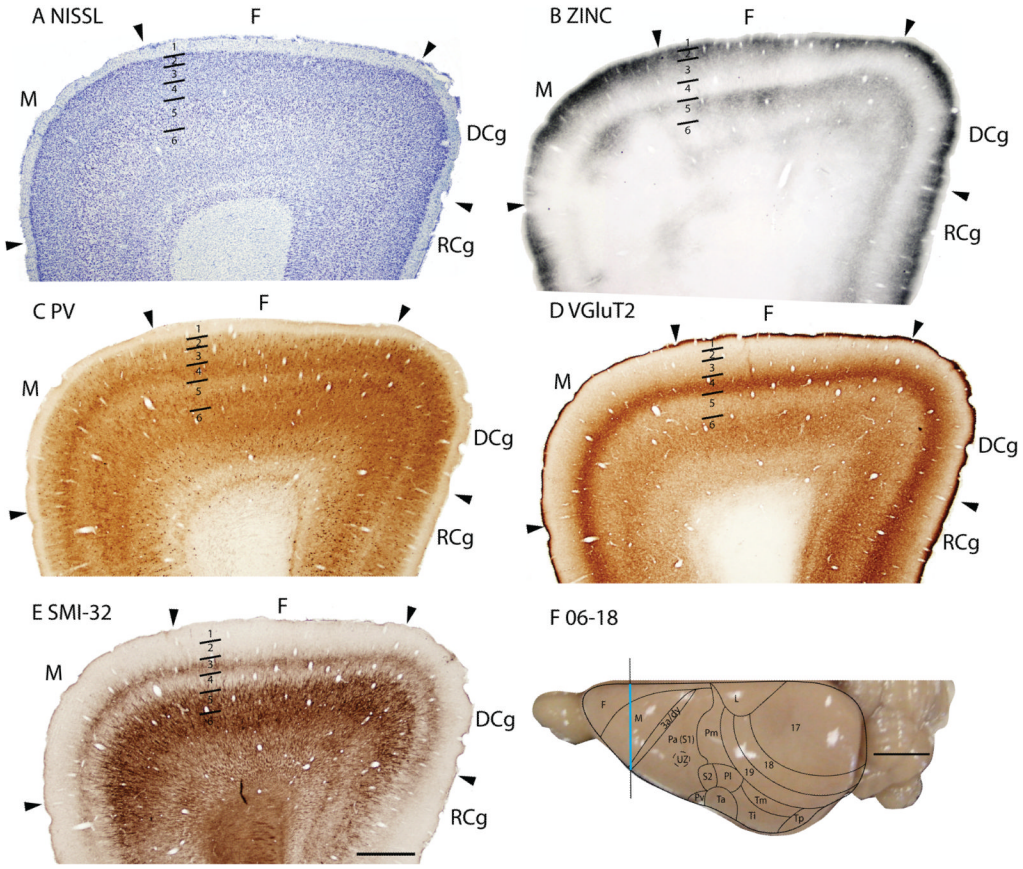

Figure 16.

Architectonic characteristics of subdivisions of the frontal cortex in squirrel 06-18. Borders of cortical layers are marked at the frontal (F) area. The blue vertical line across the cortex (panel F) indicates the location where the brain sections in panels A–E were obtained. Scale bar in panel E = 2mm, panel F = 5mm.

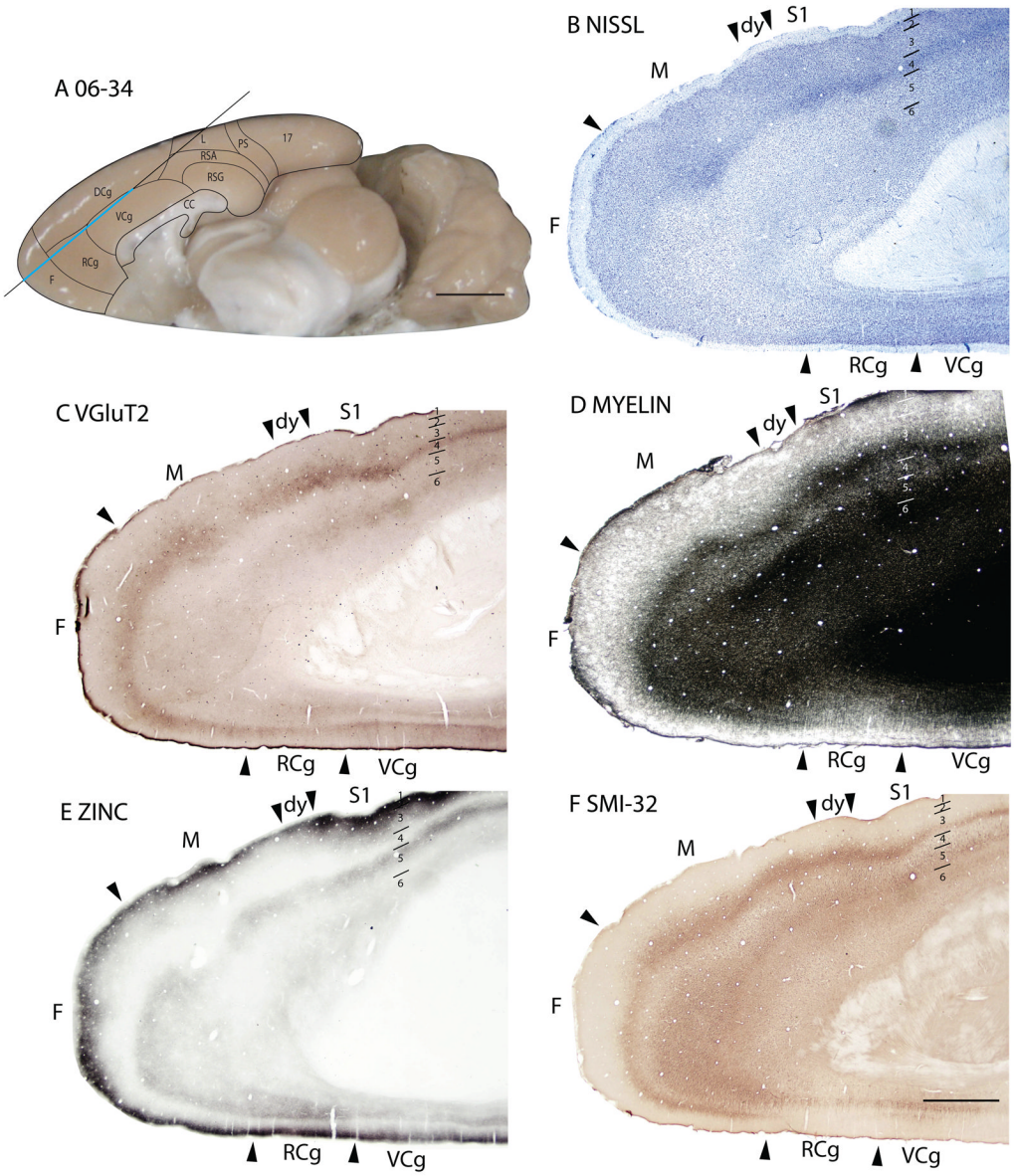

Figure 17.

Architectonic characteristics of subdivisions of frontal and cingulate cortices in squirrel 06-34. Cortical areas are shown on a medial view of the left hemisphere in panel A. The blue horizontal line across the brain indicates the location of the brain sections illustrated in panels B–F. Short horizontal lines on panels B–F show the extent of the cortical layers. Scale bar on the brain (panel A) = 5mm. Scale bar for brain sections (panel F) = 2mm.

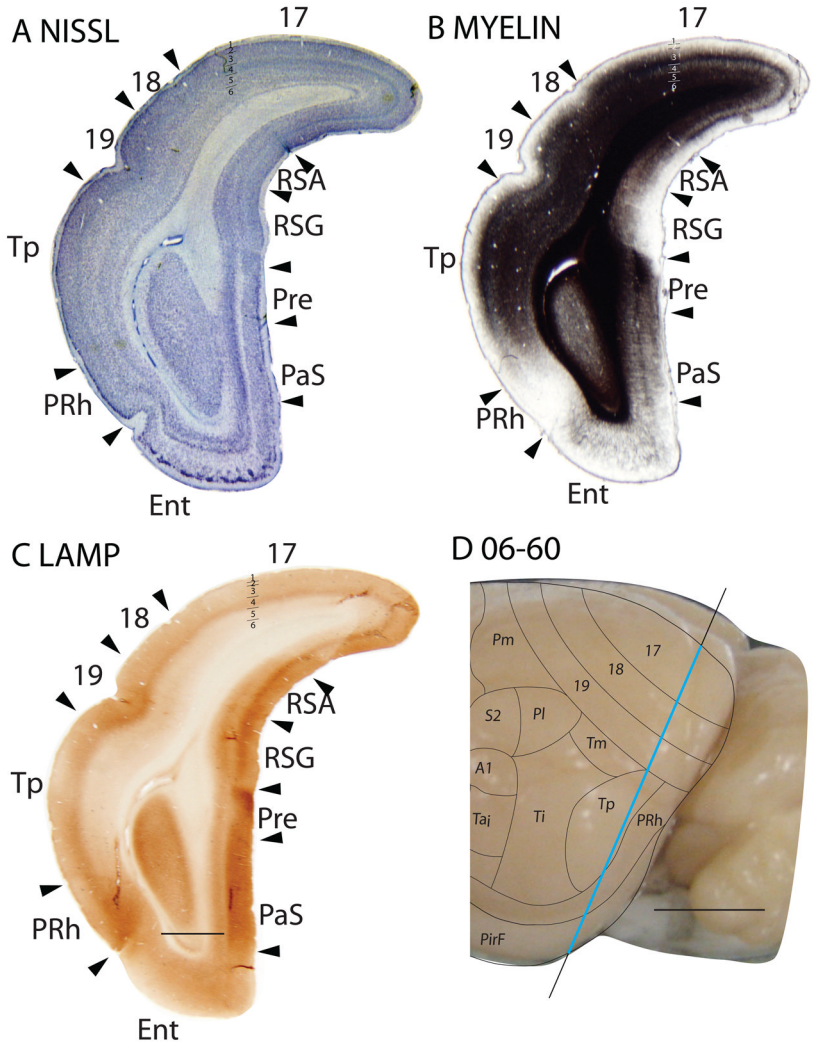

Figure 18.

Architectonic characteristics of subdivisions of retrosplenial cortex in squirrel 06-60. Cortical areas are shown on a lateral view of the left caudal hemisphere in panel D. The blue horizontal line across the brain indicates the location of the brain sections illustrated in panels A–C. Short horizontal lines on panels A–C show the extent of the cortical layers. The limbic areas show darker staining in the Limbic Associated Membrane protein (LAMP) compared to other cortical areas, such as area 17 and 18. Scale bar on the brain (panel D) = 5mm. Scale bar for brain sections (panel C) = 2mm.

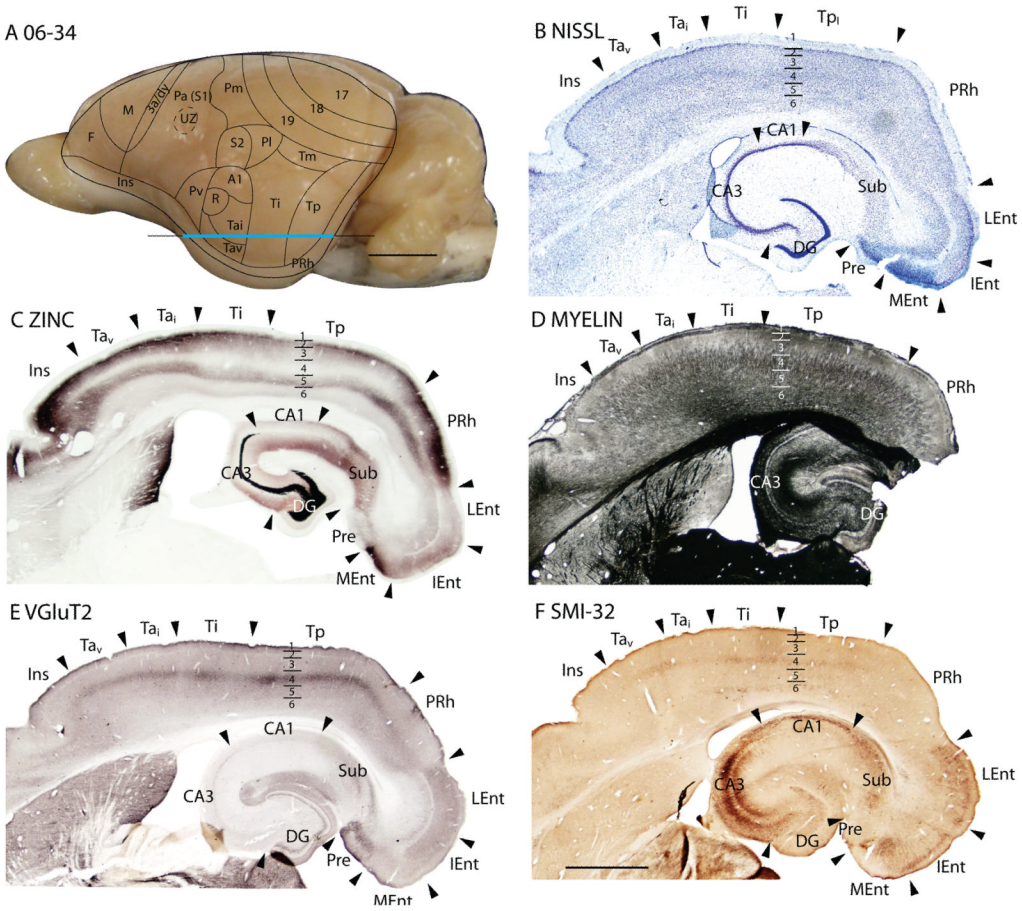

Figure 19.

Architectonic characteristics of subdivisions of temporal and insular cortices in squirrel 06-34. Cortical areas are shown on a medial view of the left hemisphere in panel A. The blue horizontal line across the brain indicates the location of the brain sections illustrated in panels B–F. Short horizontal lines on panels B–F show the extent of the cortical layers. Scale bar on the brain (panel A) = 5mm. Scale bar for brain sections (panel F) = 2mm.

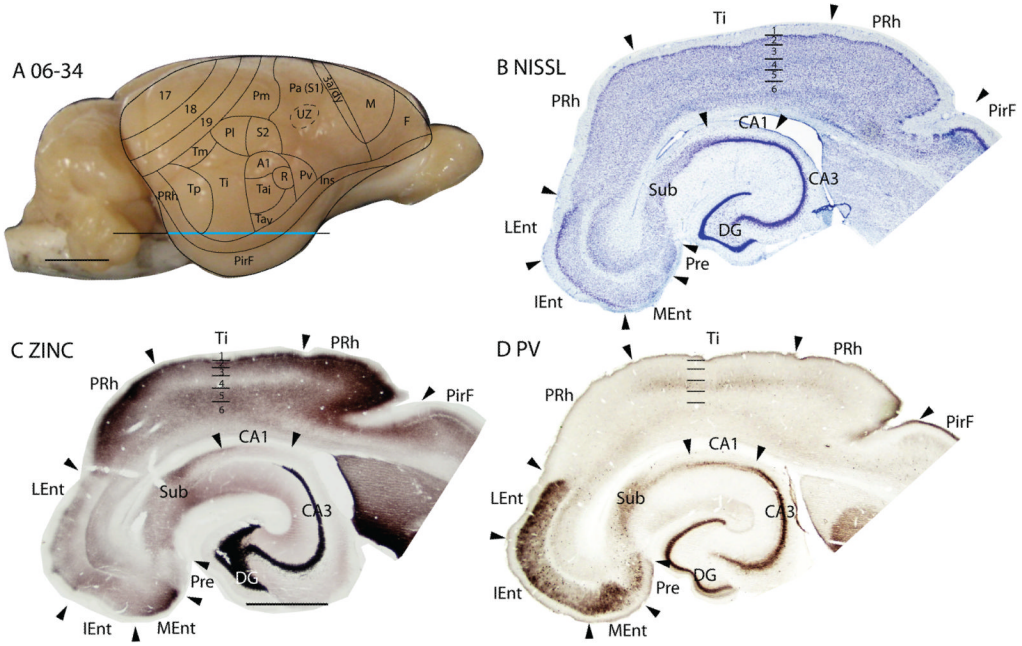

Figure 20.

Architectonic characteristics of subdivisions of rhinal cortex in squirrel 06-34. Cortical areas are shown on a lateral view of the right hemisphere in panel A. The blue horizontal line across the brain indicates the location of the brain sections illustrated in panels B–D. Short horizontal lines on panels B–D show the extent of the cortical layers. Scale bar on the brain (panel A) = 5mm. Scale bar for brain sections (panel D) = 2mm.

Table 1

Abbreviations

3a/dy	Dysgranular region
A1	Primary auditory cortex
CA1	*Cornu Ammonis 1*
CA3	*Cornu Ammonis 3*
CB	Calbindin
CO	Cytochrome oxidase
DCg	Dorsal cingulate area
DG	Dentate gyrus
Ent	Entorhinal area
F	Frontal area
Hippo	Hippocampus
IEnt	Intermediate entorhinal area
Ins	Insular area
L	Limbic area
LAMP	Limbic associated membrane protein
LEnt	Lateral entorhinal area
M1	Primary motor cortex
MEnt	Medial entorhinal area
Pa(S1)	Parietal anterior area
PaS	Parasubiculum
PB	Phosphate buffer
Pirf	Piriform cortex
Pl	Parietal lateral area
Pm	Parietal medial area
Pre	Presubiculum
PRh	Perirhinal area
PS	Prostriata
Pv	Parietal ventral area
PV	Parvalbumin
R	Rostral auditory area
RCg	Rostral cingulate area
RSA	Retrosplenial agranular area
RSG	Retrosplenial granular area
S1	Primary somatosensory cortex
S2	Secondary somatosensory cortex
Sub	Subiculum
Ta	Temporal anterior area
Ta_i	Temporal anterior intermediate area
Tav	Temporal anterior ventral area
Ti	Temporal intermediate area

Tm	Temporal mediodorsal area
Tp	Temporal posterior area
UZ	Unresponsive zone
V1	Primary visual area
V2	Secondary visual area
VCg	Ventral cingulate area
VGluT2	Vesicle glutamate transporter 2
Zn^{2+}	Zinc ions

Table 2

Antibody characterization

Antibody	Host (Type)	Source	Catalog #	Dilution factor	Isotype	Immunogen
SMI-32	Mouse (monoclonal)	Covance Inc., Princeton, NJ	SMI-32R	1:2000	IgG1	Homogenized hypothalamus of Fischer rats
PV	Mouse (monoclonal)	Sigma- Aldrich, St. Louis, Mo	P3088	1:2000	IgG1	Frog muscle parvalbumin (Clone PARV-19)
CB	Mouse (monoclonal)	Swant, Bellinzona, Switzerland	C98-48	1:5000	IgG	Calbindin D-28k purified from chicken gut
VGluT2	Mouse (monoclonal)	Chemicon now part of Millipore, Billerica, MA	MAB5504	1:2000	IgG1	Recombinant protein from rat VGluT2
LAMP	Mouse (monoclonal)	Drs Aurea Pimenta and Pat Levitt	N.A.	1:1000	IgG	Hybridoma clone 2G9 (Levitt, 1984; Horton and Levitt, 1988)